



# Tylosin Tartrate Adsorption onto Granular Activated Carbon in the Presence of Humic Acid

A Major Qualifying Project Submitted to Faculty of L'Ecole Nationale Supérieure des Industries Chimiques and Worcester Polytechnic Institute  
In Partial Fulfillment of the Requirements for the Degree of Bachelor of Science

Submitted by:

Alejandra Vargas

Submitted to:

Project Advisor:

Professor Terri Camesano  
Professor Robert Thompson

Site Advisor:

Dr. Marie Noëlle Pons

April 14, 2011

This report represents the work of an undergraduate student at WPI submitted to the faculty as evidence of completion of a degree requirement. WPI routinely publishes these reports on its web site without editorial or peer review.

## Abstract

Tylosin in the environment has increased in the past decades because of intensive use for livestock for therapeutic purpose or for growth promotion. This study investigated tylosin tartrate's removal from water by adsorption onto granular activated carbon (GAC), Acticarbone BGX, in the presence of humic acid. Humic acid was chosen as a representative compound of natural organic matter (NOM) found in surface waters, which competes with tylosin tartrate for adsorption. The concentration range of tylosin tartrate was up to several tens of mg/L; this range can represent concentrated effluents at the vicinity of farm discharge points.

Batch experiments were performed to investigate the influences of pH on humic acid adsorption. Humic acid adsorption isotherms measured at different pH's were fitted to the Langmuir and Freundlich models. The isotherms and Dissolved Organic Carbon (DOC) tests results showed that humic acid adsorption was favored at low pH's (3.5). The experiments ran with tylosin tartrate and humic acid, demonstrated that tylosin tartrate adsorption decreased in the presence of humic acid, which was assigned to competition effects.

## Acknowledgements

This project could not have been accomplished without the advice and guidance of research faculty, directors and students at L'Ecole Nationale Supérieure des Ingénieries Chimiques (L'ENSIC) and Worcester Polytechnic Institute (WPI).

I would like to express my gratitude to Marie Noëlle Pons for making this experience possible for WPI students. I would like to thank her guidance in completing and understanding the laboratory experiments as well as the significance of the results. Secondly I would like to thank the support of my advisors. Your knowledge and insights has driven this project to a level that it could not have achieved otherwise. I would like to thank Professor Comesano for her advice on how to get the most out of an abroad experience as well as her specific advice to the case of France. I would like to thank Professor Thompson for lending me as many explanations and resources needed to my continuous inquiries.

In addition, I would like to thank people that helped me along the way in Nancy, who made my learning experience a much more graceful one. First, I would like to thank Steve Pontvianne, an expert in technical issues, who taught me the way of operation as well as theory behind many important apparatus and machines. Next, I would like to thank Professor Karima Belaroui, who discussed with me many of my results and lent me some great GAC images for my report. I would also like to thank Julie Bertrou, who was my graduate student mentor, for the beginning of my stay in Nancy, even if the photocatalysis part of the project did not work at the end due to technical problems, she was extremely kind in showing and explaining to me all laboratory-related work and theory. Finally, I would like to offer special thanks to Professor Marie-Odile Simonnot, for discussing with me my results and offering useful insights.

# Executive Summary

## Introduction & Background

It is crucial to continuously characterize and understand the effects from the different compounds present in drinking water, since it represents a direct route into the human body, from which we rely upon for survival. Pharmaceuticals are progressively a concern in drinking water. Even though commonly found only in trace quantities, little is known about the chronic effects from continuous exposure to them and their sub-products in drinking water (Jones, Lester & Voulvoulis, 2005). Some speculations of these effects include abnormal physiological processes and reproductive impairment and increased incidences of cancer (Kolpin, Furlong, Meyer, Thurman, Zaugg, Barber & Buxton, 2002).

The pharmaceutical of focus in this study is tylosin tartrate; a veterinary antibiotic used for growth promotion and therapeutics. Antibiotics pose an additional concern since they interfere with the bacterial degradation of organic pollutants and foster the development of antibiotic resistant microorganisms (Alatrache, Laoufi, Pons, Van Deik & Zahraa, 2010). Therefore, it is unfeasible to treat antibiotic-containing waters with biological degradation. In light of this limitation, alternative water treatments have emerged to address this problem. They include: reverse osmosis, adsorption onto granular activated carbon (GAC), ozonation and advanced oxidation processes (AOP).

This study focuses on tylosin tartrate's abatement by adsorption onto GAC. An additional research component was to study the effect of humic acid on tylosin tartrate's adsorption. Humic acid was the model component chosen to represent natural organic matter (NOM) typically found in surface waters. Mardini and Legube (2010) found in their study that regardless of the initial target compound and HA-A concentration, significant reduction in the target compound's

adsorption capacity was noted due to the competitive effects of NOM. Direct site competition and pore blockage have been identified as the two primary mechanisms of competitive adsorption (Mardini & Legube, 2010; Carter, Weber & Olmstead, 1992; Kilduff, Karanfil & Weber, 1998; Newcombe, Morrison, Hepplewhite, Knappe, 2002).

## Methods

Initially humic acid, tylosin tartrate and a mixture of both were characterized by UV-Vis and fluorescence spectroscopy. Calibration curves were constructed in the appropriate concentration ranges for these compounds and their mixture.

Kinetic experiments were carried out to assess tylosin tartrate and humic acid's adsorption equilibrium time. Additionally, one kinetic experiment was used to compare the adsorption performance of tylosin tartrate alone and in the presence of humic acid. Equilibrium experiments were also conducted to investigate the effect of pH on adsorption of humic acid. pH's of 3.5, 7 and 8 were analyzed. Isotherms were fitted to the Freundlich and Langmuir Models.

Other analytical methods used apart from spectroscopy were the dissolved organic carbon (DOC) test, which reflects the total organic matter left in solution after adsorption, and ion chromatography used to detect inorganic matter, which in this case were calcium, chloride, carbonate, potassium, sodium, ammonium, nitrate and sulfate ions.

## Results & Conclusions

The main results with respect to the characterization of solutions show that tylosin tartrate presents a Gaussian shape curve at 290 nm in UV-Vis spectroscopy, while it shows no correlation between emission and concentration for fluorescence spectroscopy. Humic acid does not have a characteristic feature in UV-Vis spectroscopy. Even though its absorbance at any wavelength varies with concentration, the correlation between its absorbance and concentration is not as reliable as in fluorescence spectroscopy, where it shows a characteristic peak at 350 and 450 nm. In this study 450 nm was used to construct the calibration curves, since at this wavelength the peaks of varying concentrations aligned themselves better than at 350 nm.

From the kinetic experiments it was found that the equilibrium adsorption time for humic acid was around 72 hours, however there is only a slight increase in adsorption quantity between the 10 and 72-hour time range. For tylosin tartrate the equilibrium time was not obvious, however for a best-fit curve this time would be around 72 hours. For tylosin tartrate in the presence of humic acid, the equilibrium time is not obvious from the results obtained. Nonetheless from these two kinetic plots (of tylosin tartrate alone and in the presence of humic acid) it was concluded that humic acid reduced tylosin adsorption by an average of 33%.

The isotherms from the equilibrium experiments fitted reasonably well to both the Langmuir and Freundlich models. However the Langmuir model is not a realistic model for this type of adsorption, physical adsorption, where a multilayer can form on the surface of the GAC. From the model parameters it was concluded that the maximum adsorbed quantity occurred at the lowest pH (3.5). The dissolved organic carbon test as well as an unpublished study (Wang, Adouani, Pons, Gao, Sardin & Simonnot, 2010) support this conclusion.

# Table of Contents

<b>Abstract</b> .....	<b>ii</b>
<b>Acknowledgements</b> .....	<b>iii</b>
<b>Executive Summary</b> .....	<b>iv</b>
<i>Introduction &amp; Background</i> .....	<i>iv</i>
<i>Methods</i> .....	<i>v</i>
<i>Results &amp; Conclusions</i> .....	<i>vi</i>
<b>Table of Contents</b> .....	<b>vii</b>
<b>List of Figures</b> .....	<b>ix</b>
<b>List of Tables</b> .....	<b>xi</b>
<b>Introduction</b> .....	<b>1</b>
<b>Background</b> .....	<b>3</b>
Wastewater.....	3
Types of Water Contaminants .....	3
<i>Pharmaceuticals in Water</i> .....	<i>4</i>
Water Treatment.....	7
<i>Limitations to Present Treatments &amp; Emerging Alternatives</i> .....	<i>8</i>
Photocatalysis using TiO <sub>2</sub> .....	9
Titanium Dioxide.....	10
High Performance Liquid Chromatography (HPLC) .....	10
Granular Activated Carbon (GAC).....	12
Humic Acid Adsorption Competition Effects .....	13
Ultraviolet-Visible Spectrophotometry .....	15
Fluorescence Spectrophotometry.....	16
Ion Chromatography.....	17
Dissolved Organic Carbon (DOC) .....	18
<b>Materials</b> .....	<b>20</b>
<b>Methods</b> .....	<b>22</b>
Preparation Experiments.....	22
<i>Characterization of Individual Solutions</i> .....	<i>22</i>
<i>Characterization of Combined Solutions</i> .....	<i>22</i>
<i>Titrations and pH Effect on UV</i> .....	<i>22</i>
Kinetic Experiments.....	23
<i>Kinetic Experiment A</i> .....	<i>23</i>
<i>Kinetic Experiment B</i> .....	<i>24</i>
<i>Kinetic Experiment C</i> .....	<i>24</i>
<i>Kinetic Experiment D</i> .....	<i>24</i>
Equilibrium Experiments.....	25
Ion Chromatography.....	26
Dissolved Organic Carbon .....	26

<b>Results and Discussion</b> .....	<b>27</b>
Preparation Experiments.....	27
<i>UV Spectra of Individual Solutions</i> .....	27
<i>UV Spectra of Combined Solutions</i> .....	30
<i>The Effect of pH on UV Spectra</i> .....	34
<i>Fluorescence Spectra of Individual Solutions</i> .....	36
<i>Fluorescence of Combined Solutions</i> .....	39
<i>River Samples Characterization</i> .....	40
Kinetic Experiments.....	43
<i>Analysis with Ultraviolet-Visible Spectroscopy</i> .....	43
<i>Analysis with Fluorescence Spectroscopy</i> .....	47
<i>Analysis with Dissolved Organic Carbon (DOC) Test</i> .....	50
Equilibrium Experiments.....	53
<i>Isotherms from UV Analysis</i> .....	53
<i>Isotherms from Fluorescence Analysis</i> .....	56
<i>Analysis with Dissolved Organic Carbon (DOC) Test</i> .....	59
<b>Conclusions</b> .....	<b>61</b>
<b>References</b> .....	<b>63</b>
<b>Appendix</b> .....	<b>68</b>
Appendix A. Step by Step Procedures .....	68
<i>High Performance Liquid Chromatography</i> .....	68
<i>UV-Visible Spectroscopy</i> .....	71
<i>Fluorescence Spectroscopy</i> .....	72
Appendix B. Additional Data .....	73
Preparation Experiments.....	73
<i>UV Spectra of Individual Solutions</i> .....	73
<i>UV Spectra of Combined Solutions</i> .....	74
<i>Effect of pH on UV Spectra</i> .....	76
<i>Fluorescence Spectra of Individual Solutions</i> .....	77
<i>Fluorescence Spectra of Combined Solutions</i> .....	78
Kinetic Experiments.....	80
<i>Analysis with UV Spectroscopy</i> .....	80
<i>Analysis with Fluorescence Spectroscopy</i> .....	81
<i>PH at Start and End of Kinetic Experiments</i> .....	83
Appendix C. Additional GAC Acticarbone BGX Photographs.....	85

## List of Figures

Figure 1. Molecular structure of tylosin (a.) and tylosin tartrate (b.) .....	6
Figure 2. Photocatalysis Experimental Set-up (Alatrache, Laoufi, Pons, Van Deik & Zahraa, 2010). .....	10
Figure 3. Types of Chromatography (University of Johannesburg) .....	11
Figure 4. Structural unit of humic acid according to a) Orlov-Chukov and b) Stevenson (Khil'ko, Kovtun, Fainerman & Rybachenko, 2010).....	14
Figure 5. Microscope Photograph of Acticarbone BGX (Magnification=120, Voltage Acceleration=5 KV).....	20
Figure 6. Microscope Photograph of Acticarbone BGX (Magnification=1000, Voltage Acceleration=5 KV).....	21
Figure 7. UV Spectra of Varying Tylosin Tartrate Concentrations.....	28
Figure 8. Tylosin Tartrate's Calibration Curve for UV Spectroscopy (at 290 nm).....	29
Figure 9. UV Spectra of Varying Humic Acid Concentrations.....	29
Figure 10. Humic Acid Calibration Curve for UV Spectroscopy (at 250 nm) .....	30
Figure 11. UV Spectra of Humic Acid (0.05 mg/L) with Varying Tylosin Tartrate Concentrations .....	31
Figure 12. UV Spectra of Humic Acid (0.5 mg/L) with Varying Tylosin Tartrate Concentrations .....	31
Figure 13. UV Spectra of Humic Acid (5 mg/L) with Varying Tylosin Tartrate Concentrations .....	32
Figure 14. UV Spectra of Humic Acid (2.5 mg/L) with Varying Tylosin Tartrate Concentrations; pH = 7.0.....	33
Figure 16. Tylosin Tartrate in the Presence of 10 mg/L Humic Acid - Calibration Curve for UV Spectroscopy (at 290 nm) .....	34
Figure 17. UV Spectra as a function of pH for 20 mg/L Tylosin Tartrate .....	35
Figure 18. UV Spectra as a function of pH for 20 mg/L Humic Acid .....	35
Figure 19. Fluorescence Spectra of Varying Tylosin Concentrations.....	36
Figure 20. Fluorescence Spectra of Varying Humic Acid Concentrations .....	37
Figure 21. Humic Acid (0-10 mg/L) Calibration Curve for Fluorescence Spectroscopy (450 nm) .....	38
Figure 22. Humic Acid (10-80 mg/L) Calibration Curve for Fluorescence Spectroscopy (450 nm) .....	38
Figure 23. Fluorescence Spectra of Humic Acid (5 mg/L) with Varying Tylosin Concentrations .....	39
Figure 24. Fluorescence Spectra of Humic Acid (10 mg/L) with Varying Tylosin Concentrations .....	40
Figure 25. UV Spectra for Madon and Moselle Rivers .....	41
Figure 26. Fluorescence Spectra for Madon and Moselle Rivers.....	42
Figure 27. Humic Acid ( $C_0=10$ mg/L) UV-Derived Kinetics .....	43
Figure 28. Humic Acid ( $C_0=80$ mg/L) UV-Derived Kinetics .....	44
Figure 29. Humic Acid Adsorption Kinetics.....	45
Figure 30. Tylosin ( $C_0=70$ mg/L) UV-Derived Kinetics.....	45
Figure 31. Tylosin ( $C_0=70$ mg/L) and Humic Acid ( $C_0=10$ mg/L) UV-Derived Kinetics.....	46
Figure 32. Tylosin Tartrate ( $C_0 =70$ mg/L) Adsorption Kinetics with and without Humic Acid ( $C_0 =10$ mg/L).....	47
Figure 33. Humic Acid ( $C_0=80$ mg/L) Fluorescence-Derived Kinetics.....	48

Figure 34. Humic Acid ( $C_0 = 80$ mg/L) Adsorption Kinetics.....	49
Figure 35. Tylosin Tartrate ( $C_0 = 70$ mg/L) and Humic Acid ( $C_0 = 10$ mg/L) Fluorescence-Derived Kinetics.....	49
Figure 37. Humic Acid - Dissolved Organic Carbon (DOC) Test.....	51
Figure 38. Tylosin Tartrate ( $C_0 = 70$ mg/L) with and without Humic Acid ( $C_0 = 10$ mg/L) - Dissolved Organic Carbon (DOC) Test .....	52
Figure 39. Madon River Water Sample – Dissolved Organic Carbon (DOC) Test.....	52
Figure 40. Moselle River Water Sample – Dissolved Organic Carbon (DOC) Test.....	53
Figure 43. Isotherms for three different pH's (3.5, 7 and 8) .....	56
Figure 44. Freundlich Model for Humic Acid Equilibrium from Fluorescence Analysis at pH values of 3.5 and 7. ....	56
Figure 46. Isotherm for a pH of 3.5.....	58
Figure 47. Isotherm for a pH of 7. ....	59
Figure 48. Humic Acid Equilibrium Experiments – Dissolved Organic Carbon (DOC) Test. ....	59
Figure 49. UV Spectra of Varying Manure Lixivate Concentrations.....	73
Figure 50. UV Spectra as a function of pH for Manure Lixivate (x100).....	74
Figure 51. UV Spectra of Manure Lixivate (x100) with Varying Tylosin Tartrate Concentrations .....	74
Figure 52. UV Spectra of Manure (x1000) with Varying Tylosin Tartrate Concentrations	75
Figure 53. UV as a function of pH for 7 mg/L Tylosin Tartrate in KCl solution .....	76
Figure 54. Titration Curve for 7 mg/L Tylosin Tartrate in KCl solution .....	76
Figure 55. UV as a function of pH for 1 mg/L Humic Acid in KCl solution .....	77
Figure 56. Titration Curve for 1 mg/L Humic Acid in KCl solution .....	77
Figure 57. Fluorescence Spectra of Varying Manure Concentrations .....	78
Figure 58. Humic Acid (0.05 mg/L) with Varying Tylosin Tartrate Concentrations.....	78
Figure 59. Humic Acid (0.5 mg/L) with Varying Tylosin Tartrate Concentrations.....	79
Figure 60. Humic Acid (2.5 mg/L) with Varying Tylosin Tartrate Concentrations.....	79
Figure 61. Madon UV-Derived Kinetics.....	80
Figure 62. Moselle UV-Derived Kinetics.....	80
Figure 63. Humic Acid ( $C_0 = 10$ mg/L) Fluorescence-Derived Kinetics.....	81
Figure 64. Madon Fluorescence-Derived Kinetics .....	81
Figure 65. Moselle Fluorescence-Derived Kinetics .....	82
Figure 66. Tylosin ( $C_0 = 70$ mg/L) Fluorescence-Derived Kinetics .....	82
Figure 67. Acticarbone BGX Image (ACCEL_VOLT 5 KV, MAG 1000) .....	85
Figure 68. Acticarbone BGX Image (ACCEL_VOLT 5 KV, MAG 1000) .....	85
Figure 69. Acticarbone BGX Image (ACCEL_VOLT 5 KV, MAG 95).....	86
Figure 70. Acticarbone BGX Image (ACCEL_VOLT 5 KV, MAG 1000) .....	86
Figure 71. Acticarbone BGX Image (VOLT 5 KV, MAG 1000) .....	87
Figure 72. Acticarbone BGX Image (VOLT 5 KV, MAG 1000) .....	87
Figure 73. Acticarbone BGX Image (VOLT 5, MAG 85).....	88
Figure 74. Acticarbone BGX Image (VOLT 5 KV, MAG 1000) .....	88

## List of Tables

Table 1. Physical and chemical properties of tylosin tartrate .....	7
Table 2. Ion Chromatography and Dissolved Organic Carbon Test Results for Moselle and Madon Rivers.....	42
Table 3. Model Parameters for Equilibrium Experiments of all pH Values – From UV Analysis.....	55
Table 4. Model Parameters for Equilibrium Experiments of all pH Values – From Fluorescence Analysis .....	57
Table 5. Symbols that Represent Kinetic Solutions.....	83
Table 6. PH Values at the Beginning and End of Kinetic Experiments .....	83

## Introduction

Tylosin is a common veterinary antibiotic often used as a growth promoter (Jones, Lester & Voulvoulis, 2005). While it has already been banned in the EU as a feed additive, it is still been used as a therapeutic. Via lixiviation of manure in farms, this drug finds its way to ground and surface waters (Loke, Tjornelund & Halling-Sorensen, 2002; Blackwell, Kay, Ashauer & Boxall, 2009). Though it has been commonly reported in trace concentrations (ng/L - µg/L), intensive livestock or aquaculture facilities can generate effluents of up to a few mg/L (Kümmerer, 2001).

Even though little is known about health effects from exposure to trace quantities of pharmaceuticals in water, some concerns include abnormal physiological processes and reproductive impairment and increased incidences of cancer (Kolpin, Furlong, Meyer, Thurman, Zaugg, Barber & Buxton, 2002). Some further concerns relevant to antibiotics specifically are that they can interfere with the bacterial degradation of organic pollutants, foster the development of antibiotic resistant microorganisms (Alatrache, Laoufi, Pons, Van Deik & Zahraa, 2010) and could cause sensitization or an allergic response upon their ingestion (Webb, Ternes, Gibert & Olejniczak, 2003).

This study focused on the removal of tylosin tartrate via adsorption onto granular activated carbon (GAC) in the presence of humic acid. Humic acid was used as a model compound of natural organic matter (NOM) typically found in surface waters. Due to site competition and pore blockage, NOM has been found to reduce the adsorption capacity of trace organic compounds onto GAC (Mardini & Legube, 2010; Carter, Weber & Olmstead, 1992; Kilduff, Karanfil & Weber, 1998; Newcombe, Morrison, Hepplewhite, Knappe, 2002).

Equilibrium batch experiments were conducted to investigate the influence of pH on humic acid adsorbance. pH has an influence on adsorption because of its effect on humic acid's electrical charge on the surface charge of the GAC as well as its effect on the compound's molecular structure, which may vary its affinity to the carbon surface. Humic acid isotherms were fitted to the Freundlich and Langmuir models. The isotherm and Dissolved Organic Carbon (DOC) test results show that humic acid adsorption was favored at low pHs (3.5). The experiments ran with tylosin tartrate and humic acid, demonstrated that tylosin tartrate adsorption decreased in the presence of humic acid, which was attributed to competition effects.

# Background

## Wastewater

Wastewater is the flow of used water from a community or city. It includes municipal, industrial and agricultural wastewater as well as rainwater (Pauli, Jax & Berger, 2001) and groundwater that leaks into cracked pipes (Water Environment Federation, 2009). Some examples are water from showers, sinks, dishwashers, laundries, car washers, hospitals and food processing operations (Water Environment Federation, 2009). Agricultural runoffs containing fertilizer and pesticides constitute a major cause of eutrophication of lakes. Storm runoffs in highly urbanized areas may cause significant pollution effects. Whether treated or not, wastewaters are ultimately discharged into a natural body of water (ocean, river, lake, etc.) which is referred to as the receiving water (Ramalho, 1977).

Wastewater is made mostly of water (99.94%) and a small fraction of waste material dissolved or suspended in water, which includes solid waste, food particles, paper products, dirt, oil and grease, proteins, organic materials such as sugars, inorganic materials such as salts, personal care products, pharmaceuticals, cleaning chemicals, among other substances. These pollutants are usually expressed in terms of mg/l (Water Environment Federation, 2009). In untreated sewage suspended particles fall in the range of 100 to 350 mg/l (Ohio State University).

## Types of Water Contaminants

It is crucial to continuously characterize and understand the effects from the variety of substances present in drinking water, since it represents a direct route into the human body, from which we rely upon for survival. Other pathways

include bodily interaction (e.g. showering) or ingestion (eating crops grown with effluent or grown on sewage-sludge-amended soil) (Jones, Lester & Voulvoulis, 2005).

Water contaminants are classified into three categories: chemical, physical and biological contaminants. Chemical contaminants include organic and inorganic compounds. The main concern that arises from pollution by organic compounds is the oxygen depletion that is caused through the process of biological degradation. This phenomenon disrupts the normal food chain in the aquatic environment. Inorganic compounds can also cause an oxygen demand, however the main concern from these pollutants is due to their potential toxic effect. Heavy metal ions, such as  $\text{Hg}^{2+}$ , As III,  $\text{Cu}^{2+}$ ,  $\text{Zn}^{2+}$ ,  $\text{Ni}^{2+}$ ,  $\text{Cr}^{3+}$ ,  $\text{Pb}^{2+}$  and  $\text{Cd}^{2+}$ , are also a dangerous threat for human health even when present in trace quantities. Physical contaminants include: temperature change, color (e.g, cooking liquors discharged by chemical pulping plants), turbidity, foams and radioactivity. Biological contaminants are responsible for transmission of diseases by water, for example: cholera, typhoid, paratyphoid, and shistosomiasis (Ramalho, 1977).

### Pharmaceuticals in Water

Pharmaceuticals are increasingly a concern in surface waters. Even if present only in trace quantities, they have the potential to destabilize the environment and public health (Jones, Lester & Voulvoulis, 2005; Kolpin, Furlong, Meyer, Thurman, Zaugg, Barber & Buxton, 2002). Pharmaceuticals are usually present in wastewaters from hospitals, farms, and residencies as well as in solid human and animal waste (Alatrache, Laoufi, Pons, Van Deik & Zahraa, 2010). Many of them are characterized by being detrimental even without being persistent in the environment. This is because their high transformation and removal rates can be offset by their continuous introduction into the environment, frequently through sewage. Little is known about the chronic health or environmental effects from

continuous exposure to pharmaceuticals and their sub-products in drinking water (Jones, Lester & Voulvoulis, 2005). Nonetheless some concerns include abnormal physiological processes and reproductive impairment and increased incidences of cancer (Kolpin, Furlong, Meyer, Thurman, Zaugg, Barber & Buxton, 2002).

Antibiotics are of special concern in wastewaters as they interfere with the bacterial degradation of organic pollutants, foster the development of antibiotic resistant microorganisms (Alatrache, Laoufi, Pons, Van Deik & Zahraa, 2010) and could cause sensitization or an allergic response upon their ingestion (Webb, Ternes, Gibert & Olejniczak, 2003). Bacteria with antibiotic resistant genes have already been found in biofilms inoculated with drinking water bacteria in Germany (Schwartz, Kohnen, Jahnsen & Obst, 2003). This indicates the possibility of gene transfer from surface or wastewaters to the drinking water network, which could represent a public health concern if it were to occur at a widespread level (Jones, Voulvoulis & Lester, 2003).

In addition, although health risks from low concentration of pharmaceuticals found in drinking water have been proven to be low (Webb, Ternes, Gibert & Olejniczak, 2003; Schulman, Sargent, Naumann, Faria, Dolan & Wargo, 2002), the synergistic effects of repeated, unintended exposure to low concentrated doses of a mixture of drugs are not known (Kolpin, Furlong, Meyer, Thurman, Zaugg, Barber & Buxton, 2002). Furthermore, the interaction of these drugs with other intended medications could cause health problems; for example ibuprofen has been shown to interfere with the cardioprotective properties of aspirin, some cyclooxygenase-2 inhibitors may interfere with bone healing and regrowth after fracture and caffeine may intensify the effects of certain analgesics (Jones, Lester & Voulvoulis, 2005).

One very common antibiotic is tylosin, a 16-membered ring macrolide, therapeutic, veterinary drug often used as a growth promoter (Jones, Lester & Voulvoulis, 2005). It has been banned in several countries, especially in the EU where all antibiotic feed additives have been banned in 2006. However tylosin is still being used a therapeutic. It finds its way to the ground and surface by lixiviation of manure in farms (Loke, Tjornelund & Halling-Sorensen, 2002; Blackwell, Kay, Ashauer & Boxall, 2009). Common tylosin concentrations found in wastewater and surface water are in the range of ng/L to a few  $\mu\text{g/L}$  (Richardson & Bowron, 1985; Hirsch, Terner, Haberer & Kratz, 1999; Kolpin, Furlong, Meyer, Thurman, Zaugg, Barber & Buxton, 2002; Yang & Carlson, 2004; Jones, Lester & Voulvoulis, 2005) but intensive livestock or aquaculture facilities can generate effluents of up to a few mg/L (Kümmerer, 2001).

In this study tylosin tartrate is used for the adsorption experiments; its physical and chemical properties can be seen in table 1. Tylosin tartrate is a salt resulting from the combination between tylosin and tartaric acid; it has two pKa's while tylosin only has one. The difference in structures between tylosin tartrate and tylosin can be seen in Figure 1.

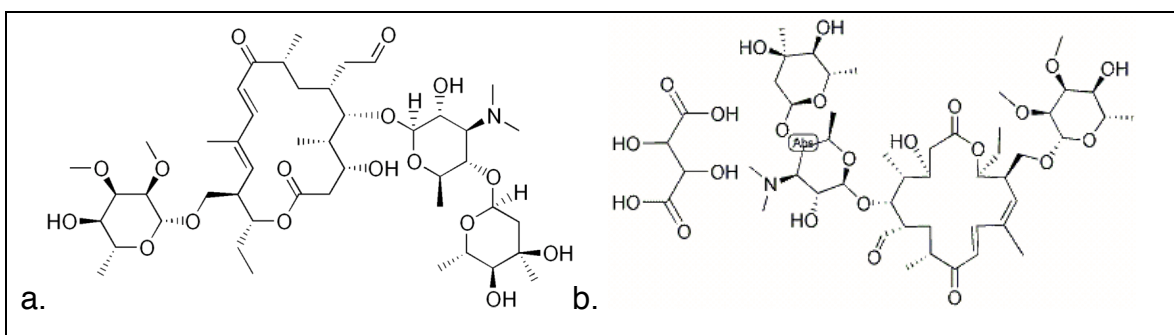


Figure 1. Molecular structure of tylosin (a.) and tylosin tartrate (b.)

Table 1. Physical and chemical properties of tylosin tartrate

pKa-1	pKa-2	Aqueous Solubility (mg/L)	Henry's Law constant (Pa m <sup>3</sup> /mol)	Proton Acceptors	Proton Donors	LogK <sub>ow</sub>	MW g/mol
25°C	25°C						
3.30	7.50	5,000	7.8*10 <sup>-36</sup>	18	5	3.41	917.1

pKa = acidity constant, LogK<sub>ow</sub>= octanol-water partition coefficient, MW= molecular weight (CAS, 2006; Qiang & Adams, 2004; Thiele-Bruhn, 2003; Hirsch, Terner, Haberer & Kratz, 1999).

Another example of a common antibiotic is sulfamethoxazole, which is a synthetic antimicrobial commonly employed: to cure urinary tract infections (Abellan, Bayarri, Gimenez & Costa, 2007), treat bronchitis, as a veterinary medicine, for prevention and treatment of infections, as well as a growth promoter (Abellan, Gimenez & Esplugas, 2009). In a study that measured concentrations of 95 different organic wastewater contaminants (OWC) within 139 selected streams in the U.S, sulfamethoxazole was found to be within the 30 most frequently detected OWC. In addition, the maximum measured concentration among the group of veterinary and human antibiotics was that of sulfamethoxazole. (Kolpin, Furlong, Meyer, Thurman, Zaugg, Barber & Buxton, 2002).

## Water Treatment

Water in a river or lake gets purified naturally by bacteria, which feed on waste and in turn reproduce themselves and produce carbon dioxide. In this process, bacteria consume oxygen, which gets naturally replenished in the ecosystem to be absorbed by the aquatic fauna and flora. The problem arises when an excess of waste is discharged into a stream and the bacteria consuming the waste deplete the available supply of dissolved oxygen that aquatic organisms need for

survival. The continuous increase in human population can cause wastewater volumes to surpass the level at which they can be naturally purified. Therefore wastewater treatment facilities are essential to maintain a balance in the environment and to supplement nature's work (Water Environment Federation, 2009).

### Limitations to Present Treatments & Emerging Alternatives

Traditional biological degradation in wastewater treatment, however, does not eliminate all type of wastes. Some of these substances encompass pesticides, heavy metals, nutrients, and pharmaceuticals (Water Environment Federation, 2009). In the previously mentioned study regarding 95 different organic wastewater compounds (OWC) detected throughout the U.S, one or more OWC was found in 80% of the 139 sampled U.S streams implying that many of these compounds survive wastewater treatment and biodegradation (Kolpin, Furlong, Meyer, Thurman, Zaugg, Barber & Buxton, 2002). One explanation to this is that it is unfeasible to treat pharmaceutical-containing waters with biological treatment due to their often-antibiotic character (Alatrache, Laoufi, Pons, Van Deik & Zahraa, 2010).

Auxiliary treatments to abate antibiotics from water include the following: reverse osmosis, adsorption onto granular activated carbon (GAC), ozonation and advanced oxidation processes (AOP). Among the AOP processes there are several: fenton or photo-fenton system, ultrasound, peroxidation and UV light, advanced oxidation hybrid processes and photocatalysis using  $TiO_2$  (Giraldo, Peñuela, Torres-Palma, Pino, Palomino & Mansilla, 2010). However, even advanced treatment processes do not always eliminate all drugs. In a study done by Tauber (Tauber, 2003) traces of carbamazepine and gemfibrozil were found in four out of ten Canadian cities, which had all used advanced treatments such as ozone or GAC (Jones, Lester & Voulvoulis, 2005).

### *Photocatalysis using TiO<sub>2</sub>*

Advanced oxidation processes are based on the production of hydroxyl radicals used to oxidize most organic contaminants. Some of its advantages are mild operation conditions and low cost. One of the most destructive types of AOP is photocatalysis using TiO<sub>2</sub> (Giraldo, Peñuela, Torres-Palma, Pino, Palomino & Mansilla, 2010).

The photocatalysis set-up, used at the photocatalysis laboratory at ENSIC, is shown in Figure 2 and it includes a pump, a reservoir flask, a reactor including the TiO<sub>2</sub> plaque and a UV lamp. To start the system about 250ml of a certain concentration of antibiotic is introduced. About half is placed into the reservoir and the other half into the reactor approximately and then the pump is started. Only the reservoir should be under agitation at all times, but not under heating conditions, since this could vary the rate of degradation. The solution is circulated throughout the system. Before turning on the lamp, about 90 min should be allowed for the antibiotic concentration to stabilize, while analyzing samples with the HPLC every 15 min to verify this. After this, the lamp can be turned on and samples can be tested every 30 min. However, the photocatalysis experiments were not carried out due to technical constraints.

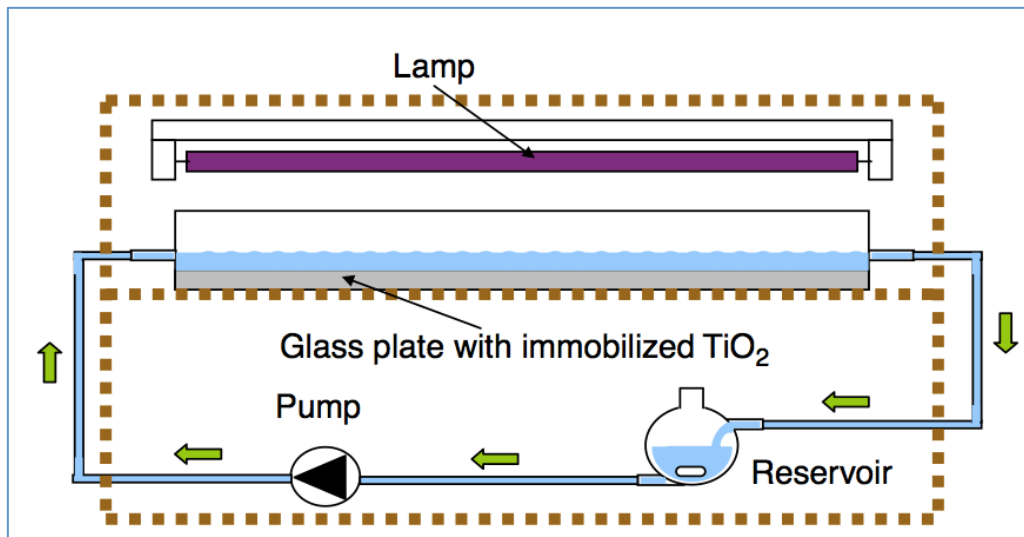


Figure 2. Photocatalysis Experimental Set-up (Alatrache, Laoufi, Pons, Van Deik & Zahraa, 2010).

### Titanium Dioxide

Titanium dioxide is a useful semiconductor metal oxide that has extensive applications in areas such as catalysis, photocatalysis, sensors and dye-sensitized solar cells (Zhao, Wan, Xiang, Tong, Dong, Gao, Shen & Tong, 2011). It is widely available, inexpensive, non-toxic and shows good chemical stability (Giraldo, Peñuela, Torres-Palma, Pino, Palomino & Mansilla, 2010). An important characteristic of this metal is its photocatalytic activity, which is determined by properties involving the crystalline phase, specific surface area and porous structures (Zhao, Wan, Xiang, Tong, Dong, Gao, Shen & Tong, 2011). For the photocatalysis experiments PC500 was the type of  $\text{TiO}_2$  that was intended for use.

### High Performance Liquid Chromatography (HPLC)

High Performance Liquid Chromatography (HPLC) is the main analytical technique used for photocatalysis in the photocatalytic laboratory of ENSIC.

HPLC is a separation technique that involves mass transfer between a stationary and mobile phase (Drenthe College). It has the ability to separate, identify and quantify the different compounds that make up any sample that can be dissolved in liquid (Waters, 2010). It was derived from column chromatography and it is a very useful tool in analytical chemistry.

The main advancements in this technique were made by the use of small particles as separators and from high pumping pressures (University of Johannesburg). Nonetheless, the high performance of the HPLC is also due to other factors such as: the narrow distribution range and uniform pore size and distribution of the particles, high-pressure column slurry packing techniques, low volume sample injectors and sensitive low volume detectors (Drenthe College). Liquid chromatography is one of three types of chromatography, as seen in Figure 3. It is used for non-volatile samples with a molecular weight smaller than 2000 (University of Johannesburg).

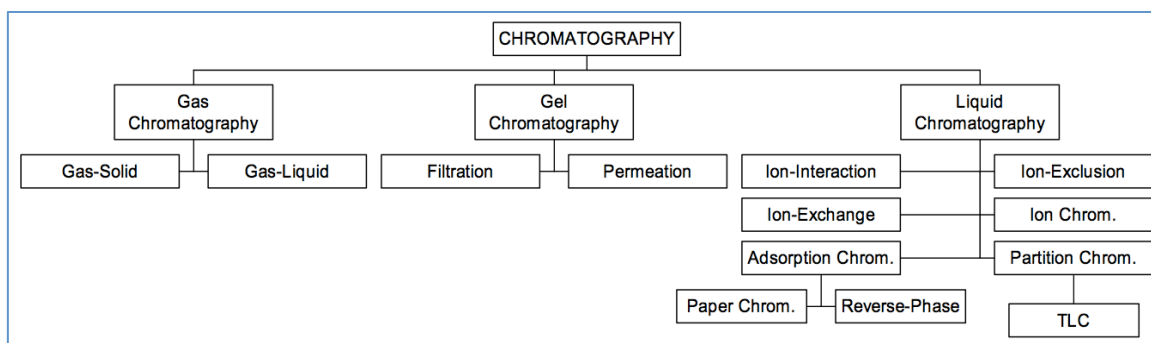


Figure 3. Types of Chromatography (University of Johannesburg)

During HPLC analysis, the analyte is forced through the column by the mobile phase at high pressure, which decreases the components' time to pass through the column known as retention time (Harris, 2007). Each compound usually corresponds to a unique retention time and thus to a unique type of peak, which is the basis of HPLC (University of Johannesburg). The set of peaks detected by a data recorder form what is known as a chromatogram. Lower retention times

translate into narrower peaks in the chromatogram as well as a better sensitivity and selectivity. Sensitivity in this context refers to the ability to differentiate the peaks from noise and selectivity refers to the ability to differentiate the peaks from each other. Common solvents used are water, methanol or acetonitrile. Often a combination of water and an organic liquid is used to speed up or slow down the analyte through the column depending on its affinity to the stationary phase (WorldIQ.com, 2010).

### *Granular Activated Carbon (GAC)*

Carbon has long been used as an adsorbent. For example, water filtration by using bone char and charred vegetation, gravel, and sand as well as sugar solution purification have been reported as early uses of charcoal (University of Waterloo). Carbon's ability to remove contaminants from water as well as the progressively stringent environmental regulations has led to its increased use in the last 30 years (Carbtrol Corporation, 1992).

Granular activated carbon is an efficient adsorbent due to its high surface area to volume ratio. One gram of commercially available activated carbon has a surface area of 1000 square meters (Carbtrol Corporation, 1992).

Adsorption is the process by which dissolved molecules adhere to a solid surface. It occurs when the attractive forces between the molecules and the adsorbent solid are greater than those between the molecules themselves (Carbtrol Corporation, 1992). There are two types of adsorption: physical and chemical adsorption. In the former a multilayer can form for which the BET (Brunauer, Emmett and Teller) equation can be used, while in the latter a monolayer can form for which the Langmuir model is typically used (Adamson, 1967).

Adsorption from solution is a complex phenomenon (Adamson, 1967). When an organic compound is adsorbed onto an adsorbent it establishes equilibrium with the amount of compound remaining in the liquid phase. It partitions among the liquid and adsorbent phases, based on its the relative affinities between both phases. Therefore, an important parameter in determining the removal percentage of a target compound is the relative amounts of both phases in solution (McQuarrie & Simon, 1998). Other factors affecting the adsorption process include: particle size and molecular weight, the solubility of the target compound, surface area, pore structure, pH, temperature, surface properties such as hydrophilicity and hydrophobicity and the nature of solute-solvent interactions in the solution phase and in the interfacial region, as well as with the adsorbent (Adamson, 1967).

#### Humic Acid Adsorption Competition Effects

Ground and surface waters contain natural organic matter (NOM), which is a mixture of humic substances, hydrophilic acids, proteins, lipids, carbohydrates, carboxylic acids, amino acids and hydrocarbons (Zhang, Shao & Karanfil, 2010), at concentrations ranging from 0.1 to 10 mg/L (Mardini & Legube, 2010). NOM can be found in dissolved, colloidal or particulate form, however the dissolved form is the predominant type found in natural waters (Zhang, Shao & Karanfil, 2010).

Competition effects from NOM have been shown to reduce the adsorption capacity of trace organic compounds in the microgram and nanogram per liter level onto activated carbon (Mardini & Legube, 2010; Carter, Weber & Olmstead, 1992; Kilduff, Karanfil & Weber, 1998; Newcombe, Morrison, Hepplewhite, Knappe, 2002).

In the activated carbon experiments, humic acid was used as a model compound of NOM. Humic acid is a terrestrial peat humic substance, which is polymeric and multifunctional with a dominant acidic character. It is often used as a model adsorbate because it is commercially available and convenient to test the effects of high concentrations (Mardini & Legube, 2010). In Figure 4, the structural unit of humic acid can be appreciated.

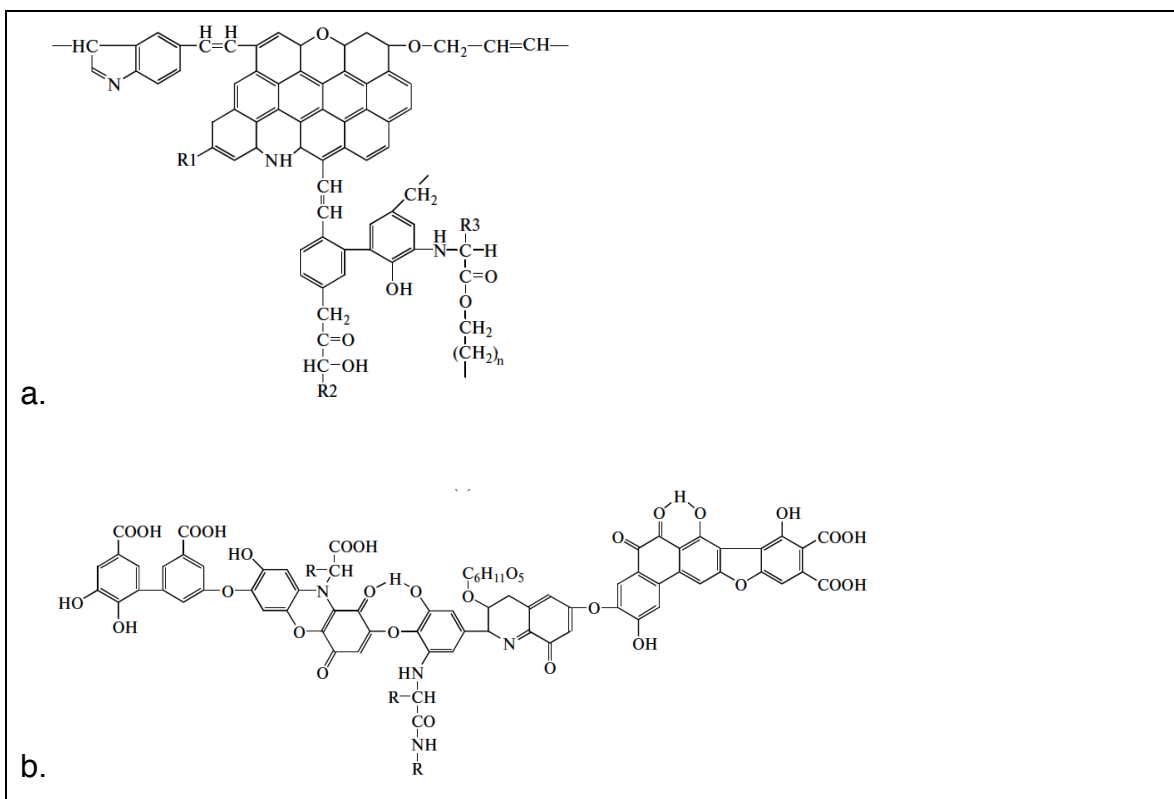


Figure 4. Structural unit of humic acid according to a) Orlov-Chukov and b) Stevenson (Khil'ko, Kovtun, Fainerman & Rybachenko, 2010).

Mardini and Legube (2010) found in their study that regardless of the initial target compound (in this case Bromacil) and HA-A concentration, significant reduction in the target compound's adsorption capacity was noted due to the competitive effects of NOM. NOM can also modify the adsorption kinetic rate of trace compounds. Direct site competition and pore blockage have been identified as the two primary mechanisms of competitive adsorption between the target compounds and NOM (Mardini & Legube, 2010; Carter, Weber & Olmstead,

1992; Kilduff, Karanfil & Weber, 1998; Newcombe, Morrison, Hepplewhite, Knappe, 2002).

Competitive effects depend on the molecular weight distribution of NOM, the pore size distribution, configuration and hydrophobicity of the activated carbon (Mardini & Legube, 2010) as well as the charge, size and polarity of the organic compounds (Zhang, Shao & Karanfil, 2010). In Mardini and Legube's study, low molecular weight NOM was found to have a greater competitive effect than high molecular weight NOM (Mardini & Legube, 2010). Zhang et al. (2010) found that the degree of NOM adsorption varied significantly depending on the type of NOM and was found to be proportional to the aromatic carbon content in NOM. This study also observed that NOM competition was more severe on a non-planar hydrophilic substance (2-phenylphenol), than on a planar hydrophobic one (phenanthrene). Additionally, hydrophobic carbon was found to have a stronger adsorption affinity to organic compounds and it also enhanced the NOM effect on the organic compound adsorption (Zhang, Shao & Karanfil, 2010).

#### Ultraviolet-Visible Spectrophotometry

Spectrophotometry analysis is the determination of the concentration of a substance according to its absorption of a specific monochromatic radiation (Trombe, 1971). When a molecule absorbs ultraviolet or visible light it is excited to a higher energy level. The absorbance of energy can be plotted against wavelength to obtain a UV-Vis spectrum. The shape of the peaks and the wavelength of maximum absorbance give information about the structure of the compound (Wake Forest University). Absorption bands correspond to functional groups within a molecule (Sheffield Hallam University). The spectra usually contain broad features that are of limited use for sample identification, but can be useful for component quantification. The concentration of a component can be

determined by applying the Beer-Lambert Law to a specific absorbance, wavelength and path length (Harris, 2007).

Ultraviolet radiation has wavelengths of 200-400 nm, while visible light has wavelengths of 400-800 nm. Plastic cuvettes can be used for the visible light wavelength range, however since plastic absorbs ultraviolet light, quartz cuvettes are used for the ultraviolet wavelength range (Wake Forest University).

Some of the uses of UV-Vis spectrophotometry include: detection of eluting components in HPLC; determination of the oxidation state of a metal center of a cofactor; determination of the maximum absorbance of a compound prior to a photochemical reaction (Wake Forest University); and absorption, reflectivity, and transmission characterization of materials such as pigments, coatings, windows and filters (Tissue B, 2000).

#### Fluorescence Spectrophotometry

Molecules are generally present in their lowest level of energy, known as ground electronic state; here is where they are more stable. Within each electronic state there are several state levels called vibrational states. In fluorescence spectroscopy light passes through a liquid sample, which causes the molecules in the sample to absorb the light in the form of discrete quanta and to rise to a more excited energy state. After colliding, the molecules quickly lose their extra energy and fall back to their ground state, releasing the energy in the form of photons (Harris, 2007). Since molecules may fall down to any of the vibrational states comprised in the ground state, each emitted photon will have a different energy and thus a different frequency. These set of frequencies along with their intensities form the different absorption bands on what is known as an emission spectrum (PerkinElmer, INC, 2006). Qualitative analysis is based on the location

of the lines in the spectrum, while quantitative analysis on the intensity of these lines (Trombe, 1971).

Fluorescence may be susceptible to temperature variations, since a change in temperature will change the medium's viscosity, which will change the number of collisions of the molecules. Fluorescence intensity is sensitive to such changes, and thus many fluorophores, which refer to the molecule's components that cause it to be fluorescence, are temperature dependent. Therefore, any sample procedure involving heating or cooling must allow for sufficient time before its fluorescence analysis (PerkinElmer, INC, 2006). In addition, fluorescence can also be sensitive to even small changes in pH, thus an accurate control and measure of this property is essential for constant and accurate results (PerkinElmer, INC, 2006).

### Ion Chromatography

Ion Chromatography is a type of liquid chromatography used to quantify and identify the cations, anions and organic acids in a given solution (Library4science.com, 2008). This technique has been specified as the method of choice by the Environmental Protection Agency (EPA) for the detection of chloride, nitrate, sulfate and phosphate. It is often preferred due to its improved sensitivity over other analytical methods and because of its high degree of accuracy and reliability (Dionex Corporation, 1992).

Its retention is determined by the ionic interactions between solute ions and charged sites bound to the stationary phase (Harris, 2007). This type of chromatography is one of the most difficult ones to carry out and it is typically used for the analysis of anions for which there is no other practical analytical

alternative (Library4science.com, 2008). It is also used for cations and biochemical species such as amino acids and proteins (Tissue, 2000).

Apart from its useful application in water treatment, ion chromatography is also used for: the determination of sugar and salt content in foods, the isolation of select proteins, the determination of water chemistries in aquatic ecosystems (Bruckner, 2009), acid rain monitoring (Dionex Corporation, 1992), and anion and cation monitoring in the semiconductor industry (Harris, 2007).

The ion chromatograph located in the wastewater laboratory in L'Ecole National Supérieure des Industries Chimiques (L'ENSIC) consists of an auto sampler, a chromatographic detector, a dual pump and an eluent generator. The two pumps are for the two solvents: one for the anions, which should be basic, and one for the cations, which should be acidic. In the software linked to this machine, the parameters to control are either the solvents' flowrate or pressure of the column, the concentration of the sample or its pH and the temperature of the column or of the samples, which will affect their conductivity. This instrument was used in the activated carbon experiments in order to characterize the water samples from the rivers of Madon and Moselle.

#### Dissolved Organic Carbon (DOC)

Dissolved organic carbon refers to the amount of organic material contained in water. It is derived from the degradation of plants and animals that come into contact with water and it is found predominantly in surface waters rather than ground water. It may be dangerous due to its synergistic effects in the presence of chlorine. This combination produces trihalomethanes that may have negative long-term health effects. In addition, DOC may interfere with the usual water purification processes of chlorination, ultraviolet and ozone sterilization as well as

promote the growth of microorganisms by representing a source of nutrition (Government of Saskatchewan, 2009).

Advanced oxidation technologies to eliminate DOC from water include: granular activated carbon, coagulation/flocculation processes, biological filtration and distillation. Water treatment costs will drastically increase as DOC concentration in water increases. Usually concentrations of 5mg/L or higher complicate water treatment, while those of 2mg/L or lower tend to be a less significant problem (Government of Saskatchewan, 2009).

## Materials

The type of granular activated carbon (GAC) used was Acticarbon BGX produced from pinewood charcoal chemical activation, provided by CECA (France). Its particle size is in the range of 0.4 – 1.6 mm; its surface area, measured by N<sub>2</sub> adsorption at 77 K (Sorptomatic 1990, Thermoquest Instruments) is 1583 m<sup>2</sup>/g and its pore volume is 1.05 g/cm<sup>3</sup>. Its pore size is distributed from micro to macropores.

Some magnifications for this type of carbon, in which the porous structure is appreciated, can be seen in Figures 5 and 6. Additional pictures can be found in Appendix C. These pictures were taken by Professor Karima Belaroui with an environmental scanning electron microscope (ESEM), model JEOL.

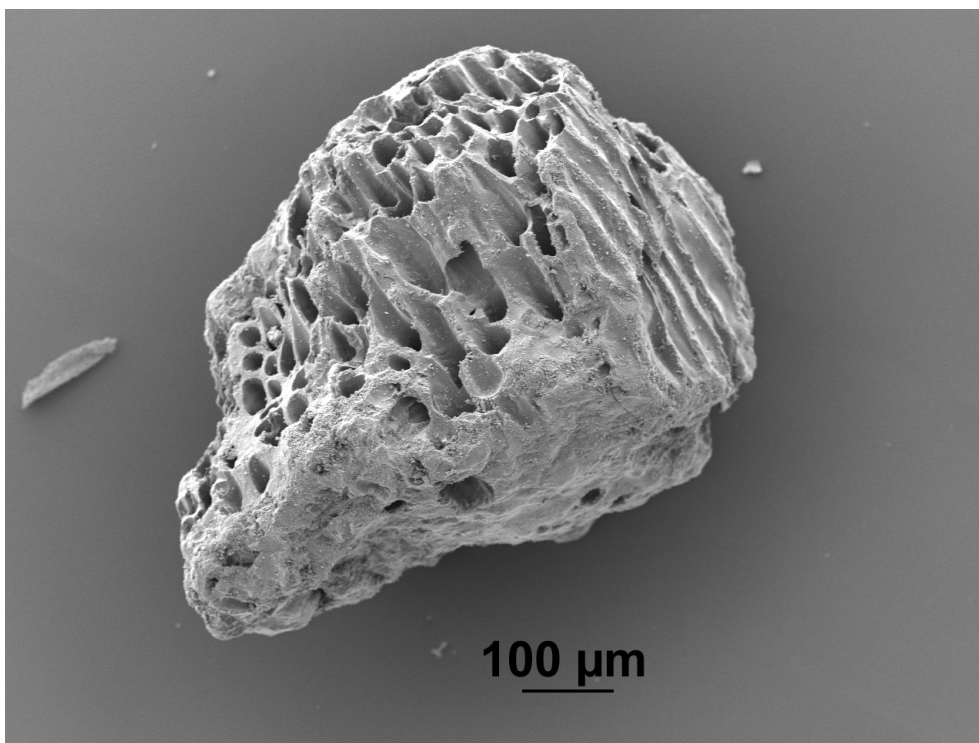


Figure 5. Microscope Photograph of Acticarbon BGX (Magnification=120, Voltage Acceleration=5 KV)

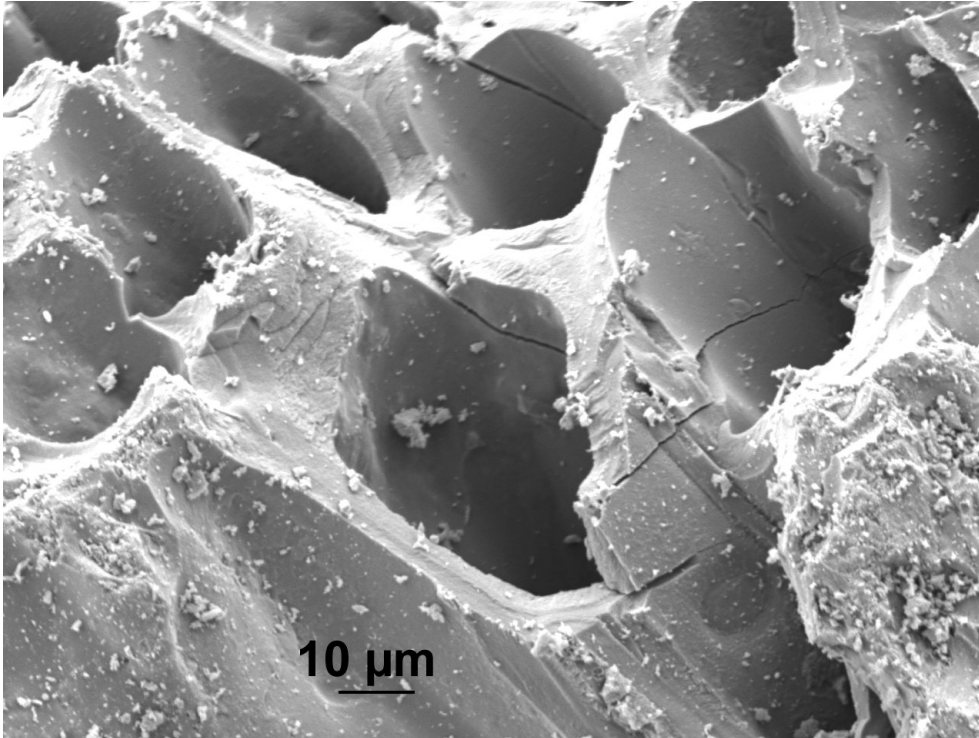


Figure 6. Microscope Photograph of Acticarbon BGX (Magnification=1000, Voltage Acceleration=5 KV)

Tylosin tartrate and humic acid (HA) (CAS 1415-93-6) were purchased from Sigma-Aldrich (Saint Quentin Fallavier, France). Tylosin tartrate and humic acid solutions at concentrations of 70 mg/L and 100 mg/L respectively were prepared using ultra-pure water and stored at 4 °C in the darkness for further use. A 0.1 M NaOH and 0.5 M H<sub>2</sub>SO<sub>4</sub> solution were prepared and used to adjust pH.

The manure lixivate solution was obtained from 'La Bouzule Farm', which is an experimental station of the Institut National Polytechnique de Lorraine (INPL).

The UV-Vis spectrophotometer used was an Anthelie Light spectrophotometer (Secomam, Domont, France) with a quartz cuvette (optical path length = 1cm). The fluorescence machine was a Hitachi F-2500 spectrofluorometer.

## Methods

### Preparation Experiments

#### Characterization of Individual Solutions

Initially tylosin tartrate, humic acid and manure lixivate solutions were characterized by UV-Vis and fluorescence spectrophotometry. The tylosin tartrate and humic acid solutions of 70 mg/L and 100 mg/L respectively, were diluted by 1, 10, 20 and 100 and tested by each type of analytical technique. The river samples from Madon and Moselle were also analyzed by these two techniques. pH was not adjusted for these solutions.

#### Characterization of Combined Solutions

Combinations of solutions were prepared and tested by the techniques previously mentioned. All possible combinations containing 5 ml of 0.1, 1, 5 and 10 mg/L humic acid solution and 5 ml of 0.07, 0.7, 3.5 and 7 mg/L tylosin tartrate solution (16 solutions total) were made and tested.

#### Titration and pH Effect on UV

10 mg/L humic acid and tylosin tartrate solutions were titrated by first dissolving them into 0.1 M KCl and adjusting their pH to 2.5 with 0.1 M HCl. Aliquots of 0.01-0.4 ml KOH solution were added to the solution up to a pH of 10. After almost each aliquot added, the solution was analyzed by UV. This procedure was done in order to obtain a graph of UV as a function of pH as well as a titration curve for humic acid and tylosin tartrate.

After realizing that the UV-pH graphs were not what were expected, solutions at pHs of 6, 7 and 8 were prepared by using buffer solutions. A buffer solution of pH of 6 was prepared by dissolving 50 ml of 0.1 M potassium dihydrogen phosphate with 5.6 ml of 0.1 M NaOH. Buffer solutions of pH of 7 and 8 were done in an analogous way except that they contained 29.1 and 46.1 ml of NaOH instead, respectively.

## **Kinetic Experiments**

### Kinetic Experiment A

The kinetic experiments were designed to analyze how tylosin tartrate and humic acid adsorb onto the activated carbon with time. Thirty grams of GAC was prepared by first completely submerging it in ultra-pure water for about 2.5 hours. This was done to purify the carbon for it to be at its maximum adsorption capacity. Then the carbon was filtered and dried at 40 °C for about 45 hours. To conduct the experiment 12-glass bottles were filled each with 100 mg of GAC and 100 ml of humic acid solution.

For kinetic experiment A, half of the bottles contained a 10 mg/L solution and the other half an 80 mg/L one. The former concentration represents the case of a river moderately impacted by organic matter, while the latter one represents the case of a river more severely impacted by it. All solutions were adjusted to a pH of 7 using either 0.1 M NaOH or 0.1 M HCl as needed. All the bottles were stirred at 150 rpm in darkness. Each solution was withdrawn, filtered and stored at 4°C after 1, 5, 10, 24, 48 and 72 hours. All 12 solutions were then measured for their pH and analyzed by UV-Vis and fluorescence spectroscopy and dissolved organic carbon content (DOC).

### Kinetic Experiment B

The second kinetic experiment was done in the same way as the first one except that this time only 6 glass bottles were filled with 100 ml of tylosin tartrate (70 mg/L). The rest of the procedure was the same as the one described for kinetic experiment A. After having analyzed the results from this experiments and realizing that adsorption equilibrium steady state was questionable, an extra run for 96 hours was done.

### Kinetic Experiment C

The third kinetic experiment was also analogous to the previous ones in terms of procedure, but this time 6 glass bottles were filled with a mixture of tylosin tartrate (70 mg/L) and humic acid (10 mg/L). This was done to understand how differently tylosin tartrate adsorbs onto GAC in the presence of humic acid in low concentrations.

For the construction of the transient adsorbed quantity plot ( $q_t$  vs time), the adsorbed quantity of humic acid measured by fluorescence was subtracted at each time point from the adsorbed quantity of the mixture measured by UV-Vis spectroscopy. This was done because UV-Vis spectroscopy is not selective; its results reflect adsorption influenced from all the organic matter present in the sample.

### Kinetic Experiment D

The last kinetic experiment conducted involved using water samples from the nearby rivers 'Madon' and 'Moselle'. Therefore this time there were 12 glass

bottles prepared with GAC and water samples from each river. The samples' pHs were not adjusted in this case but rather left as the natural rivers' pHs.

## Equilibrium Experiments

The isotherm experiments consisted of 21 glass bottles, which in turn consisted of 3 sets, each of a different pH (6,7 and 8), each with 7 different solutions of humic acid. The seven different solutions were: 5,10, 20, 40, 60, 80 and 100 mg/L of humic acid. The pH was adjusted as described earlier. Each bottle contained 100 mg of GAC. The objective of this experiment was to analyze how the maximum adsorbed quantity varied with varying initial concentrations of the compound of interest, in this case humic acid. All other conditions for this experiment were the same as the ones described for the kinetic ones.

After analyzing the kinetic experimental results it was concluded that 96 hours of contact time would suffice for the solutions to reach adsorption equilibrium. Therefore after this time, the bottles were collected, filtered and stored at 4°C. Then they were analyzed by aforementioned techniques used in the kinetic experiments.

An alternative to this procedure is to use the same solution concentration in all bottles and vary the GAC mass in each bottle. This technique has been more recently employed since the error from weighing masses is more likely to be lower than the accumulated errors from a series of dilutions. However it should theoretically give the same outcome.

## Ion Chromatography

This experiment was conducted by the technician Steve Pontvianne on a ICS-3000 Ion Chromatography System (Dionex). The solvent used for the experiment was water. Several water samples were passed through the column before injecting the samples of interest, which were water samples from the Moselle and Madon rivers. The machine was run under isocratic mode (constant solvent mixture). The ions being tested for were calcium, chloride, carbonate, potassium, sodium, ammonium, nitrate and sulfate.

## Dissolved Organic Carbon

This experiment was also run by the technician Steve Pontvianne. Ten water samples were run through the system to condition and clean it before the samples of interest were introduced. The samples of interest included vials from all the kinetic and equilibrium experiment. In addition, between each set of 13 samples, 3 water samples were run to clean the column.

The procedure by which the samples go through to be analyzed is the following: they are first heated up to 690 °C while the reaction is sped up by using platinum catalyst. Then the vapors from this reaction pass through a halogen suppressor. Next, water and carbon dioxide are cooled to room temperature so that only carbon dioxide will remain in the gaseous state. Finally, carbon dioxide gas is quantified by the machine analyzer. All the carbon detected is considered non-purgeable-organic-carbon.

## Results and Discussion

### Preparation Experiments

For the activated carbon experiments tylosin tartrate was the antibiotic used and monitored throughout. Humic acid was also monitored simultaneously. Humic acid represents the natural organic matter that would normally be found in discharge waters and which has been found to reduce the adsorption capacity of trace organic compounds onto GAC as discussed in the background section.

### UV Spectra of Individual Solutions

Several UV runs were carried out with varying concentrations of each solution in order to obtain an idea of what level of absorbance corresponded to what concentration of each substance<sup>1</sup>. All curve distortions at 340 nm are due to the lamp change in the UV machine. The spectra and calibration curves obtained for the different concentrations of tylosin tartrate and humic acid are shown in Figures 7, 8, 9, and 10.

---

<sup>1</sup> Manure lixivate was another substance characterized by various techniques, however due to time constraints it did not form part of the GAC experiments. Therefore most of its spectra and additional information is presented in Appendix B.

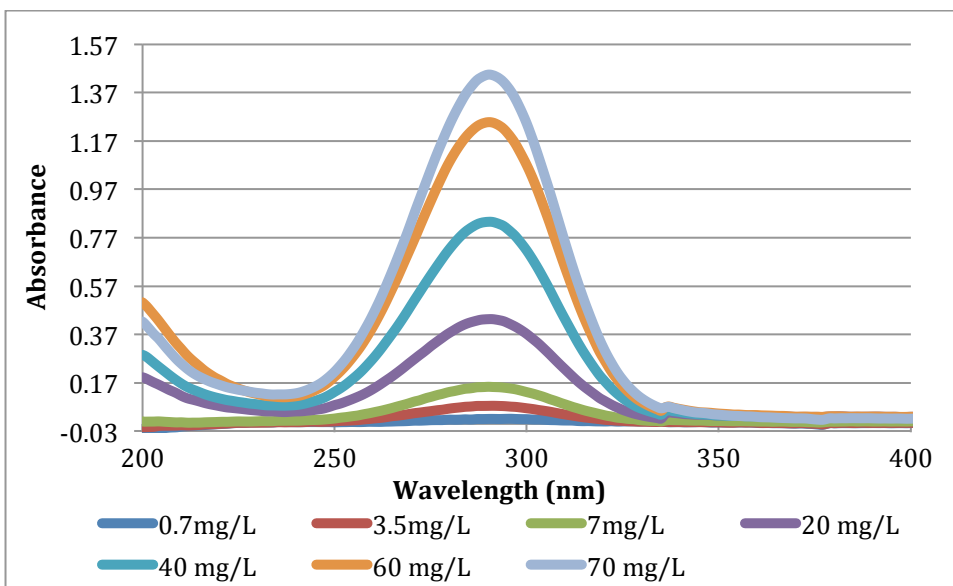


Figure 7. UV Spectra of Varying Tylosin Tartrate Concentrations

From the tylosin tartrate spectra the maximum absorbance reached with a concentration of 70mg/L is approximately 1.4. Since the maximum detectable absorbance for the UV machine being used in this experiment was 3, this concentration was an acceptable one with which to start an activated carbon experiment.

It is evident that tylosin tartrate presents a characteristic Gaussian UV-curve shape, with the maximum absorbance occurring at a wavelength of about 290nm. Therefore a calibration curve was constructed for this wavelength as shown in Figure 8. This calibration was then used to determine the concentrations of tylosin tartrate solutions after varying times of contact with GAC.

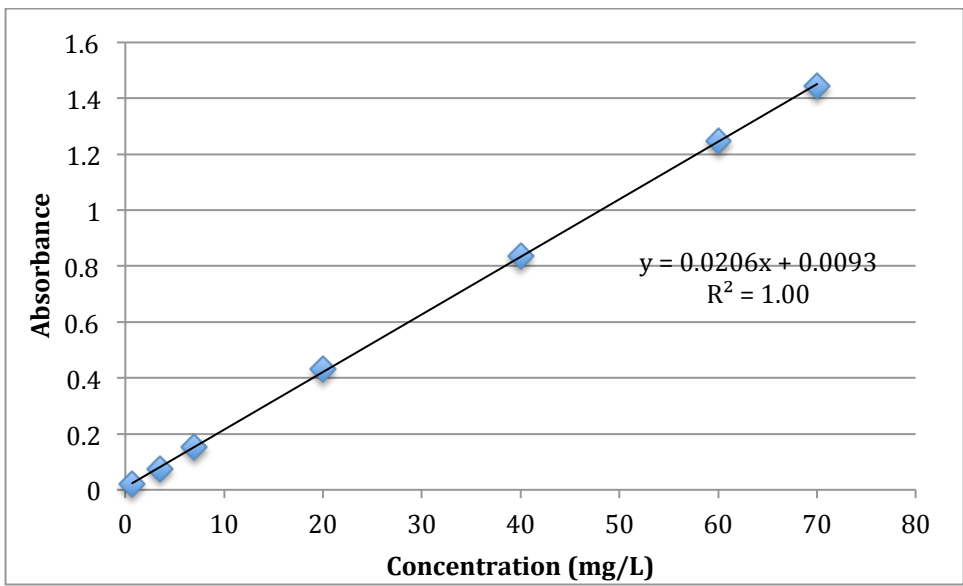


Figure 8. Tylosin Tartrate's Calibration Curve for UV Spectroscopy (at 290 nm)

The humic acid spectra are shown in Figure 9. These spectra show a completely different shape, which resemble more to a decreasing exponential curve. It is not clear which is the wavelength of interest here, since there is no characteristic feature with which to easily detect humic acid presence in solution. Nonetheless, a wavelength of 250 nm was chosen to plot a calibration curve from as shown in Figure 10. The regression is very accurate showing a coefficient of determination of one exact to the second decimal place.

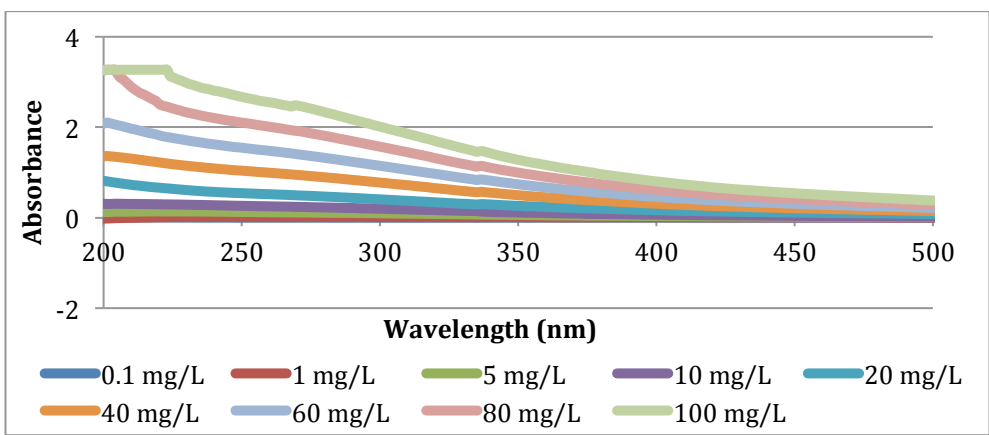


Figure 9. UV Spectra of Varying Humic Acid Concentrations

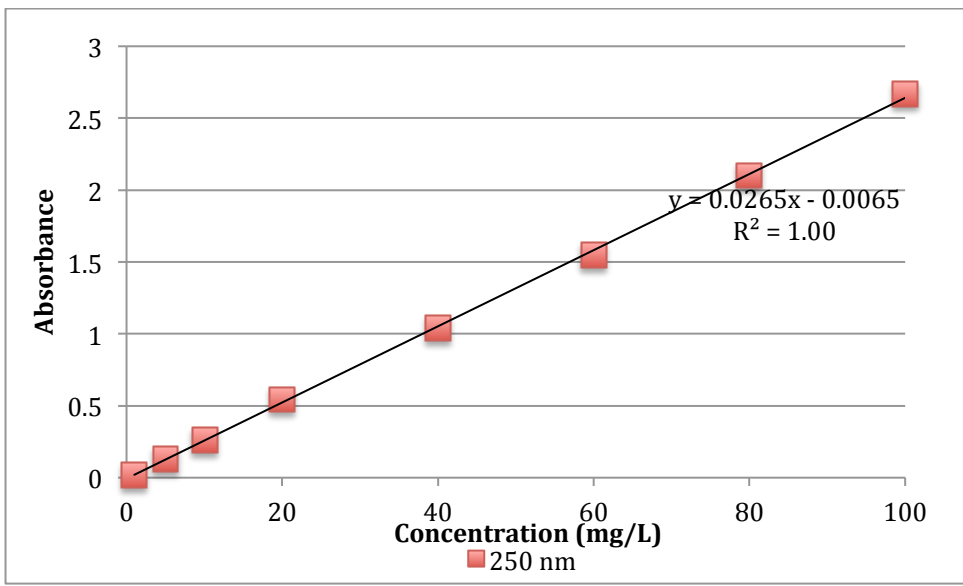


Figure 10. Humic Acid Calibration Curve for UV Spectroscopy (at 250 nm)

The objective of understanding how the UV curves behave with varying concentrations of tylosin tartrate and humic acid is to be able to relate a type and shape of curve to a specific concentration of each substance. This information, especially the calibration curves were used in the interpretation of the UV spectra from the GAC kinetic and equilibrium experiments. However, since there is no characteristic UV feature for humic acid, fluorescence was more heavily relied upon to analyze the kinetics and equilibrium of this substance during the GAC experiments.

[UV Spectra of Combined Solutions](#)

Further UV runs were made with different combinations of humic acid and tylosin tartrate. The purpose of these runs was to obtain an idea of how the UV spectra behave with varying combinations of the components' concentrations, which is the case during the adsorption experiments. The combination of humic acid and tylosin tartrate graphs are shown in the following spectra.

Figures 11 and 12 show spectra with a lot of noise, since the concentrations of both humic acid and tylosin tartrate are reaching their limits of detection. However in Figure 13 the spectra present smoother lines due to higher humic acid concentration. From these three sets of spectra it is evident that tylosin tartrate concentrations below 0.35 mg/L are no longer detectable by UV spectroscopy. It is also noteworthy that even with constant concentrations of tylosin tartrate, the absorbance levels at 290 nm change with varying humic acid concentrations.

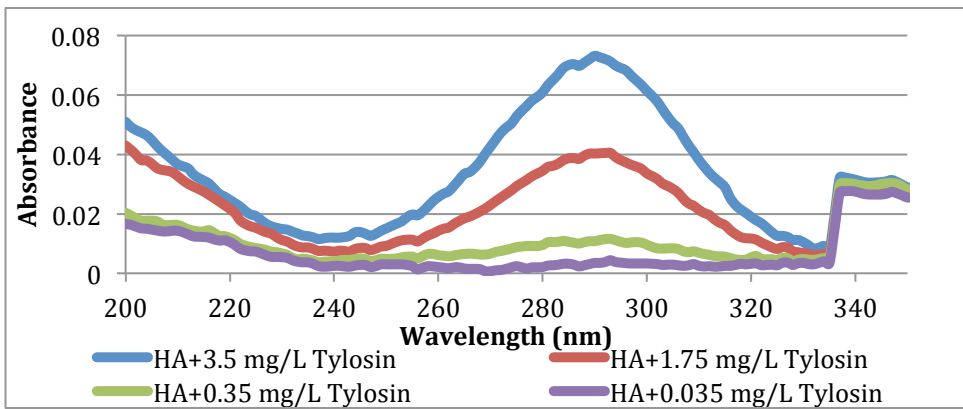


Figure 11. UV Spectra of Humic Acid (0.05 mg/L) with Varying Tylosin Tartrate Concentrations

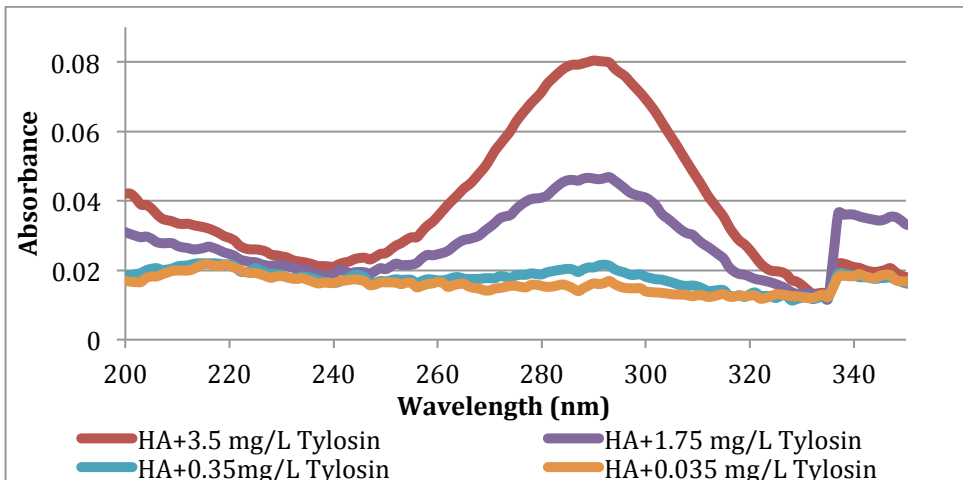


Figure 12. UV Spectra of Humic Acid (0.5 mg/L) with Varying Tylosin Tartrate Concentrations

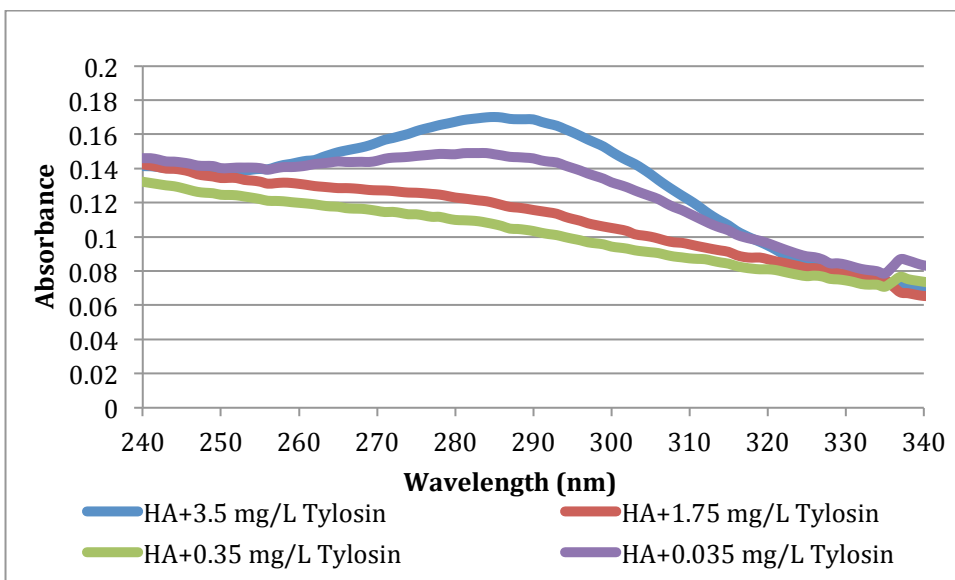


Figure 13. UV Spectra of Humic Acid (5 mg/L) with Varying Tylosin Tartrate Concentrations

The combination of 2.5 mg/L humic acid with varying tylosin tartrate concentrations at a pH of 7 (a pH of 7 was achieved by diluting the solutions in a buffer of potassium dihydrogen phosphate and sodium hydroxide) was also done as seen in Figure 14. A different range of concentrations was used for this experiment (between 0 and 20mg/L of tylosin), in which the development of the Gaussian shape curve at 290 nm with increasing tylosin tartrate concentration can be better appreciated.

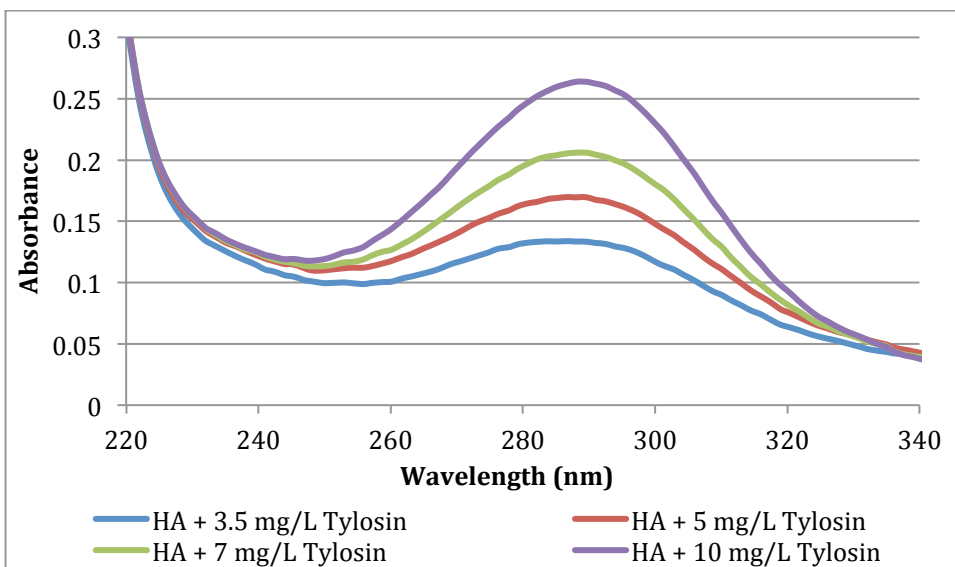


Figure 14. UV Spectra of Humic Acid (2.5 mg/L) with Varying Tylosin Tartrate Concentrations; pH = 7.0.

Finally UV spectra of humic acid (10 mg/L) with a tylosin tartrate concentration in the range of 0 – 70 mg/L were constructed as seen in Figure 15. Here the curves are smooth and their absorbances show a clear correlation with tylosin tartrate’s concentrations. In addition, a calibration curve was constructed from these spectra as shown in Figure 16.

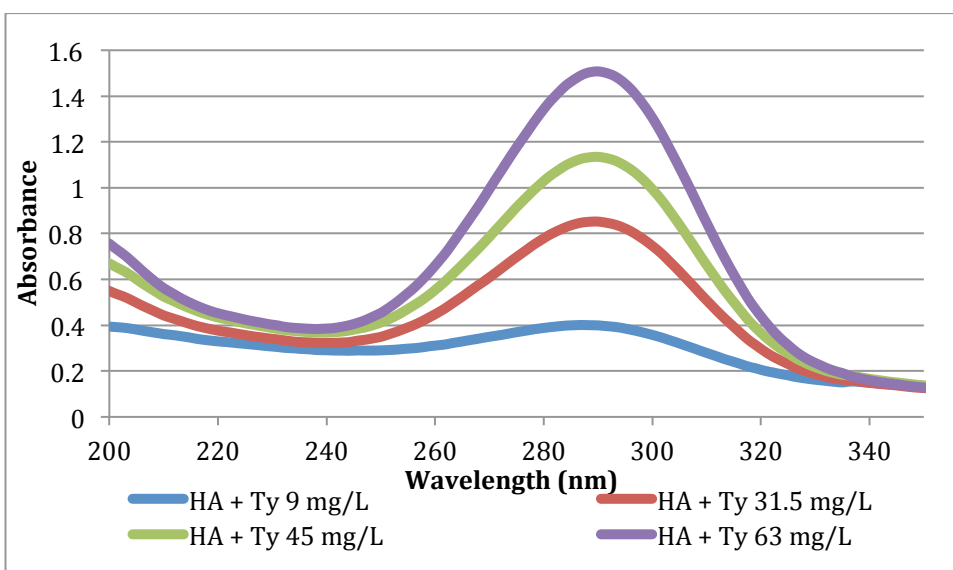


Figure 15. UV Spectra of Humic Acid (10 mg/L) with Varying Tylosin Tartrate Concentrations

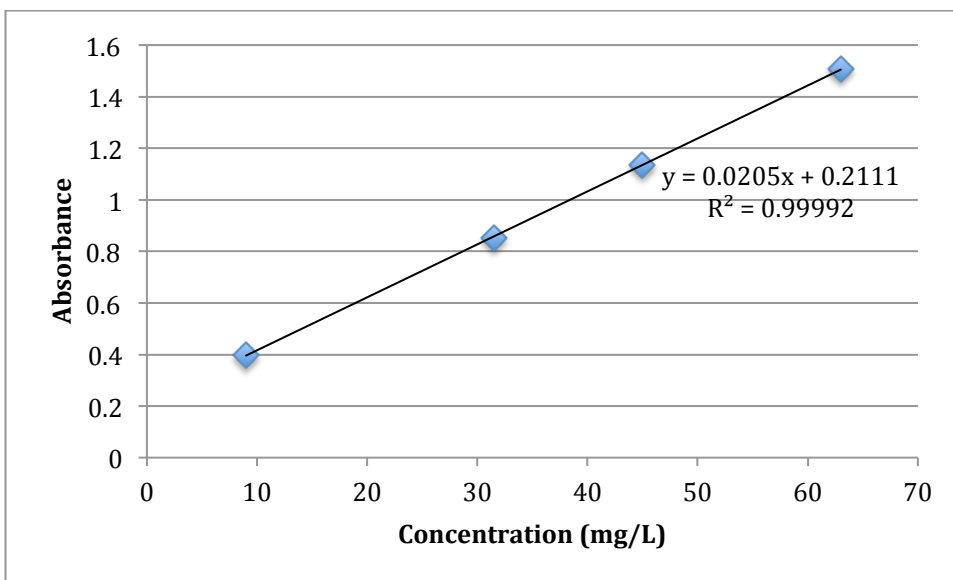


Figure 16. Tylosin Tartrate in the Presence of 10 mg/L Humic Acid - Calibration Curve for UV Spectroscopy (at 290 nm)

### The Effect of pH on UV Spectra

Initially titrations were carried out to obtain UV curves for a wide range of pH values from 2.5 to 10. However, the curves obtained for all solutions resemble each other too much, and this suggests that something in the titration procedure went wrong (Appendix B). One possibility for this is that the hydrochloric acid used for the titration could have reacted with the tylosin tartrate, especially at low pH values, considering its pKa of 3.8 (Khil'ko, Kovun, Fainerman & Rybachenko, 2010).

Therefore to obtain varying pH's, buffer solutions for a pH of 6, 7 and 8 were made as explained in the methodology. These pH values were chosen since these are the values typically found in river water samples. The graphs of UV as function of pH are the following for tylosin tartrate and humic acid respectively:

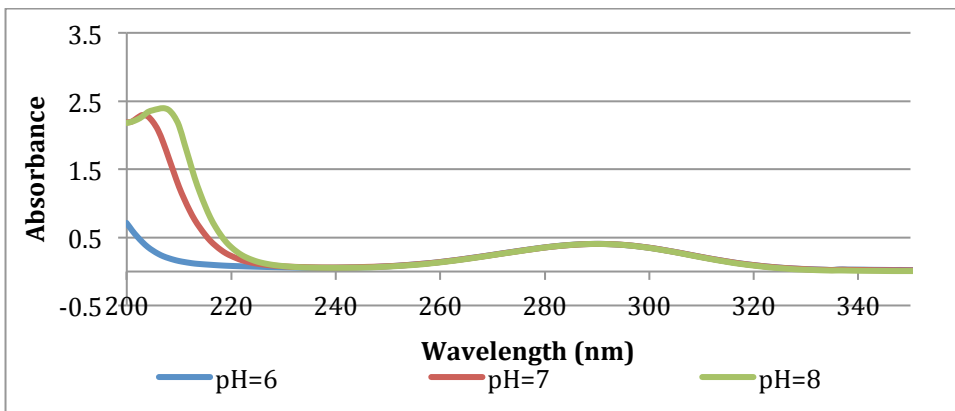


Figure 17. UV Spectra as a function of pH for 20 mg/L Tylosin Tartrate

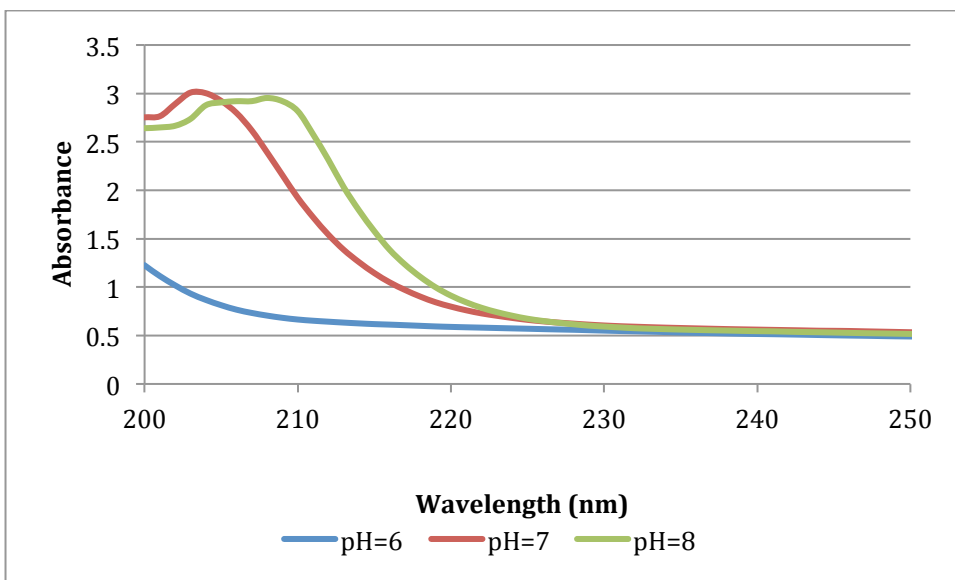


Figure 18. UV Spectra as a function of pH for 20 mg/L Humic Acid

From the UV graphs as a function of pH for a pH range of 6 to 8 it can be seen that both solutions present almost the same trend of increasing absorbance with increasing pH. The noteworthy difference between the curves for the three pH's is that the curves for a pH of 6 is the only one that does not reach a maximum absorbance within the wavelength range studied. The tylosin tartrate graphs once again present a small gaussian shape at a wavelength of about 290 nm.

## Fluorescence Spectra of Individual Solutions

All solutions were characterized by fluorescence spectroscopy. Solutions with various concentrations of tylosin tartrate (0.07 – 70 mg/L) and humic acid (0.1 – 80 mg/L) were analyzed with this technique and are shown in the following spectra.

The tylosin tartrate fluorescence seen in Figure 19 shows some characteristic traits for the compound. The most evident trait is the broad, Gaussian shaped peak at about 352 nm. Next there is a shallow, broad peak at around 280 nm. An interesting observation is that the spectra of all the concentrations tested lie almost perfectly on top of each other. They all reach a maximum fluorescence of about 50 for a wavelength of 352 nm.

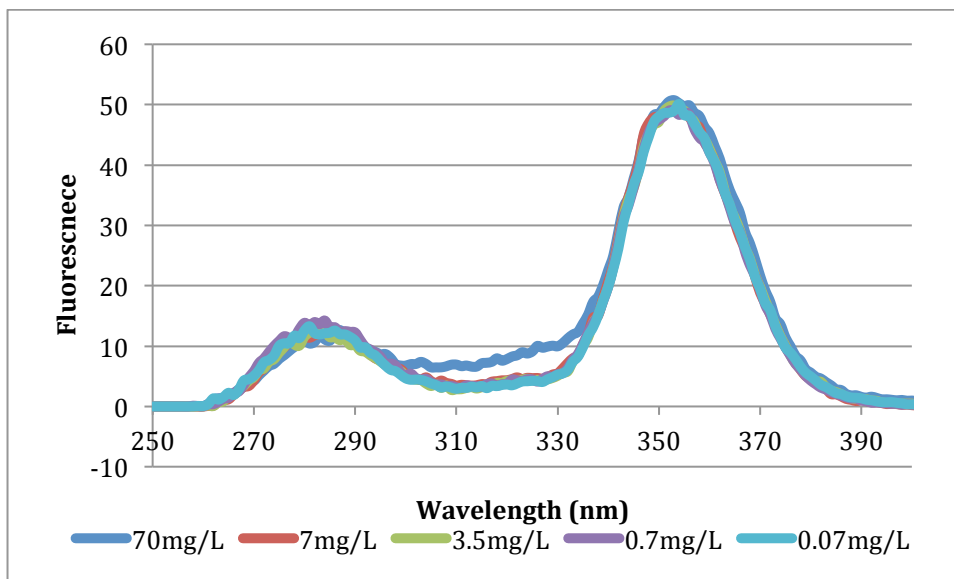


Figure 19. Fluorescence Spectra of Varying Tylosin Concentrations

From Figure 19 it can be seen that while fluorescence spectroscopy could be used to identify tylosin tartrate it cannot be used to quantify it since tylosin tartrate's fluorescence does not vary with concentration. In other words no useful correlation can be derived between concentration and fluorescence for tylosin

tartrate. However this was not the case in a previous work done on this subject [unpublished data; Wang, Adouani, Pons, Gao, Sardin & Simonnot, 2010].

The spectra for humic acid solutions are shown in Figure 20. The characteristic traits for this compound are a well-defined peak at 350 nm (but narrower than that of tylosin tartrate) and a broader peak at around 450 nm that only starts to show at a humic acid concentration of 5 mg/L. In these spectra, there is a visible difference of fluorescence emission among the different concentrations. As expected the fluorescence increases with increasing concentration of the solution. Calibration curves to show this trend were constructed and are shown in Figures 21 and 22.

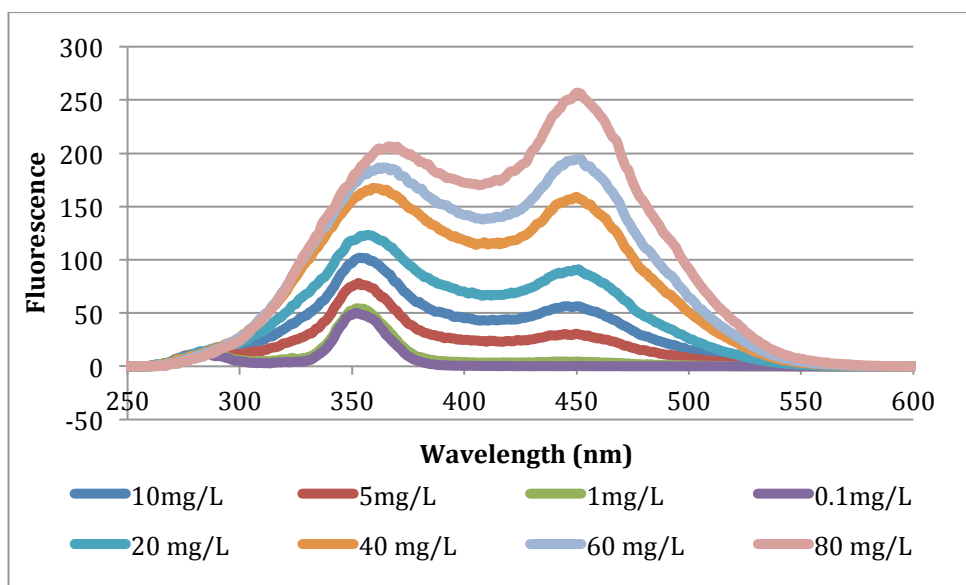


Figure 20. Fluorescence Spectra of Varying Humic Acid Concentrations

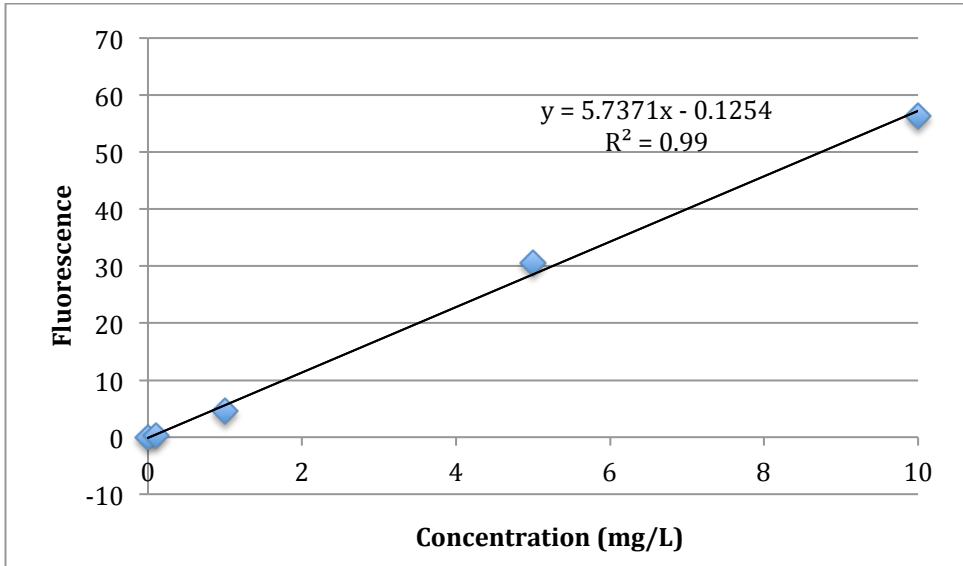


Figure 21. Humic Acid (0-10 mg/L) Calibration Curve for Fluorescence Spectroscopy (450 nm)

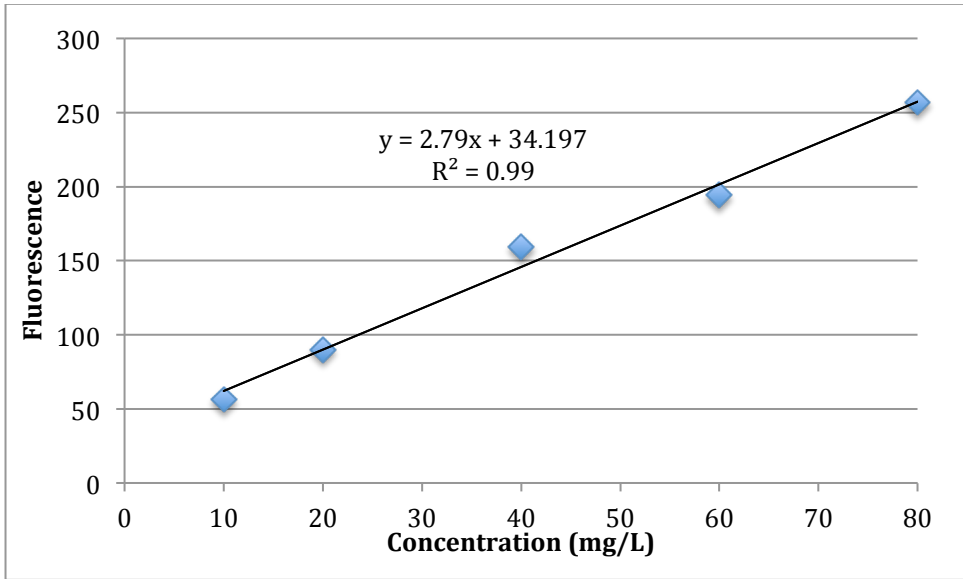


Figure 22. Humic Acid (10-80 mg/L) Calibration Curve for Fluorescence Spectroscopy (450 nm)

The reason Figure 22's plot does not pass through the origin is that at high sample concentrations, there are interferences that occur during the fluorescence run. If the data throughout a large range of concentrations were all put in the

same graph, one would probably see a curve instead of a line (Marie Noëlle Pons).

### Fluorescence of Combined Solutions

The combinations were made by keeping humic acid's concentration constant and varying that of tylosin tartrate's. Since tylosin tartrate's fluorescence has been shown to not vary with concentration (Figure 19) and humic acid is kept constant the fluorescence spectra for combined solutions are expected to lie on top of each other and indeed this is what is observed in Figures 23, 24 and in several others in Appendix B.

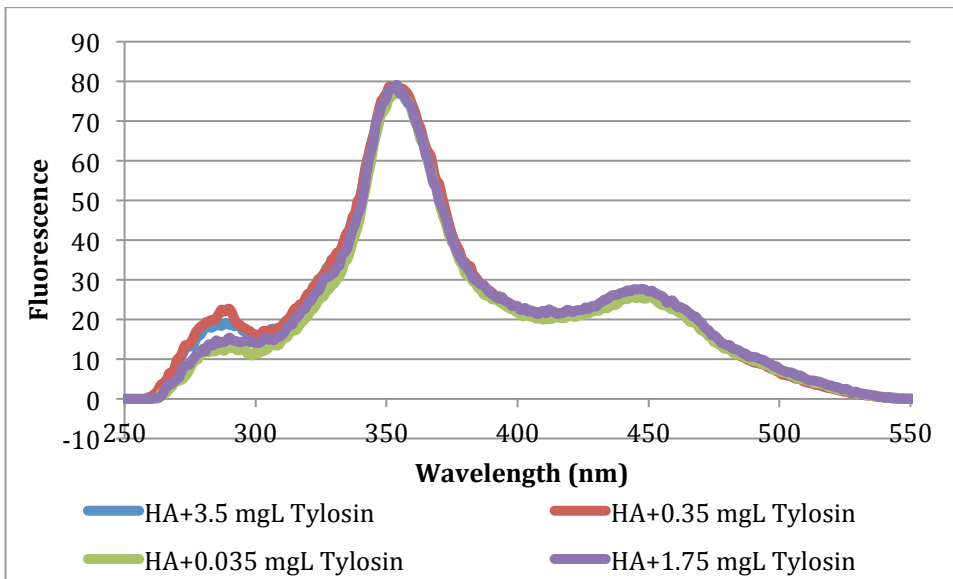


Figure 23. Fluorescence Spectra of Humic Acid (5 mg/L) with Varying Tylosin Concentrations

The fluorescence spectra shown in Figure 24 show the same trend from the previous figure but with higher tylosin tartrate concentrations (9 – 63 mg/L). Fluorescence spectra for other combinations of humic acid and tylosin tartrate are shown in Appendix B.

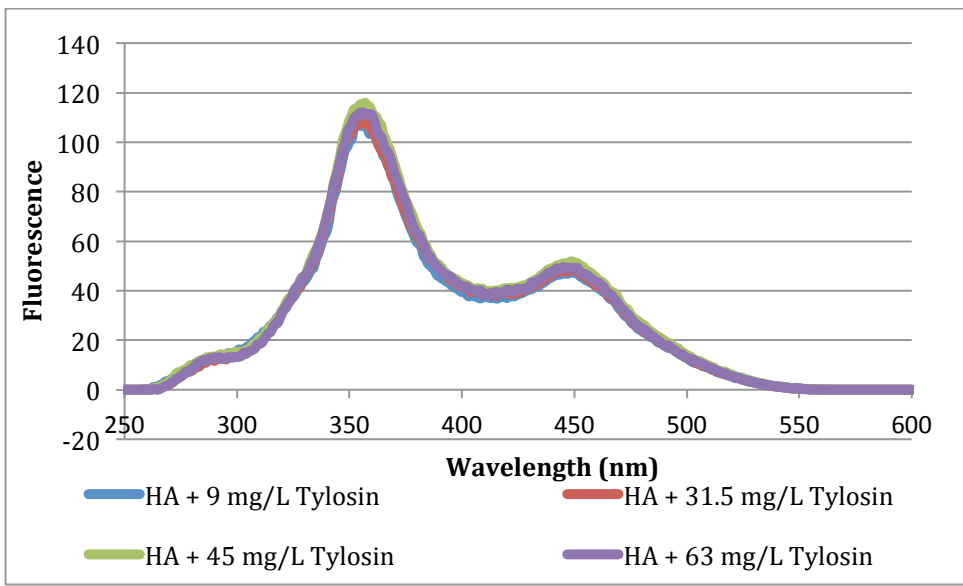


Figure 24. Fluorescence Spectra of Humic Acid (10 mg/L) with Varying Tylosin Concentrations

River Samples Characterization

River samples from the Madon and Moselle rivers were characterized via UV and fluorescence spectroscopy, ion chromatography and dissolved organic carbon test. Contaminants found in the Madon river are most probably of agricultural origin, while those of the Moselle river are due to the wood industries and pulp and paper mills (Marie Noëlle Pons).

From the UV spectra for the river water samples shown in Figure 25, it is evident that no tylosin tartrate was detected at 290 nm. Nonetheless, this compound may still be found in these rivers but in quantities lower than 0.7 mg/L, which was the concentration identified as the limit of detection by the UV machine from earlier sections (Figure 7). Another observation from the rivers' UV spectra is that this water probably contains nitrate and/or nitrite. This is inferred due to the slight maxima in the spectra, especially in Madon's spectrum, at around 200 nm.

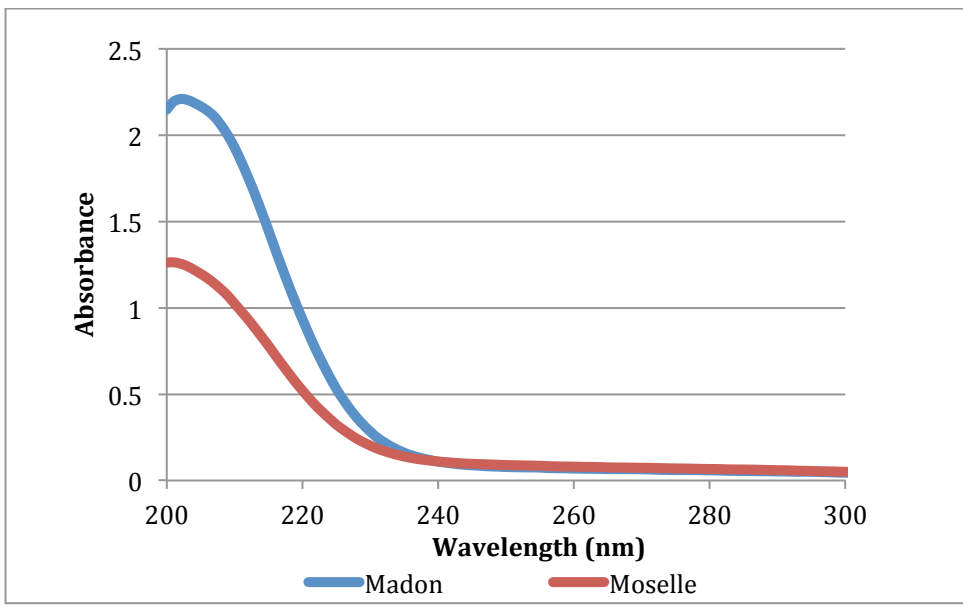


Figure 25. UV Spectra for Madon and Moselle Rivers

With regards to fluorescence, the rivers present clear peaks at 350 nm and small ones around 280 nm as seen in Figure 26. The ideal situation would have been to see a similar fluorescence between the river samples and that of humic acid; this would have shown that the humic acid being used in this study is a good model of natural organic matter. One similarity is that both the rivers and humic acid present peaks at 350 nm (Figures 26 and 20). Therefore this fluorescence from the river can be associated to some composition of natural organic matter. On the other hand, the rivers spectra do not fluoresce at 450 nm as humic acid does (Figure 20). Also, the rivers spectra show an additional wavelength of interest at 280 nm, not found in humic acid and which may be due to proteins from urine.

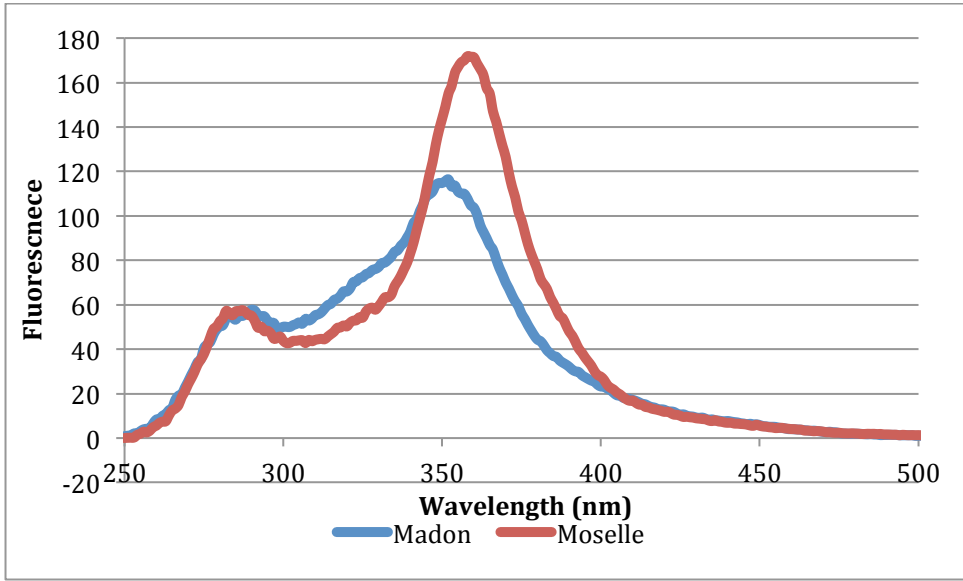


Figure 26. Fluorescence Spectra for Madon and Moselle Rivers

The different salts and organic carbon found in the Moselle and Madon rivers can be seen in Table 2. These values were obtained by the techniques of ion chromatography and dissolved organic carbon test respectively.

Table 2. Ion Chromatography and Dissolved Organic Carbon Test Results for Moselle and Madon Rivers

Technique	Component	Concentration (mg/L)	
		Moselle	Madon
Ion Chromatography	Ca	24.42	42.8
	Cl	2.52	4.63
	CO3	13.1	38.1
	K	n.a.	0.621
	Na	4.77	6.95
	NH4	n.a.	n.a.
	NO3	0.793	1.73
Dissolved Organic Carbon	SO4	5.52	29.9
	C	2.78	2.60

## Kinetic Experiments

### Analysis with Ultraviolet-Visible Spectroscopy

The UV spectra for humic acid's adsorption kinetics for a range of time of 0 to 72 hours and for initial concentrations of 10 mg/L and 80 mg/L are shown in Figures 27 and 28 respectively. The maximum time of contact used was 72 hours, which had been reported as enough time for adsorption equilibrium for these solutions [unpublished data; Wang, Adouani, Pons, Gao, Sardin & Simonnot, 2010].

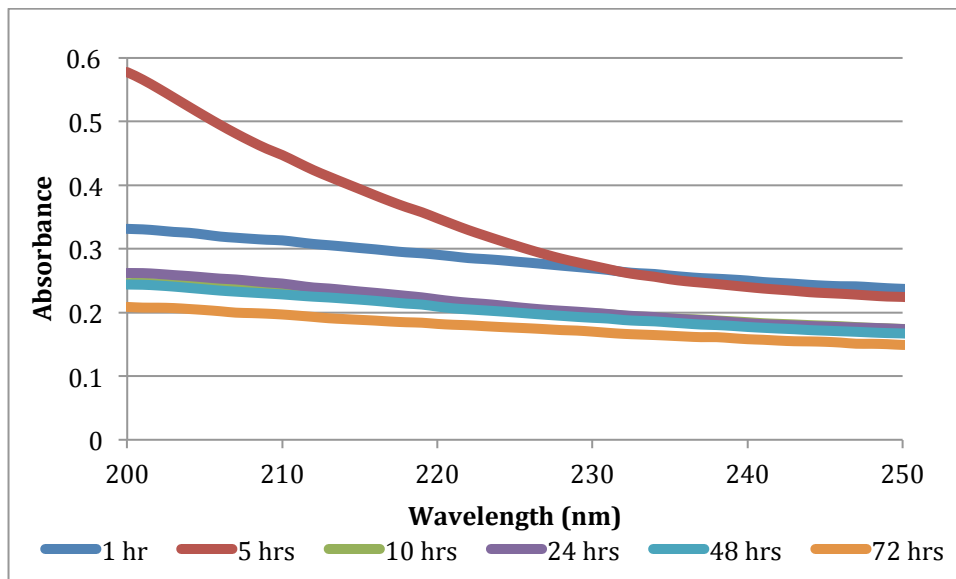


Figure 27. Humic Acid ( $C_0=10$  mg/L) UV-Derived Kinetics

Since the UV spectrum for humic acid at an initial concentration of 10 mg/L at 5 hours (Figure 27) presents a strange behavior between the wavelength range of 0-230 nm; a calibration based on a wavelength of 250 was used for this case. For consistency this wavelength of interest was chosen as well for humic acid at an initial concentration of 80 mg/L.

From the previous spectra the adsorbed quantity was plotted as a function of time, as shown in Figure 29, by using humic acid's calibration curve (Figure 10) and the following equation:

$$q_t = \frac{(C_0 - C_t)V}{W} \quad \text{(Equation 1)}$$

Where,

$q_t$  = Adsorbed quantity (mg/g)

$C_0$  = Initial concentration of target compound (mg/L)

$C_t$  = Concentration of target compound after time  $t$  (mg/L)

$V$  = Volume of solution (ml)

$W$  = Weight of adsorbent (mg)

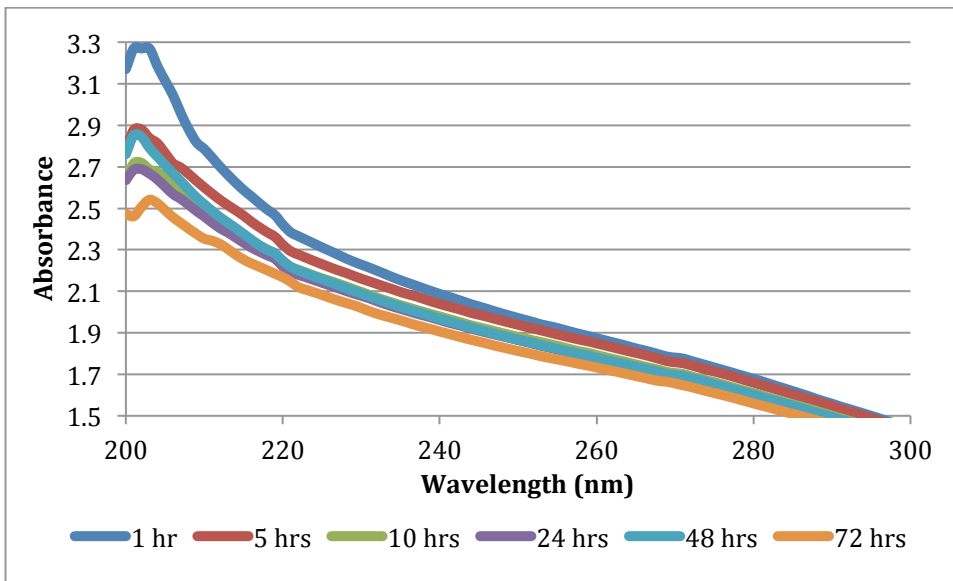


Figure 28. Humic Acid ( $C_0=80$  mg/L) UV-Derived Kinetics

In Figure 29 it is not clear when the humic acid solution in contact with GAC comes to adsorption equilibrium. From the start up to 10 hours the adsorption occurs at a fast pace, resulting in a steep increase of the adsorbed quantity

during that range of time. Between 24 hours and 48 the quantity adsorbed stays quite constant, however it then increases slightly at the 72-hour point.

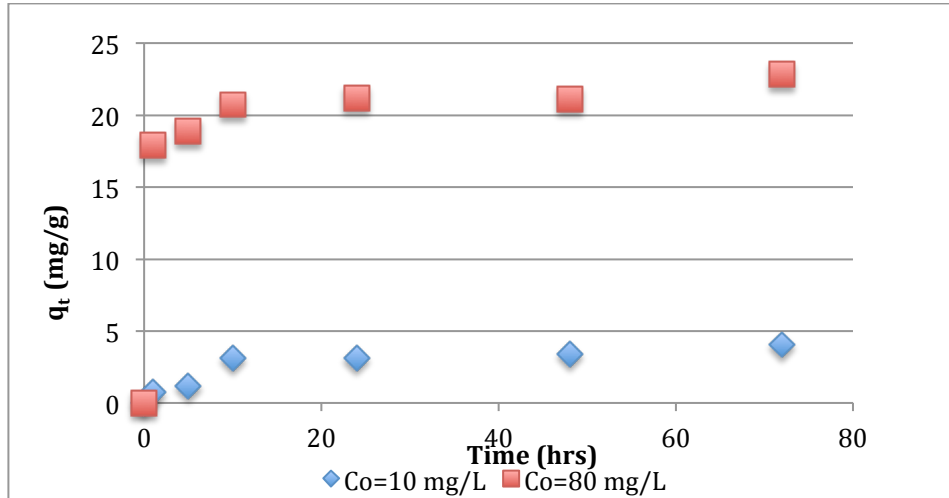


Figure 29. Humic Acid Adsorption Kinetics

In Figure 30, tylosin tartrate's adsorption kinetics is seen in the form of UV spectra. For the most part tylosin tartrate's adsorption seems to advance with time proportionally. However between the 24 and 48-hour gap the compound's concentration seems to stay stable. Also, the 72-hour curve seems to not follow the trend proportionally, since it shows less absorbance than the 96-hour one.

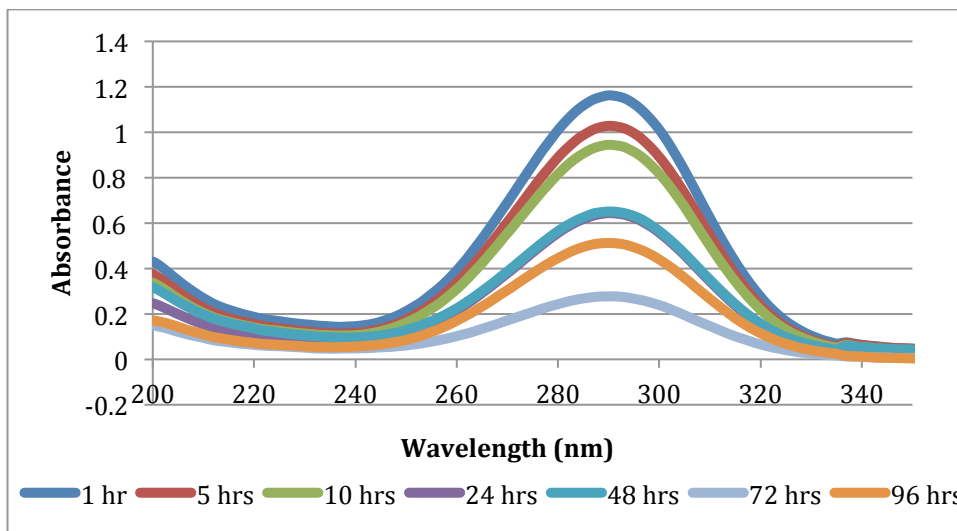


Figure 30. Tylosin ( $C_0=70$  mg/L) UV-Derived Kinetics

In Figure 31 the adsorption kinetics of a mixture of tylosin tartrate and humic acid at initial concentrations of 70 and 10 mg/L respectively is shown in the form of UV spectra. In this case, tylosin tartrate does follow a proportional trend of UV absorption with respect to its concentration.

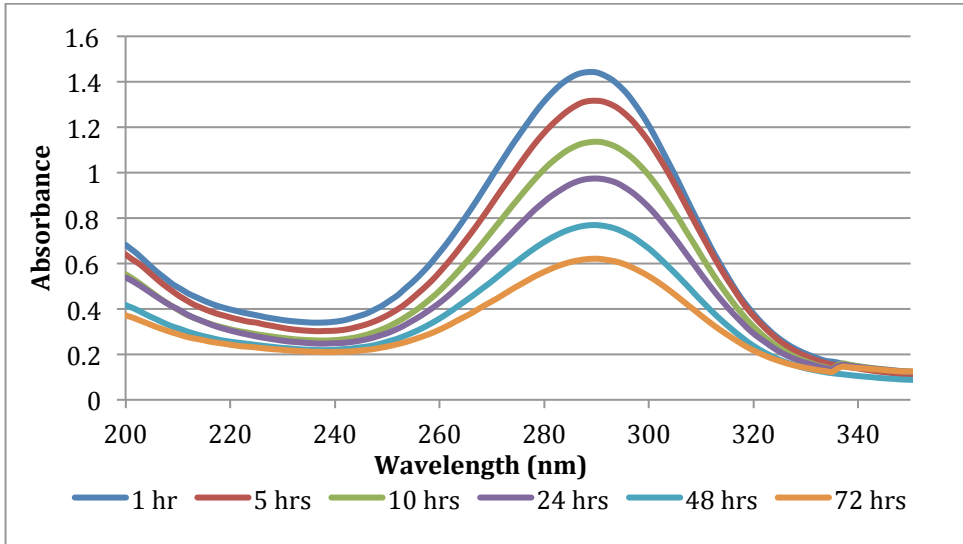


Figure 31. Tylosin ( $C_0=70$  mg/L) and Humic Acid ( $C_0=10$  mg/L) UV-Derived Kinetics

The calibration curves pertaining to this mixture and that of tylosin tartrate alone (Figures 16 and 8 respectively) were used together with Equation 1 to obtain the graph of adsorption kinetics shown in Figure 32. From this graph it seems that the 48-hour point for the kinetics of tylosin alone is an outlier. Additionally, as noted earlier the 72-hour point is most likely overestimating the adsorbed quantity. Taking into account these two possibilities it would be reasonable to infer that equilibrium adsorption for tylosin tartrate ( $C_0 = 70$  mg/L) happened between 72 and 96 hours. For tylosin tartrate in the presence of humic acid (blue points), the points do not seem to attain a plateau for the range of time studied; therefore it is not certain when this solution reaches equilibrium adsorption.

In spite of a few outliers, all of the data points in Figure 32 corresponding to the adsorbed quantity of tylosin tartrate alone are above those from tylosin tartrate in

the presence of humic acid. This shows that humic acid reduces tylosin tartrate adsorption onto GAC. The average reduction is 33%. Competition between tylosin and humic acid can be partly due to steric reasons; since humic acid is a macromolecule it can cause pore blockage on the GAC (Mardini & Legube, 2010; Carter, Weber & Olmstead, 1992; Kilduff, Karanfil & Weber, 1998; Newcombe, Morrison, Hepplewhite, Knappe, 2002).

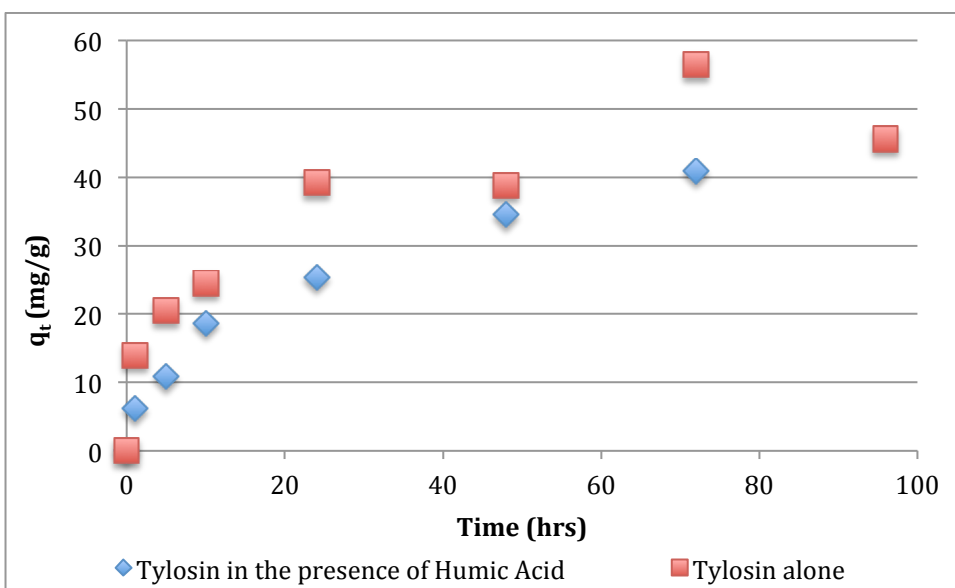


Figure 32. Tylosin Tartrate ( $C_0 = 70$  mg/L) Adsorption Kinetics with and without Humic Acid ( $C_0 = 10$  mg/L)

### Analysis with Fluorescence Spectroscopy

The kinetic experiments were also analyzed by fluorescence spectroscopy. As illustrated in Figure 19, tylosin tartrate is not quantifiable by fluorescence spectroscopy; therefore the difference in fluorescence with time seen in the spectra of Figures 33 and 35 is caused only by humic acid. Nonetheless, tylosin tartrate, together with humic acid, plays a role in defining the shape of the curve as can be seen from the small peaks at 280 nm in Figure 35 which are characteristic to tylosin.

In addition, in Figure 35 it is clear how after 72 hours of contact only about 5 mg/L or less of humic acid remains in solution since at that point there is no longer a visible fluorescence maximum at 450 nm, which is characteristic to humic acid at a concentration of 5 mg/L and onward as evidenced from Figure 20.

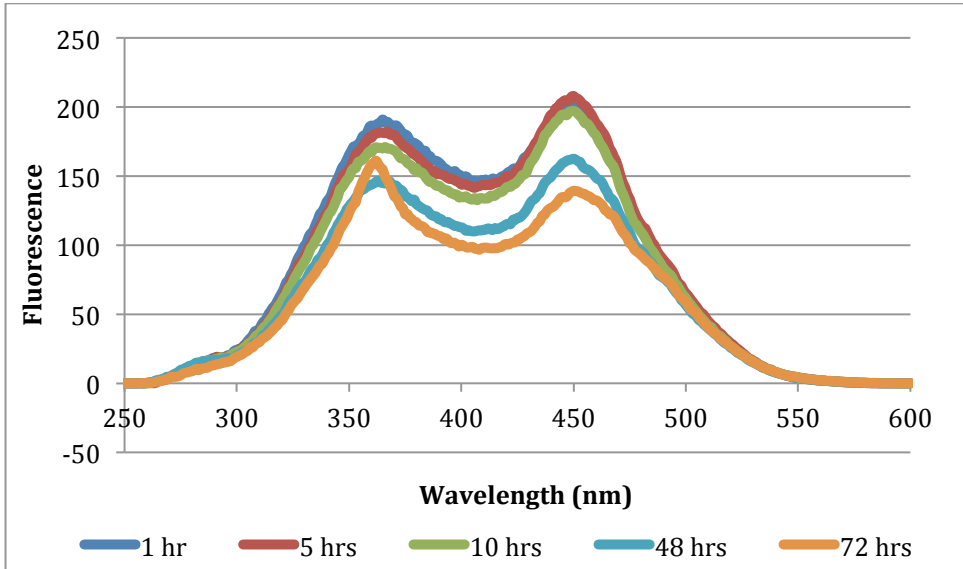


Figure 33. Humic Acid ( $C_0=80$  mg/L) Fluorescence-Derived Kinetics

In Figure 34 the adsorption kinetics of humic acid at an initial concentration of 80 mg/L is shown. From the plot, the point that corresponds to 1 hour seems to be an outlier. While from Figure 29 it was inferred that equilibrium adsorption occurred very closely after 72 hours, in the case of the adsorption kinetics derived from fluorescence this cannot be assumed. Also, note that the upper limit in Figure 29 (for  $C_0 = 80$  mg/L) is approximately 22 mg/g, while in Figure 34 it exceeds 40 mg/g.

Conversely, the mixture of humic acid ( $C_0=10$  mg/L) and tylosin tartrate ( $C_0=70$  mg/L) reach more of a plateau during the last set of hours of contact as seen in Figure 35.

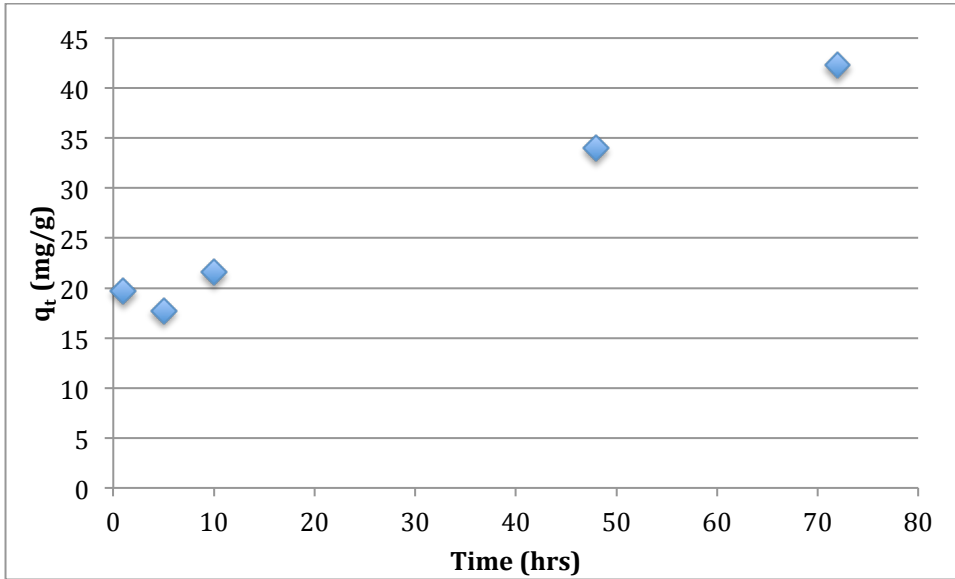


Figure 34. Humic Acid ( $C_0 = 80$  mg/L) Adsorption Kinetics

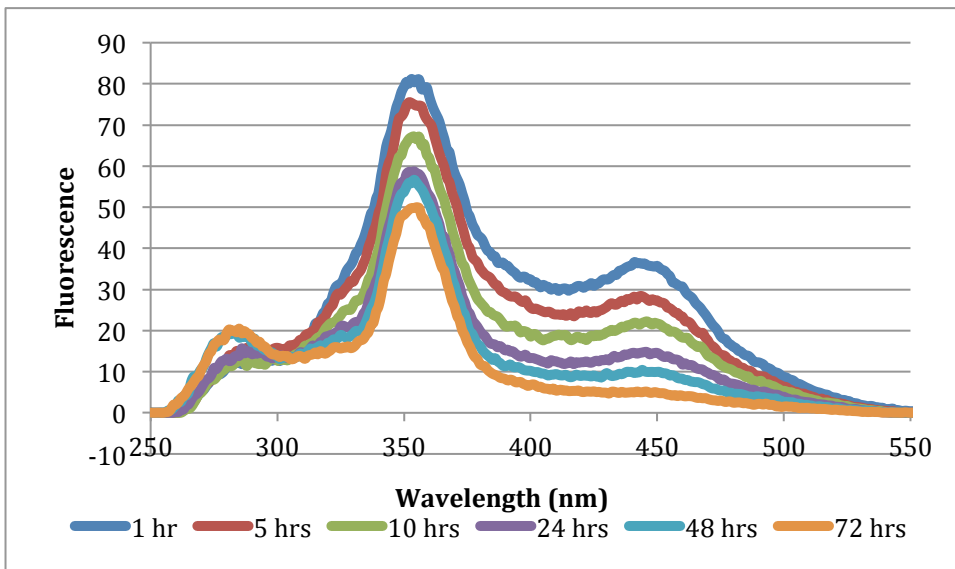


Figure 35. Tylosin Tartrate ( $C_0 = 70$  mg/L) and Humic Acid ( $C_0 = 10$  mg/L) Fluorescence-Derived Kinetics

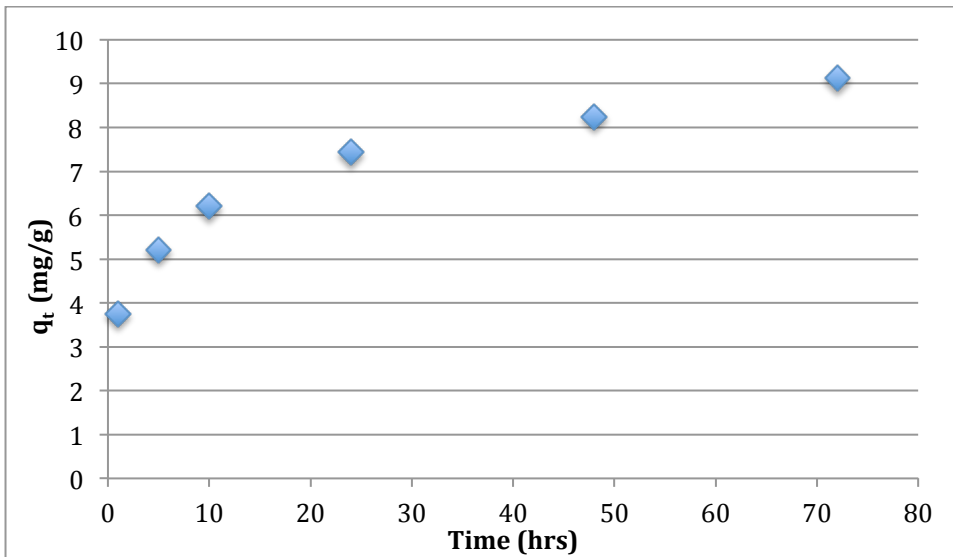


Figure 36. Tylosin Tartrate ( $C_0 = 70$  mg/L) and Humic Acid ( $C_0 = 10$  mg/L) Adsorption Kinetics (Note: this graph was done using a calibration curve for humic acid fluorescence only since tylosin tartrate does not have fluorescence.)

Even though 72 hours seemed very close to enough time for adsorption equilibrium of the solutions in the above discussion, the equilibrium experiments conducted afterwards were allowed 96 hours of contact time.

#### Analysis with Dissolved Organic Carbon (DOC) Test

The dissolved organic carbon (DOC) test measures the amount of non-purgeable organic carbon in solution. Since the organic materials in this study's adsorption experiments consisted of tylosin tartrate and humic acid, the DOC results should theoretically be correlated to the amount of these substances left in solution. Therefore the expected plot trend for this test is a curve similar to a decreasing exponential curve, since the organic material should decrease with time as adsorption takes place and then it should stabilize as adsorption equilibrium is reached.

The majority of the dissolved organic carbon results, shown in Figures 37 – 40, were not very clear. Many of the graphs seem to have the 48-hour point as an

outlier. When this point was unreasonably high, it was eliminated from the plot as shown in Figures 38 (for tylosin tartrate alone) and 40. Humic acid's remaining organic carbon seems quite stable with time, suggesting that it was not getting much adsorption. However, this is not the case in the kinetic plots for humic acid (Figure 29).

In disregard of the 48-hour point, the rest of the solutions' organic carbon, Figures 38-40, seems to decrease for the first 24 hours. Only tylosin tartrate's organic carbon (Figure 38) keeps decreasing until 72 hours. After the decreasing phase of these solutions some of them show an increase in dissolved organic carbon content. One possibility for this observed phenomenon is that impurities are detaching from the GAC.

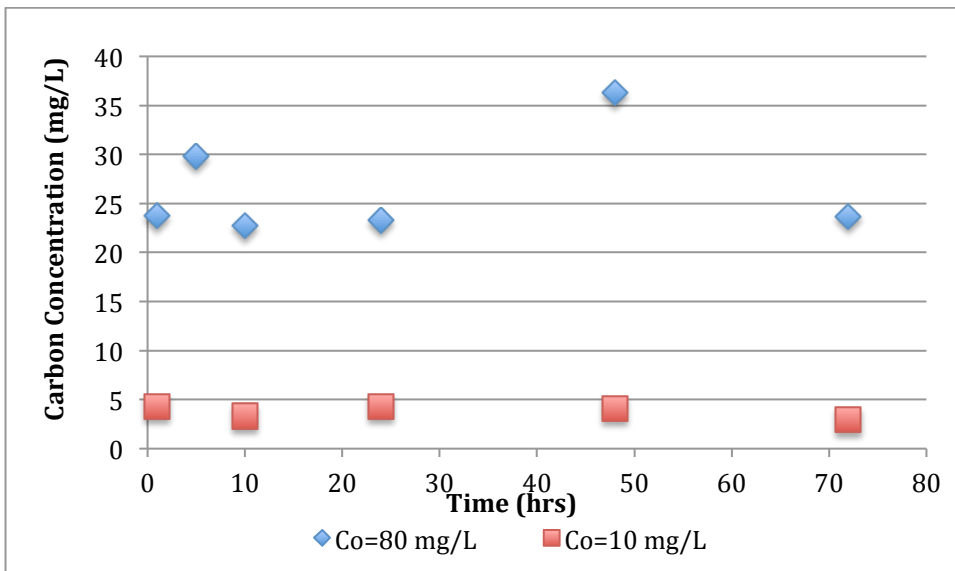


Figure 37. Humic Acid - Dissolved Organic Carbon (DOC) Test

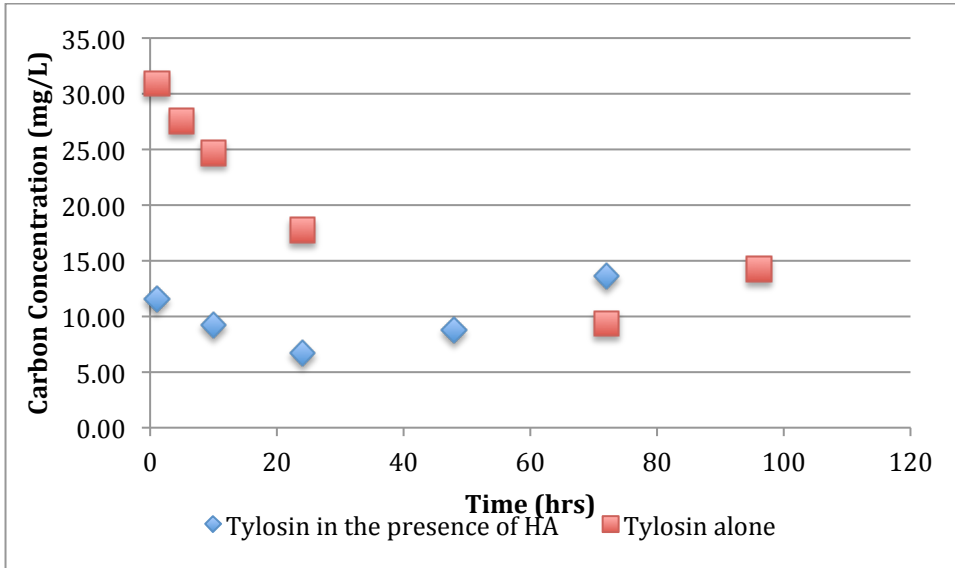


Figure 38. Tylosin Tartrate ( $C_0 = 70$  mg/L) with and without Humic Acid ( $C_0 = 10$  mg/L) - Dissolved Organic Carbon (DOC) Test

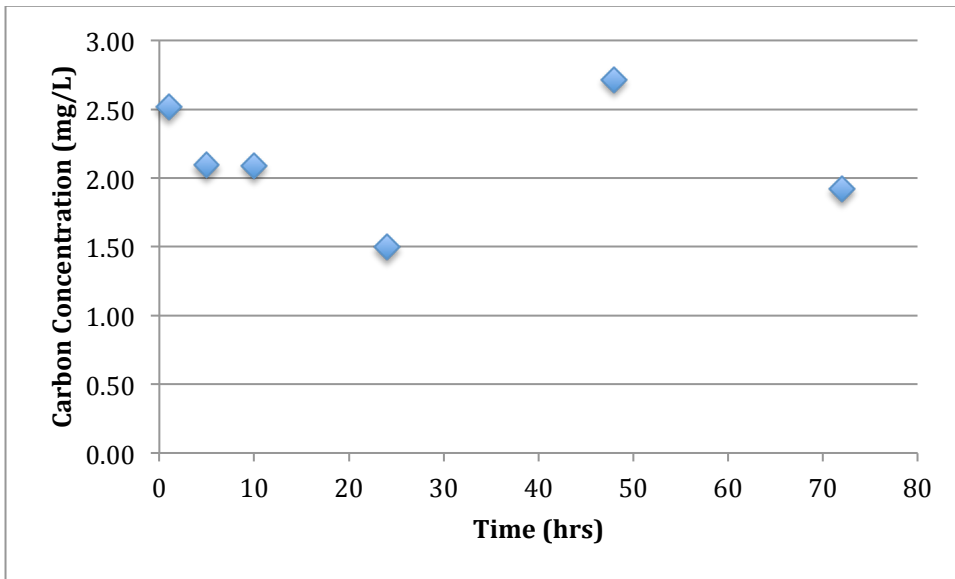


Figure 39. Madon River Water Sample – Dissolved Organic Carbon (DOC) Test

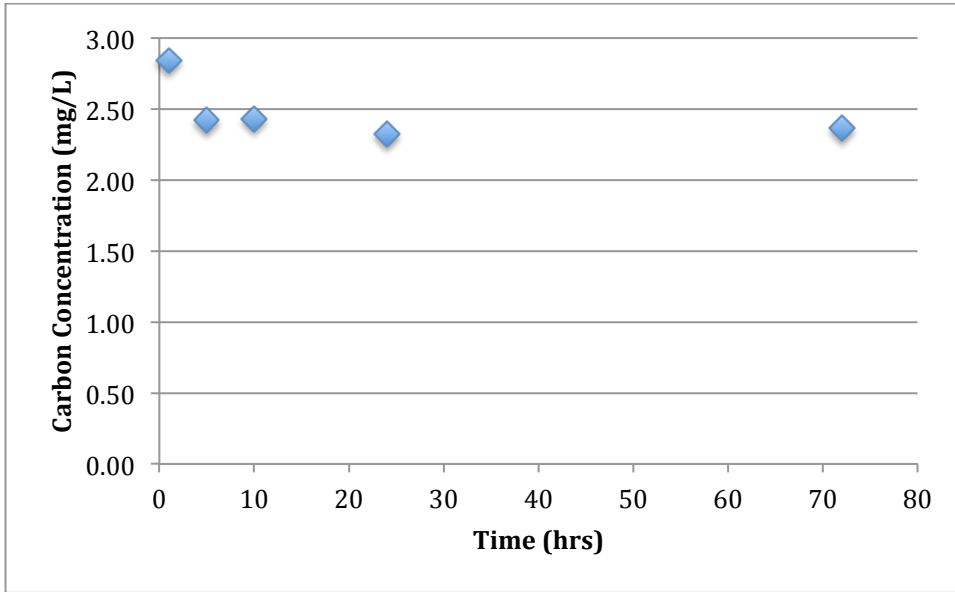


Figure 40. Moselle River Water Sample – Dissolved Organic Carbon (DOC) Test

## Equilibrium Experiments

### Isotherms from UV Analysis

The isotherms constructed based on the Freundlich and Langmuir models can be seen in Figures 41 and 42. The equations used for these models respectively are the following:

$$\ln q_e = \ln K_F + \left(\frac{1}{n}\right) \ln C_e \quad \text{Equation 2}$$

$$\frac{1}{q_e} = \frac{1}{Q_0 b C_e} + \frac{1}{Q_0} \quad \text{Equation 3}$$

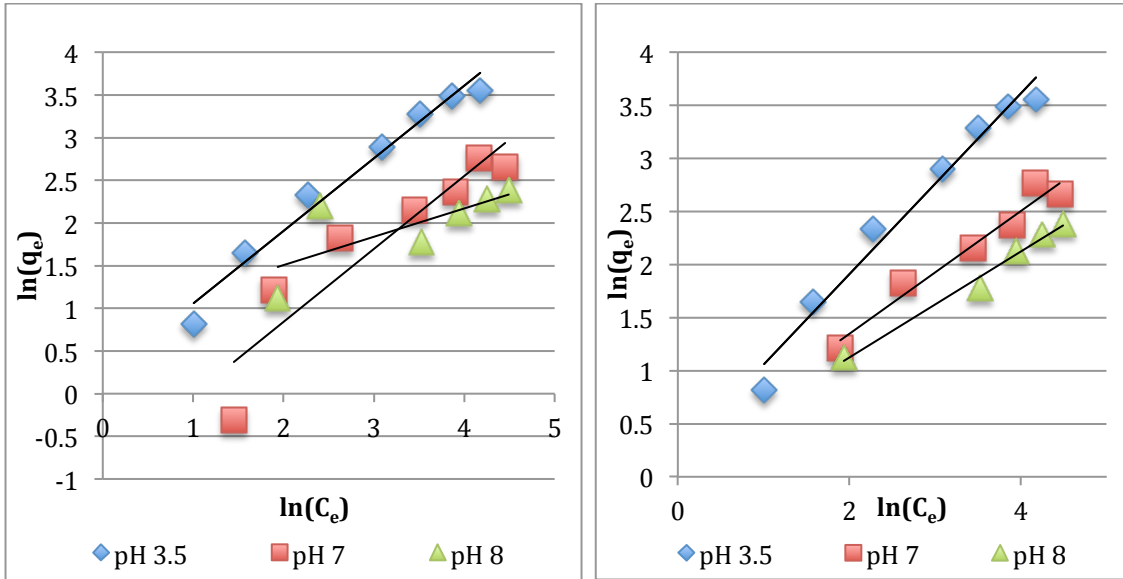


Figure 41. Freundlich Model for Humic Acid Equilibrium from UV Analysis at pH values of 3.5, 7 and 8. (The left graph includes all points, while in the right one, one outlier has been removed from the pH 7 and pH 8 series of points).

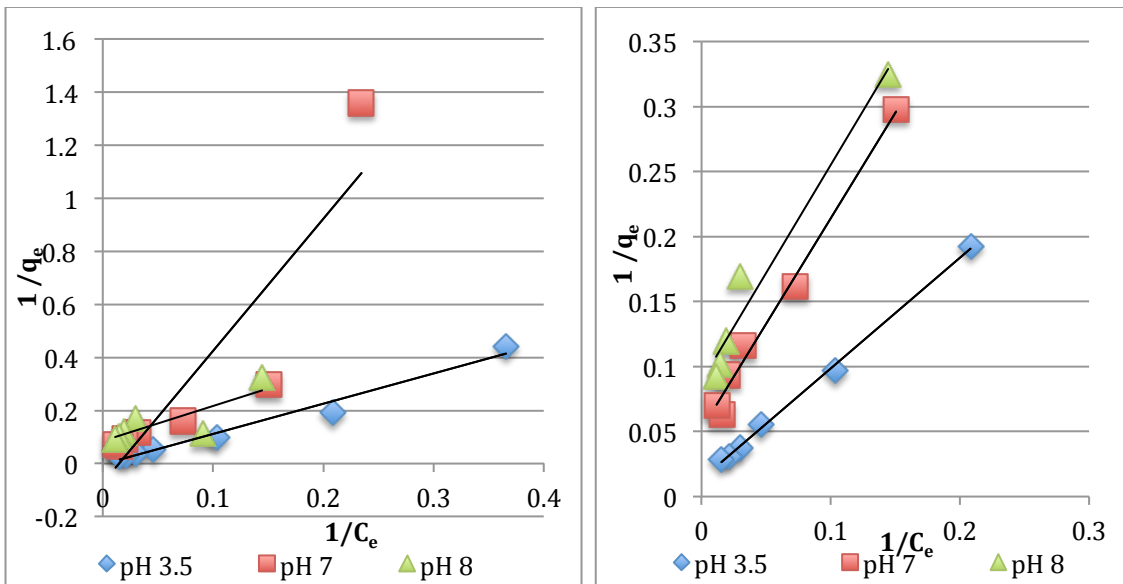


Figure 42. Langmuir Model for Humic Acid Equilibrium from UV Analysis at pH values of 3.5, 7 and 8. (The left graph includes all points, while in the right one, one outlier has been removed from each set of lines).

In Table 2 the different model parameters acquired from the equilibrium plots from Figures 41 and 42 are listed. It is noteworthy how the lowest pH (pH 3.5) shows the greatest maximum adsorbed quantity. This result was also obtained in

a previous study on this topic [unpublished data; Wang, Adouani, Pons, Gao, Sardin & Simonnot, 2010]. The distribution coefficients are comparable between both models.

Table 3. Model Parameters for Equilibrium Experiments of all pH Values – From UV Analysis

Model Parameters	$K_F$	$n$	$Q_0$ (mg/g)	b	$R^2$	
					Freundlich	Langmuir
pH 3.5	1.23	1.17	-417.7	-0.0210	0.974	0.976
Without outlier	1.23	1.17	<b>74.6</b>	0.0157	0.974	0.998
pH 7	0.419	1.17	-13.6	-0.0147	0.860	0.815
Without outlier	1.21	1.73	<b>19.3</b>	0.0319	0.962	0.987
pH 8	2.32	3.01	11.7	0.0647	0.541	0.655
Without outlier	1.13	2.00	<b>11.2</b>	0.0535	0.985	0.963

In Figure 43 the plateau values for the equilibrium adsorbed quantity ( $q_e$ ) should correspond to the maximum adsorbed quantity ( $Q_0$ ) derived from the Langmuir model equation (Table 3 – bold figures). For a pH of 3.5 the data points in Figure 43 do not seem to plateau therefore a comparison cannot be made between this two quantities. For a pH of 7 the maximum adsorbed quantity reached from the graph is about 16 mg/g while the one from the model is 19.3 mg/g. Finally for a pH of 8, these two quantities are about 10 and 11.2 mg/g respectively. The solid lines in Figure 43 were constructed with the model parameters from the Langmuir model derived from Figure 42 (the graph without a few outliers). They are in reasonable agreement with the raw data points obtained.

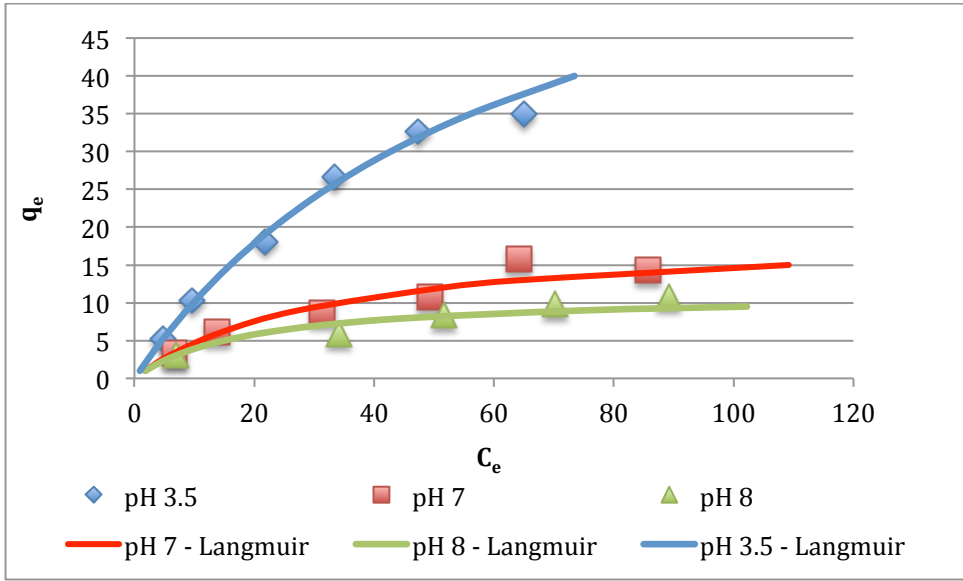


Figure 43. Isotherms for three different pH's (3.5, 7 and 8)

Isotherms from Fluorescence Analysis

Isotherms were also derived using fluorescence analysis. They show the same trend in terms of y-intercept level as those derived from ultraviolet analysis; the isotherm with a pH of 3.5 shows the highest y-intercept in the Freundlich models and the lowest in the Langmuir ones.

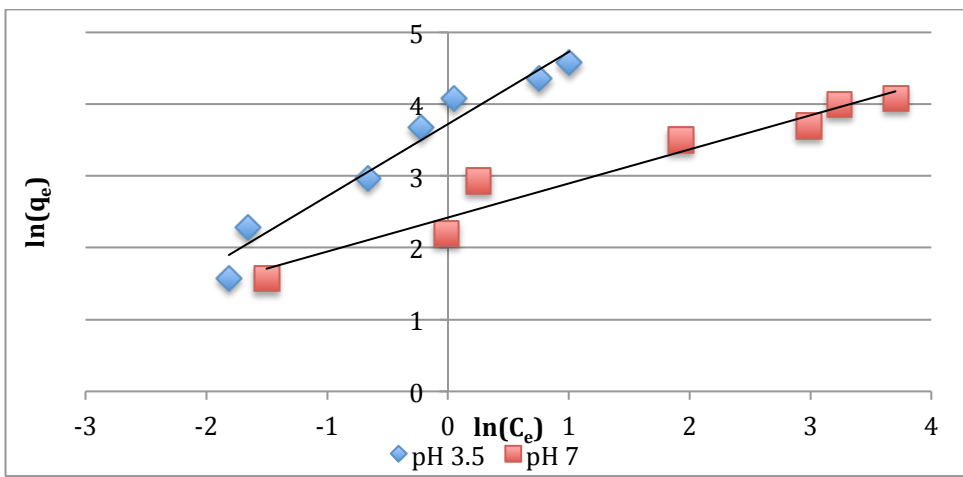


Figure 44. Freundlich Model for Humic Acid Equilibrium from Fluorescence Analysis at pH values of 3.5 and 7.

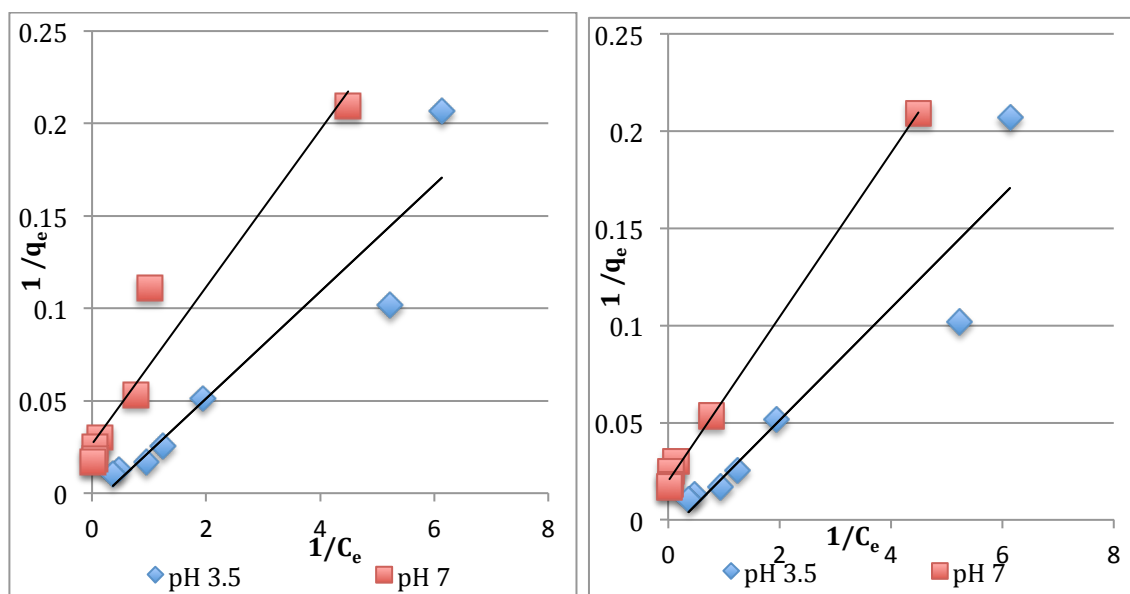


Figure 45. Langmuir Model for Humic Acid Equilibrium from Fluorescence Analysis at pH values of 3.5 and 7. (The left graph includes all points, while in the right one; one outlier has been removed for the pH 7 isotherm).

No outliers were removed from the fluorescence-derived isotherms, except for the Langmuir model at a pH 7. The isotherms for a pH of 8 were not shown since they showed a very poor fit to the models ( $R^2 < 0.1$  for both models).

Table 4. Model Parameters for Equilibrium Experiments of all pH Values – From Fluorescence Analysis

Model Parameters	$K_F$	$n$	$Q_0$ (mg/g)	b	$R^2$	
					Freundlich	Langmuir
pH 3.5	41.4	0.995	<b>152</b>	0.228	0.958	0.897
pH 7	11.3	2.01	37.6	0.626	0.949	0.933
Without outlier	-	-	<b>50.3</b>	0.472	-	0.998

Once again the lowest pH showed the highest value for maximum adsorbed quantity,  $Q_0$ , as shown in Table 4. In addition the isotherms derived from fluorescence seem to fit the Freundlich model better than they fit the Langmuir

one as reported in a previous study [unpublished data; Wang, Adouani, Pons, Gao, Sardin & Simonnot, 2010].

Once again, in Figures 46 and 47 the plateau values for the equilibrium adsorbed quantity ( $q_e$ ) should correspond to the maximum adsorbed quantity ( $Q_0$ ) derived from the Langmuir model equation (Table 4 – bold figures). For a pH of 3.5 the data points in Figure 46 do not seem to plateau nor do they align to the Langmuir model; thus the maximum adsorbed quantities, about 100 and 152 mg/L for the raw data and the model-derived parameter respectively, do not match. For a pH of 7 in Figure 47 the maximum adsorbed quantity reached from the graph is about 60 mg/g while the one from the model is 50.3 mg/g (Table 4). The Langmuir model in this case seems to align itself better to the raw data.

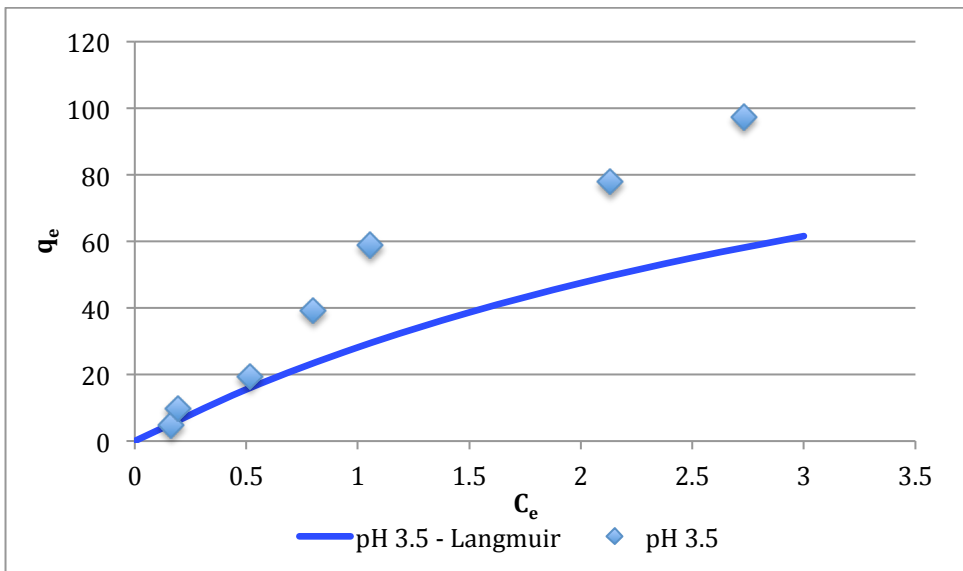


Figure 46. Isotherm for a pH of 3.5.

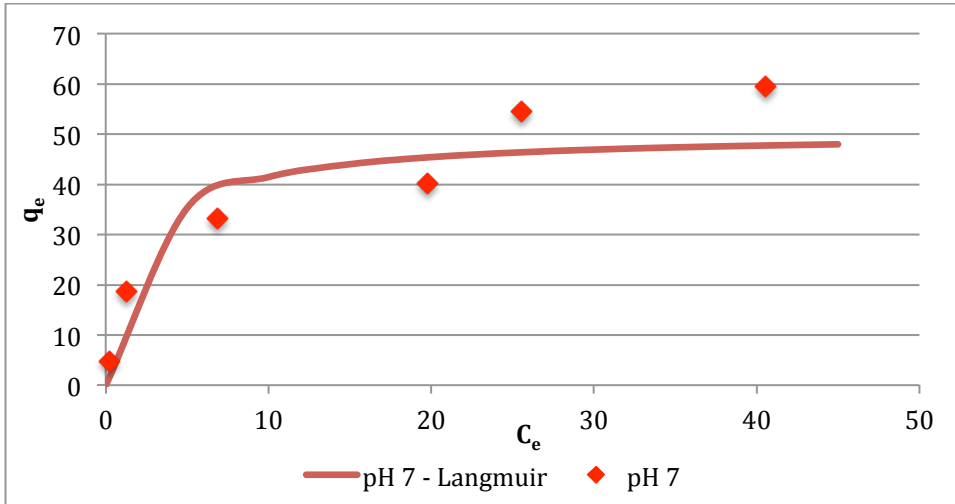


Figure 47. Isotherm for a pH of 7.

#### Analysis with Dissolved Organic Carbon (DOC) Test

In Figure 48 the dissolved organic carbon that remained in solution after 96 hours of contact is shown for the range of concentrations used. In the Figure it is seen that the solution with the lowest pH (pH 3.5) show the lowest concentration of remaining carbon in solution. Therefore, this confirms again that the most adsorption occurred at this pH as shown in Table 3 and 4.

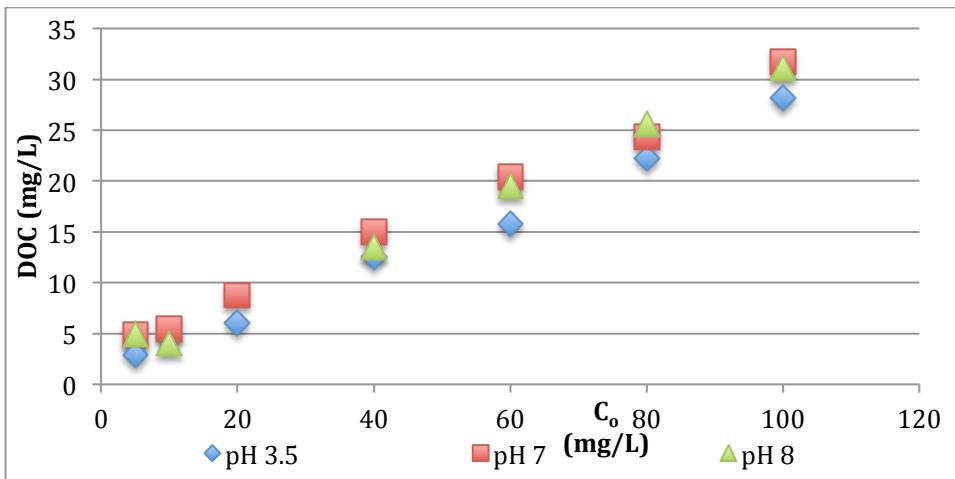


Figure 48. Humic Acid Equilibrium Experiments – Dissolved Organic Carbon (DOC) Test.

Depending on the degree of dissociation of functional groups such as  $\text{-COOH}$  and  $\text{-OH}$ , humic acid molecules can occur in different conformational states from flexible linear chains to random coils (Khil'ko, Kovun, Fainerman & Rybachenko, 2010). Reported  $\text{pK}_a$ 's for humic acid are 3.8 and 8.5 (Khil'ko, Kovun, Fainerman & Rybachenko, 2010), suggesting that at a pH of 3.5, humic acid may exist in a different structure, and according to the results of this study it may have a better affinity for the GAC surface under this condition. In addition, pH has an influence on adsorption because of its effect on humic acid's electrical charge and on the surface charge of the GAC.

## Conclusions

From Figure 32 it is concluded that humic acid reduces the adsorption capacity of tylosin onto GAC by an average of 33%. As noted in the background section, this can be due to pore blockage as well as site competition. In addition, from Figure 48 and Tables 3 and 4 it is concluded that the highest humic acid adsorption occurred at the lowest pH of 3.5. This may be due to structural and electrical charge changes of humic acid at different pH's due to the changes at specific pKa's; however this conclusion requires further study. Also further study is needed to evaluate at which pH does the highest adsorption occur for tylosin tartrate; this may help elucidate the optimal pH at which to run tylosin tartrate adsorption experiments involving natural surface waters.

As far as adsorption equilibrium time, it was unclear for both tylosin tartrate and humic acid. The most reasonable inference from the kinetic graphs is that tylosin tartrate adsorption equilibrium occurred at around 96 hours of contact, while humic acid's occurred at around 72 hours. This, however, should be confirmed by repeating these kinetic experiments, which was not possible in the present study due to time constraints.

The isotherms derived from fluorescence analysis fitted the Freundlich Model better than the Langmuir one, which agrees with previous data on this matter [unpublished data; Wang, Adouani, Pons, Gao, Sardin & Simonnot, 2010]. The Langmuir equation may not be an ideal model for this type of adsorption, physisorption, in which a multilayer can form. Further modeling should be done on this type of adsorption by using a BET (Brunauer, Emmett and Teller) Model, which can be applied to multilayer coverage as noted in the background section. Also, further studies should be done on deriving isotherms for solutions of tylosin in the presence of humic acid.

One possible source of error during the kinetic and equilibrium experiments was the granular activated carbon sticking to the sides of the glass bottles, which impeded it from being in solution. Therefore, this could have misleadingly reduced the adsorption of the target compound, leading to wrong conclusions from the results.

## References

- Abellan, M.N., Bayarri, B., Gimenez, J. & Costa, J. (2007). *Photocatalytic degradation of sulfamethoxazole in aqueous suspension of TiO<sub>2</sub>*. Applied Catalysis B: Environmental 74: 233-241, Elsevier.
- Abellan, M.N., Gimenez, J. & Esplugas, S. (2009). *Photocatalytic degradation of antibiotics: The case of sulfamethoxazole and trimethoprim*. Elsevier.
- Adamson, A.A. (1967). *Physical Chemistry of Surfaces*, John Wiley & Sons, NY.
- Alatrache, A., Laoufi, N. A., Pons, M. N., Van Deik, J. & Zahraa, O. (2010). *Tylosin abatement in water by photocatalytic process*. Water Science & Technology, IWA Publishing.
- Carbtrol Corporation (1992). *Granular Activated Carbon For Water & Wastewater Treatment*. Retrieved from: <http://www.carbtrol.com/water&waste.pdf>
- Blackwell P.A., Kay P., Ashauer R. & Boxall A.B.A. (2009). *Effects of industrial conditions on the leaching behavior of veterinary antibiotics in soils*. Chemosphere, 75: 13-19.
- Bruckner, M.Z. (2009). *Bio-geochemical Methods: Ion Chromatography*. Montana State University. Retrieved from: [http://serc.carleton.edu/microbelife/research\\_methods/biogeochemical/ic.html](http://serc.carleton.edu/microbelife/research_methods/biogeochemical/ic.html)
- Carter, M.C., Weber, Jr. W.J. & Olmstead, K.P. (1992). *Effects of background dissolved organic matter on TGE adsorption by GAC*. Journal of American Works Association, 84(8), 81-91.
- Dionex Corporation (1992). *Determination of Anions in Acid Rain by Ion Chromatography*. Retrieved from: [http://www.dionex.com/en-us/webdocs/4124-AN31\\_V15.pdf](http://www.dionex.com/en-us/webdocs/4124-AN31_V15.pdf)
- Drenthe College. *Standardbase Techniques: High Performance Liquid Chromatography*. Retrieved from: <http://www.standardbase.hu/tech/HPLC.pdf>
- Harris D.C. (2007). *Quantitative Chemical Analysis – Seventh Edition*. New York: New York, W.H Freeman and Company.
- Hirsch R., Ternes T., Haberer K. & Kratz K.L. (1999). *Occurrence of antibiotics in the aquatic environment*. Sci. Total Environ. 225: 109-118.

Jones, O., Voulvoulis, N. & Lester, J. (2003). *Potential impact of pharmaceuticals on environmental health*. Bull World Health Organ, 81(10): 768-769.

Jones, O., Lester, J. & Voulvoulis, N. (2005). *Pharmaceuticals: a threat to drinking waters?* Trends in Biotechnology 24(4).

Khil'ko S.L., Kovtun A. I., Fainerman V.B. & Rybachenko, V.I. (2010). *Adsorption and Rheological Characteristics of Humic Acid Salts at Liquid-Gas Interfaces*. Colloid Journal, 72(6): 857-865.

Kilduff, J.E., Karanfil, T. & Weber, W.J. (1998). *Competitive effects of nondisplaceable organic compounds on trichloroethylene uptake by activated carbon*. II. Model verification and applicability to natural organic matter. Journal of Colloid and Interface Science, 205(2), 280-289.

Kolpin, D., Furlong, E., Meyer, M., Thurman, E. M., Zaugg, S., Barber, L. & Buxton, H. (2002). *Pharmaceuticals, Hormones and other Organic Wastewater Contaminants in U.S Streams, 1999-2000: A National Reconnaissance*. Environmental Science & Technology, 36(6): 1202-1211.

Kümmerer K. (2001). *Drugs in the environment: emission of drugs, diagnostic aids and disinfectants into wastewater hospitals in relation to other sources – a review*. Chemosphere. 45: 957-969.

Giraldo, A. L., Peñuela, G. A., Torres-Palma, R. A., Pino, N. J., Palominos, R. A. & Mansilla, H. D. (2010). *Degradation of the antibiotic oxolinic acid by photocatalysis with TiO<sub>2</sub> in suspension*. Elsevier.

Government of Saskatchewan (2009). *Dissolved Organic Carbon (DOC): for private water and health regulated public water supplies*. Factsheet. Retrieved from: <http://www.saskh2o.ca/PDF-WaterCommittee/DissolvedOrganicCarbon.pdf>

Library4science.com (2008). *Ion Chromatography*. Retrieved from: <http://www.chromatography-online.org/topics/ion/chromatography.html>

Loke M.L., Tjornelund J. & Halling-Sorensen B. (2002). *Determination of the distribution coefficient (log K<sub>d</sub>) of oxytetracycline, tylosin A, olaquinox and metronidazole in manure*. Chemosphere, 48: 351-361.

Mardini, F.A. & Legube, B. (2010). *Effect of the adsorbate (Bromacil) equilibrium concentration in water on its adsorption on powdered activated carbon. Part 3: Competition with natural organic matter*. Journal of Hazardous Materials 182, 10-17.

- McQuarrie, D.A. & Simon, J.D. (1998). *Physical Chemistry: a molecular approach*. University Science Books, Sausalito, California.
- Newcombe, G., Morrison, J., Hepplewhite, C. & Knappe, D.R.R. (2002). *Simultaneous adsorption of MIB and onto activated carbon – II. Competitive effects*. *Carbon* 40(12), 2147-2156.
- Ohio State University. *Wastewater Treatment Principles and Regulations*. Ohio State University Extension Fact Sheet. Retrieved from file:///Users/alejandravargas/Documents/WPI/Senior%20Year%20MQP/Wastewater%20Treatment%20Principles%20and%20Regulations,%20AEX-768-96.html
- Pauli, W., Jax, K. & Berger, S., (2001). *Protozoa in Wastewater Treatment Function and Importance*. The Handbook of Environmental Chemistry Vol. 2 Part K Biodegradation and Persistence, Springer-Verlag Berlin Heidelberg.
- PerkinElmer, INC (2006). *An Introduction to Fluorescence Spectroscopy*. PerkinElmer Life and Analytical Sciences. Retrieved from: <http://www.bioch.ox.ac.uk/aspsite/services/equipmentbooking/biophysics/introfluor.pdf>
- Qiang, Z. & Adams, C. (2004). *Potentiometric determination of acid dissociation constants (pka) for human and veterinary antibiotics*, *Water Res.*, 38: 2874-2890.
- Ramalho, R. S. (1977). *Introduction to Wastewater Treatment Processes*. Academic Press, New York, San Francisco, London.
- Richardson M.L. & Bowron J.M. (1985). *The fate of pharmaceutical chemicals in the aquatic environment*. *J. Pharma. Pharmacol.* 37: 1-12.
- Schulman, L., Sargent, E., Naumann, B., Faria, E., Dolan, D. & Wargo, J. (2002). *A human health risk assessment of pharmaceuticals in the aquatic environment*. *Human and Ecological Risk Assessment: An International Journal*, 8(4): 657-680.
- Schwartz, T., Kohnen, W., Jansen, B. & Obst, U. (2003). *Detection of antibiotic resistant bacteria and their resistance genes in wastewater, surface water, and drinking water biofilms*. *Microbiology Ecology*, 43(3).
- Sheffield Hallam University. *UV-VIS Absorption Spectroscopy: Theoretical Principles*. Retrieved from: <http://teaching.shu.ac.uk/hwb/chemistry/tutorials/molspec/uvvisab1.htm>
- Thiele-Bruhn, S. (2003). *Pharmaceutical antibiotic compounds in soils – a review*. *Journal of Plant Nutrition and Soil Science*, 166(2): 145-167.

Tissue, B.M. (2000). *Ion Chromatography*. Retrieved from:  
<http://www.files.chem.vt.edu/chem-ed/sep/lc/ion-chro.html>

Tissue, B.M. (2000). *Ultraviolet and Visible Absorption Spectroscopy (UV-Vis)*. Retrieved from: <http://www.files.chem.vt.edu/chem-ed/spec/uv-vis/uv-vis.html>

Trombe, F. (1971). *Detection and Determination of Trace Elements: Absorption Spectrophotometry, Emission Spectroscopy, Polarography*. Paris, Keter Press.

University of Johannesburg. *High Performance Liquid Chromatography*. Retrieved from:  
<http://152.106.6.200:8080/dspace/bitstream/10210/379/1/11Ch3HPLC.pdf>.

University of Waterloo. *Water Treatment*. Retrieved from:  
<http://www.science.uwaterloo.ca/~cchieh/cact/applychem/watertreatment.html>

Wake Forest University. *UV-VIS Spectroscopy*. Retrieved from:  
<http://www.wfu.edu/chem/courses/organic/UV/index.html>

Wang L., Adouani N., Pons M.N, Gao N.Y, Sardin M. & Simonnot M.O. (2010-unpublished). *Tylosin adsorption onto granular activated carbon*.

Waters (2010). *HPLC-High Performance Liquid Chromatography*. Waters: The Science of What's Possible. Retrieved from:  
[http://www.waters.com/waters/nav.htm?locale=en\\_US&cid=10048919](http://www.waters.com/waters/nav.htm?locale=en_US&cid=10048919)

Water Environment Federation, (2009). *Following the Flow: An Inside Look at Wastewater Treatment*. Water Environment Federation. Retrieved from  
[www.wef.org/publicinformation/default.aspx](http://www.wef.org/publicinformation/default.aspx).

Webb, S., Ternes, T., Gibert, M. & Olejniczak, K. (2003). *Indirect human exposure to pharmaceuticals via drinking water*. *Toxicology Letters*, 143(3): 157-167

WorldIQ.com (2010). *HPLC-Definition*. Retrieved from:  
<file://localhost/Users/alejandravargas/Documents/WPI/Senior%20Year%20MQP/literature/HPLC/HPLC%20-%20Definition.html>

Yang S. & Carlson K.H. (2004). *Solid-phase extraction-high-performance liquid chromatography-ion trap mass spectrometry for analysis of trace concentrations of macrolide antibiotics in natural and waste water matrices*. *J. Chromatogr. A*. 1038: 141-155.

Zhao, J., Wan, P., Xiang, J., Tong, T., Dong, L., Gao, Z., Shen, X & Tong, H.

(2011). *Synthesis of highly ordered macro-mesoporous anatase TiO<sub>2</sub> film with high photocatalytic activity*. Microporous and Mesoporous Materials, Elsevier.

## Appendix

### Appendix A. Step by Step Procedures

#### High Performance Liquid Chromatography

To run a separation and obtain a chromatogram:

1. Press the 'power' buttons on the top two boxes in the HPLC machine.
2. When the green light has turned on in the machine, open the two black knobs by turning them counterclockwise.
3. Then press 'purge' for on both boxes. (The purge is normally done only with Methanol. However, if you are having problems with bubbles in the cables, then you can do the purge after having put each cable in its appropriate solvent.)
4. Put one plastic cable into each solvent (normally one in water with formic acid and one in methanol).
5. Close black knobs. Once the knobs are closed the end of the cables submerged in the solvents should not come into contact with air, otherwise this will cause huge bubbles in the system.
6. Press the 'pump' buttons in both boxes. Wait until pressure stabilizes to continue. The pressure should reach a level of approximately 150 bar.
7. Press 'power' on the detector (the bottom-most box)
8. Once the readings on the detector are stable press 'zero' on it.
9. Start the HPLC software called 'LC Solution'.
10. Press on #1 to start an analysis.
11. Once the program says 'Ready' in green letters, one can inject about 20 microliters of the sample. (If more than 20 microliters is injected the difference will be discarded automatically by the machine into a vial that should be emptied every so often. Make sure that the metal knob is turned to lead when you inject the sample).

12. Press the green button on the program called 'single start' to start the separation.
13. Save run under you name, sample name and concentration and date.
14. Click on 'ok'.
15. When a window pops up asking to star the run, turn the metal knob from 'load' to 'inject', then your separation will start.
16. To view and/or manipulate the chromatogram afterwards click on 'postrun' in the main program window.
17. To shut down the machine, first leave the column rinsing with both solvents for about 20 minutes. Then turn press 'power' again on all the boxes and finally return all cables to the methanol solvent.

To calculate the area under the peaks:

1. Click on 'postrun' in the main program window.
2. Go to File-Open to open your desired chromatogram.
3. Click on 'Wizard' in the left toolbar of the window.
4. Click on 'Program' on the next window that will pop up.
5. Now you are ready to manipulate your graph as desired. With the top left buttons you can choose to 'reject peak', 'adjust peak' and others but these are the most frequently employed. With the 'adjust peak' button adjust the red measuring lines on the graph to select what area you want to measure under the peak.
6. Click on 'ok'.
7. Click on 'suivant' to read the areas corresponding to each peak on the graph including the one you adjusted.

To construct a calibration curve:

1. Run several known concentrations of your sample on the HPLC. You should include the lowest concentration detectable by the machine and the highest one that you can possibly obtain.
2. Measure the areas under the curves for each concentration.
3. Construct a graph of areas versus concentrations. You should obtain a directly proportional relationship between both variables.

Troubleshooting the HPLC:

1. If the pressure is too low (lower than 100 bar) then this indicates that probably there is an obstruction in the plastic cables. Possibilities to troubleshoot:
  - a. Check that the cables are not tangled or blocked by the HPLC machine.
  - b. If the problem continues, run a purge without changing the cables from their corresponding solvents. This should eliminate any bubbles.
  - c. If the bubbles persist, use a syringe to force them out.
  - d. It is useful to sonicate the solvents to eliminate any small bubbles contained in the solution.
2. If the program starts detecting sharp peaks even without any sample injections, one could:
  - a. Turn around the column so that the mobile phase passes in the opposite direction. Let it rinse for a couple of hours. This will allow the column to unclog, which is sometimes the case due to the high pressure.
  - b. Replace column if problem persists.

- c. If problem persists, this is an indication that it might have nothing to do with the column itself. Replace the detector lamp.

## UV-Visible Spectroscopy

1. Turn on the UV machine with a button in the back of it.
2. Check that there is no cuvette within it and press 'val' after the machine asks: Porte-cuvette vide? The machine will now run an autotest that takes approximately 5 minutes.
3. When the autotest is done the machine will ask 'imprimer?' you should then use the right arrow to select 'abandonner'.
4. Then use the down arrow upto 'Configuration' and then to the right up to 'Liaison RS232' and press 'val' (validate).
5. Login to the computer using the name Eccma9 and password eccma and then open the program called LabPowerJ.
6. Under 'Methods', under 'nouvelle methode' choose 'Balayage du Spectre'
7. Then go to the bottom of the window and click on edit. Set the minimum and maximum wavelengths to 200 and 700 nm respectively. Click on ok.
8. Insert your reference (usually water) into the UV machine and click on ok. The baseline will take about 1 minute. Make sure to introduce the quartz cuvette with the transparent side facing the source of light. In addition, only hold the quartz cuvette by the non-transparent parts.
9. The machine is ready to be used. Rinse cuvette with desired sample first and then fill it up and insert it in the UV machine cuvette holder.
10. Press the yellow button 'Measure' in the top toolbar of the program. The running time takes about 1 minute.
11. Then go to File-Export-Excel and save the document with you name, sample name and concentration and date.
12. To finish just close the program and then turn off the machine.

## Fluorescence Spectroscopy

1. Turn on the fluorescence machine by pressing on-off switch in the bottom front of the machine.
2. Login to the computer using the name and password pons, then open the software called FL Solutions.
3. Click on 'Method' to add a new method. Then click on Load and go to 'disque C', then 'Program Files', then 'FL Solutions', folder 'mnp' and choose 'raman\_eau.flm'. The scan mode should be 'emission'.
4. Introduce a plastic cuvette filled with water into the machine and click on 'Measure'.
5. Once run is completed click on 'Report'. This will take you to an excel sheet where you can save your data under your preference.
6. Repeat this run by choosing this time the method 'eau usee'. The scan mode should be 'synchronous'.
7. Once both raman and eau usee are ran and saved the samples of interest can be run under the same method/mode that was used for eau usee.
8. All samples should be saved via the 'Report' button.
9. To finish close the program. When it asks you if it should just close the program or also turn off the lamp chose the latter one, but also manually switch off the lamp on the machine.

## Appendix B. Additional Data

### Preparation Experiments

Some graphs are briefly discussed others are not.

#### UV Spectra of Individual Solutions

Manure lixiviate was also intended to form part of the GAC experiments, however due to time constraints this was not possible. Manure often ends up in surface waters due to runoff waters from farms. It is of interest because, similarly to humic acid, it can compete for GAC adsorption and thus limit the target compound's abatement from water.

The manure lixiviate spectra in Figure 49 show that manure lixiviate dilutions by 10 and 20 result in an absorbance over the limit of detection for the UV machine. Therefore a dilution of at least 100 should be used for the GAC experiments. Since no exact concentration was known for these solutions, no calibration curve was constructed for this substance.

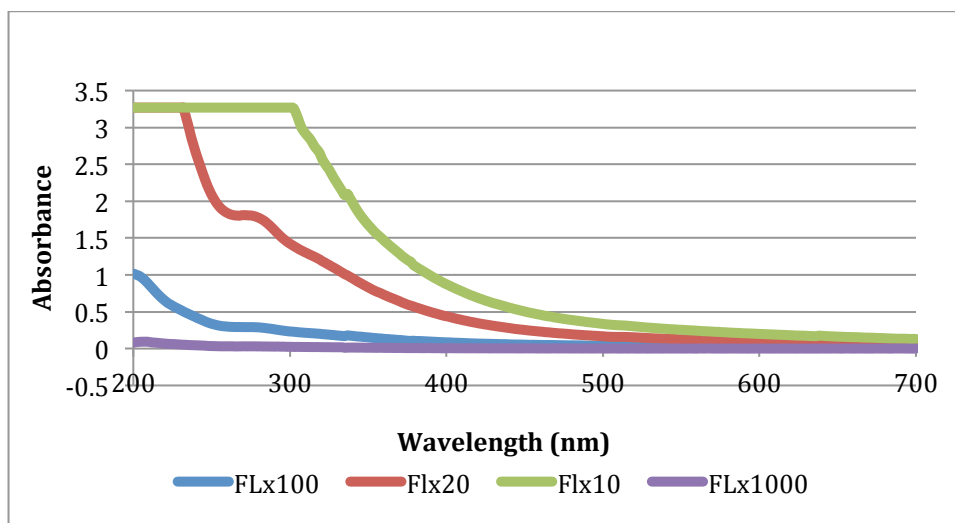


Figure 49. UV Spectra of Varying Manure Lixiviate Concentrations

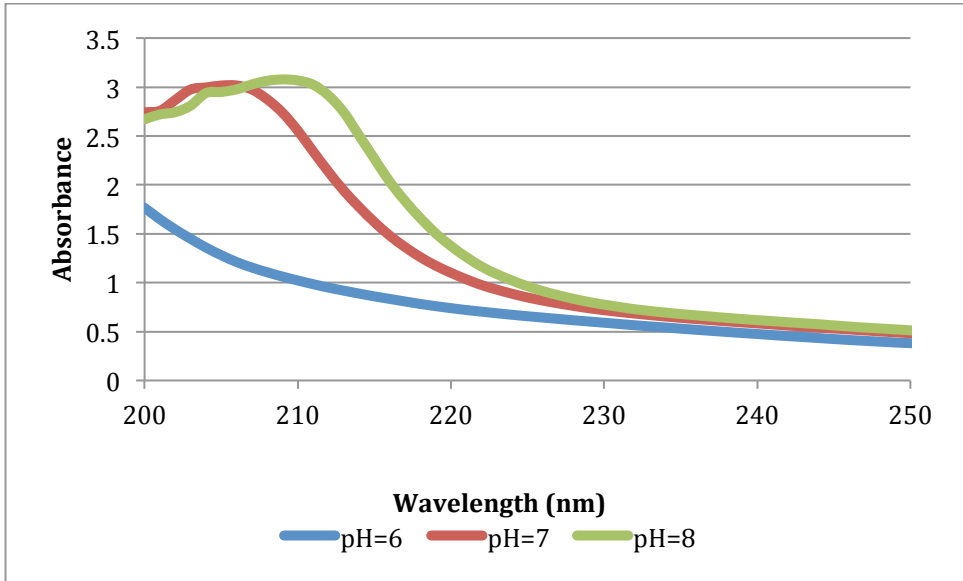


Figure 50. UV Spectra as a function of pH for Manure Lixivate (x100)

UV Spectra of Combined Solutions

The combinations of manure lixiviate and tylosin tartrate concentrations are shown in the following spectra in Figures 51 and 52.

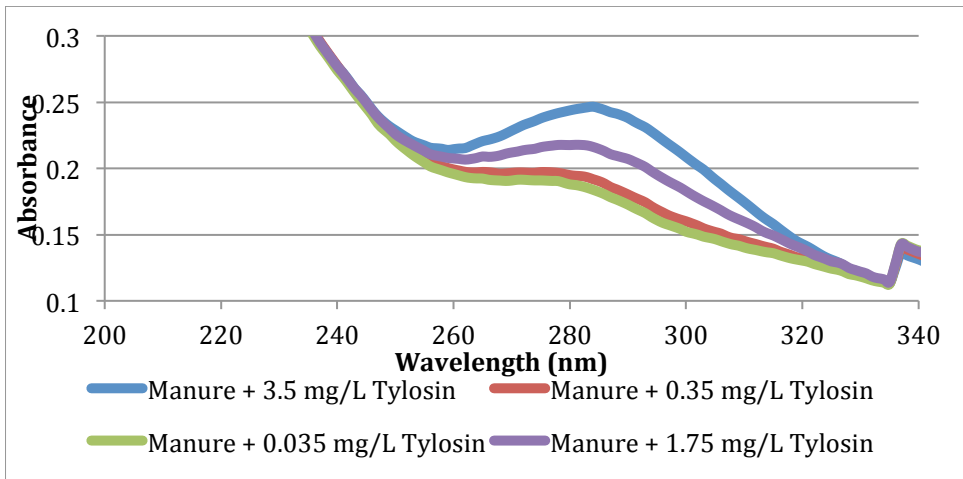


Figure 51. UV Spectra of Manure Lixivate (x100) with Varying Tylosin Tartrate Concentrations

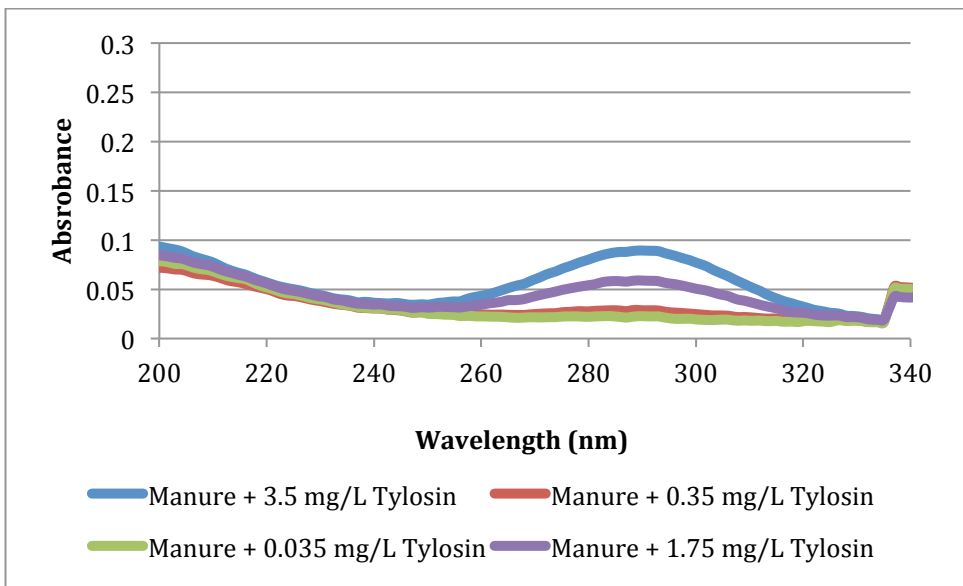


Figure 52. UV Spectra of Manure (x1000) with Varying Tylosin Tartrate Concentrations

The spectra from stronger manure lixiviate concentrations, as shown in Figure 51, tend towards the negative x-axis much more steeply than those with weaker manure presence, as shown in Figure 52. This causes the tylosin tartrate peaks to shift upwards in Figure 51 and reach an absorbance of about 0.25 for a tylosin concentration of 7 mg/L, while the highest peak in Figure 52 only reaches one of about 0.09.

## Effect of pH on UV Spectra

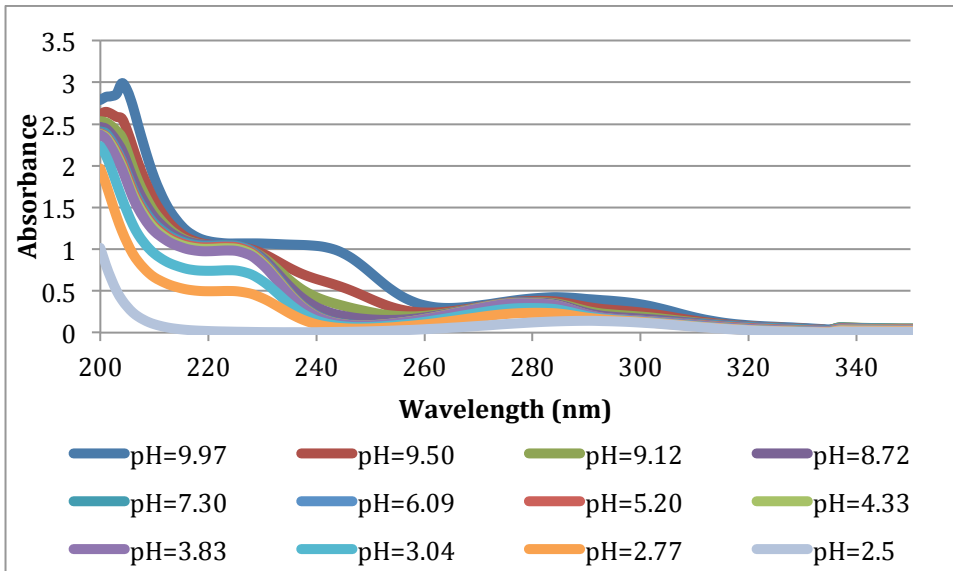


Figure 53. UV as a function of pH for 7 mg/L Tylosin Tartrate in KCl solution

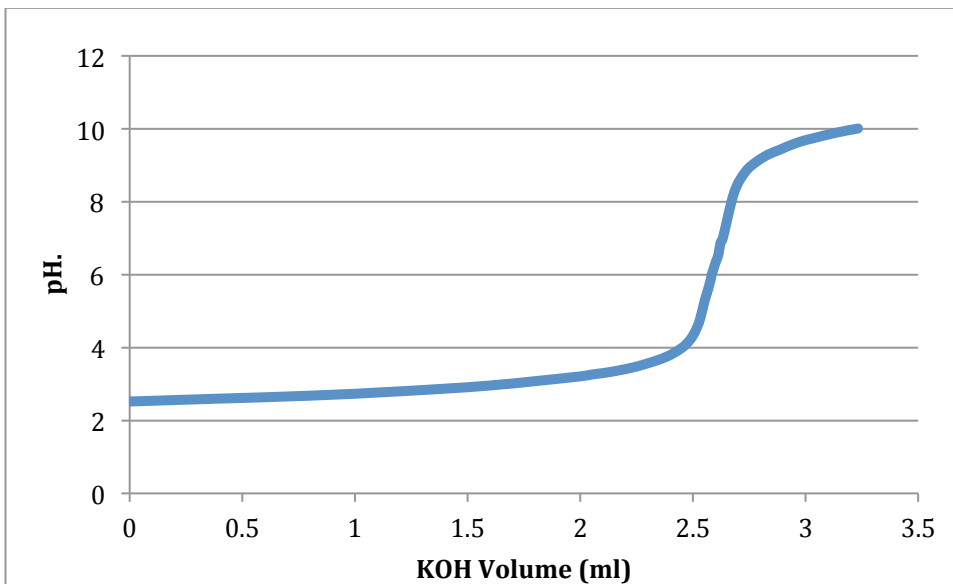


Figure 54. Titration Curve for 7 mg/L Tylosin Tartrate in KCl solution

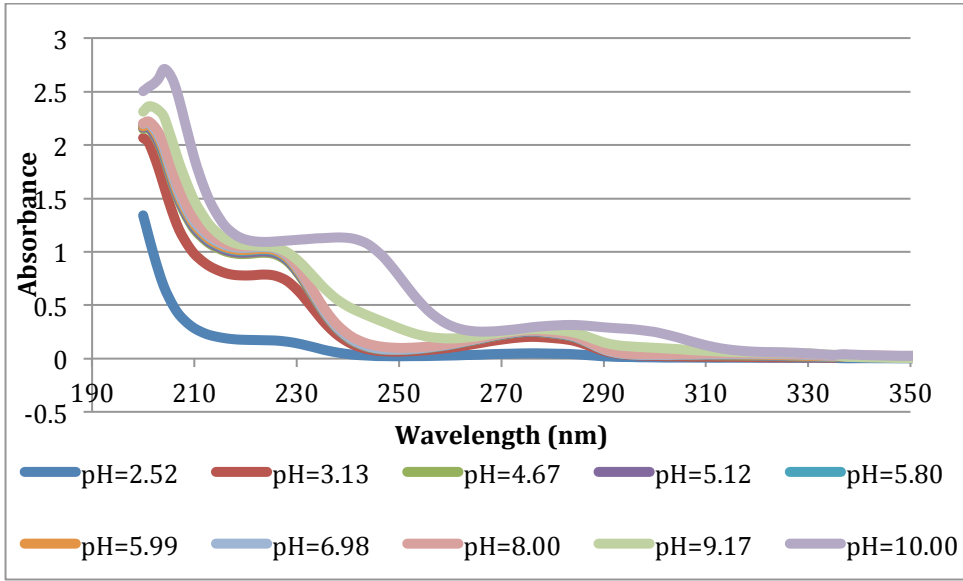


Figure 55. UV as a function of pH for 1 mg/L Humic Acid in KCl solution

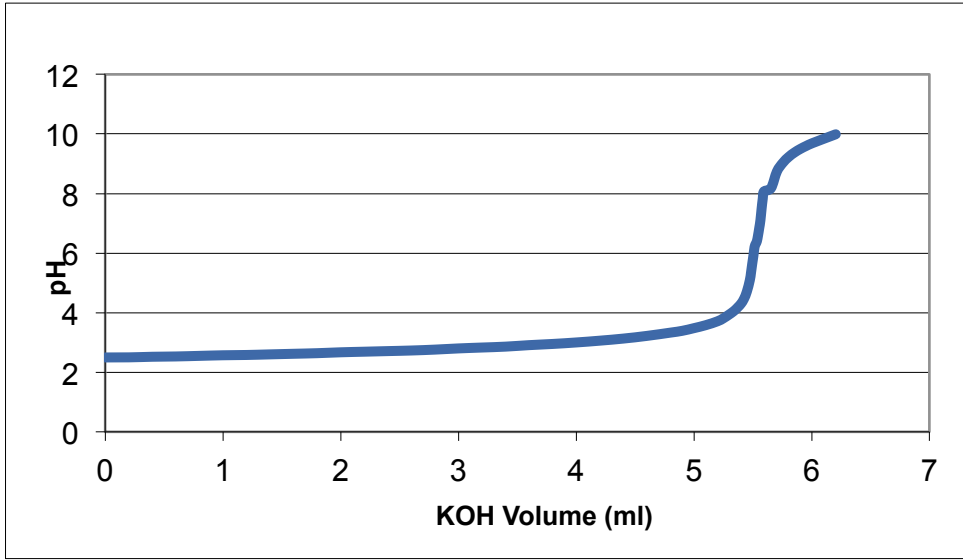


Figure 56. Titration Curve for 1 mg/L Humic Acid in KCl solution

Fluorescence Spectra of Individual Solutions

The fluorescence spectra for manure lixiviate solutions are shown in Figure 57. Since the UV spectra for manure dilutions of x10 and x20 showed absorbance levels over the limit of detection fluorescence traits for dilutions of x100 and x1000 only will be discussed in this section.

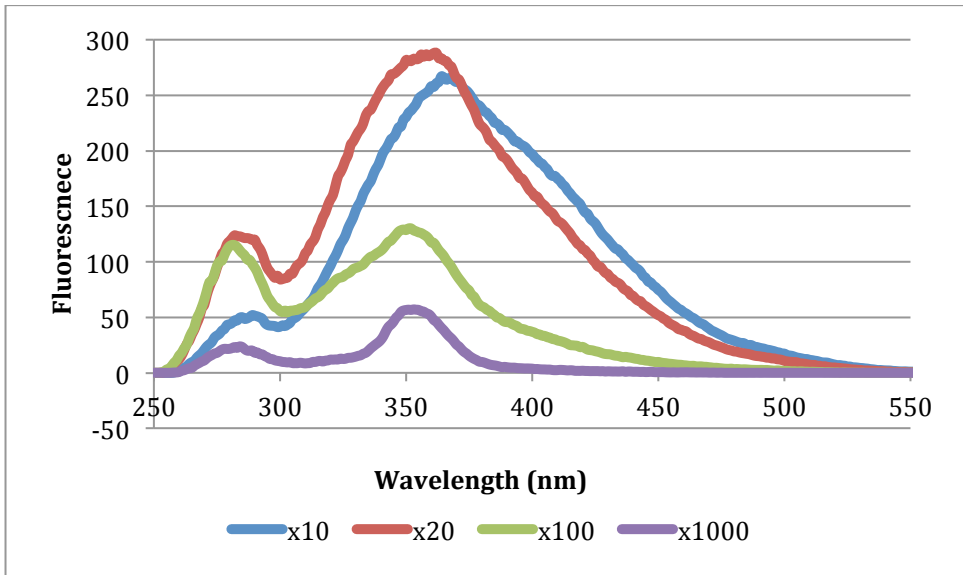


Figure 57. Fluorescence Spectra of Varying Manure Concentrations

Manure shows a rather broad peak at a wavelength of 350 nm and another broad but smaller one at around 280. However these spectra do not show a consistent trend between fluorescence and concentration, nor do they show peaks at a consistent wavelength of interest. These spectra were all obtained from the same sample and they were all taken at the same time.

#### Fluorescence Spectra of Combined Solutions

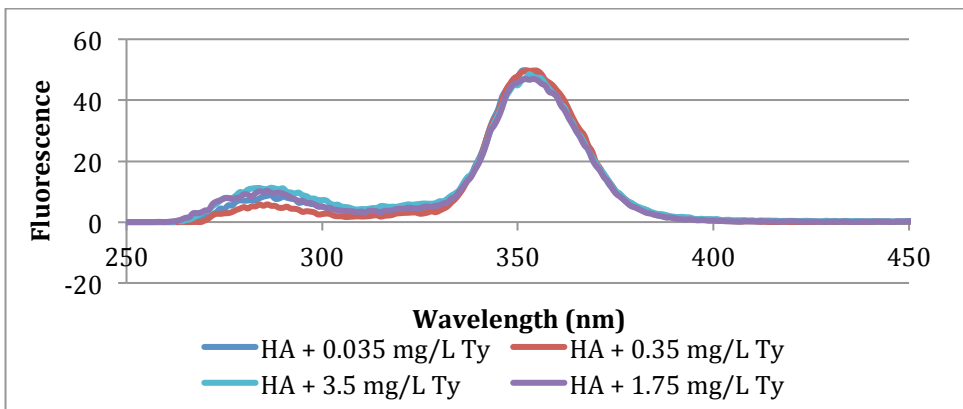


Figure 58. Humic Acid (0.05 mg/L) with Varying Tylosin Tartrate Concentrations

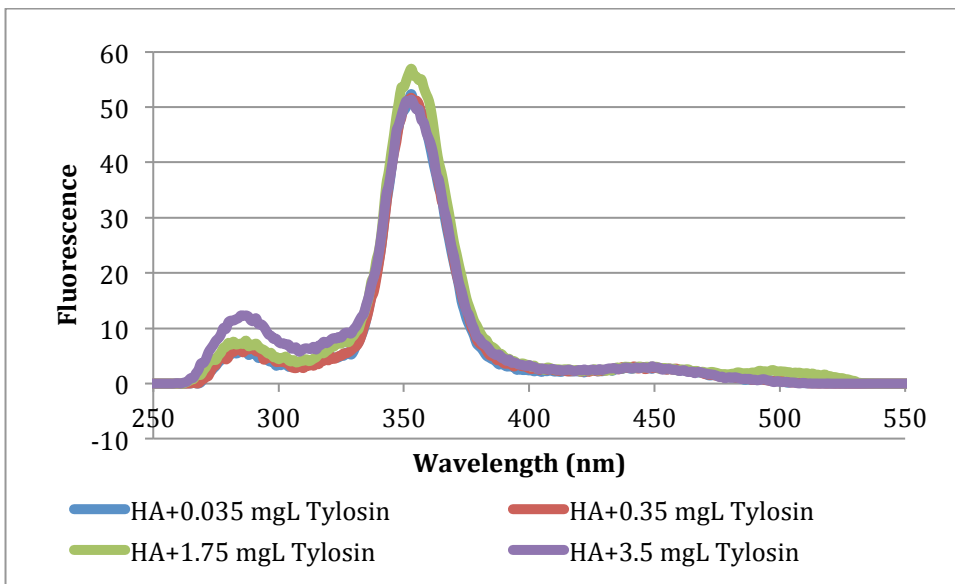


Figure 59. Humic Acid (0.5 mg/L) with Varying Tylosin Tartrate Concentrations

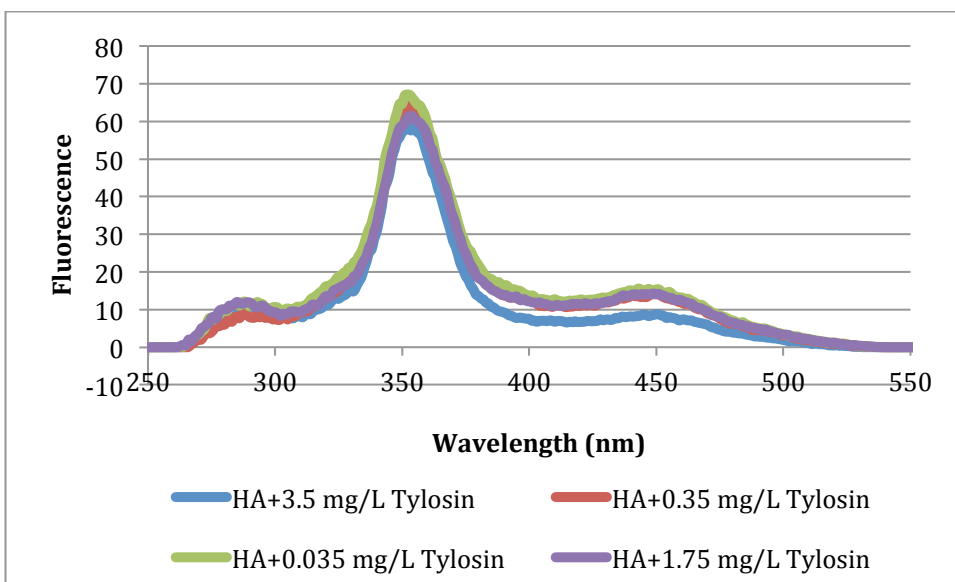


Figure 60. Humic Acid (2.5 mg/L) with Varying Tylosin Tartrate Concentrations

## Kinetic Experiments

### Analysis with UV Spectroscopy

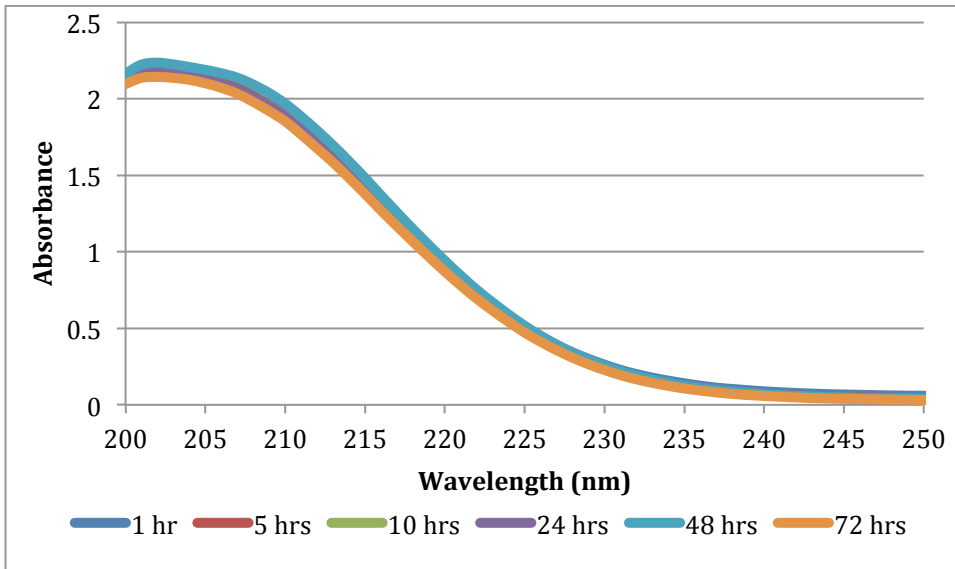


Figure 61. Madon UV-Derived Kinetics

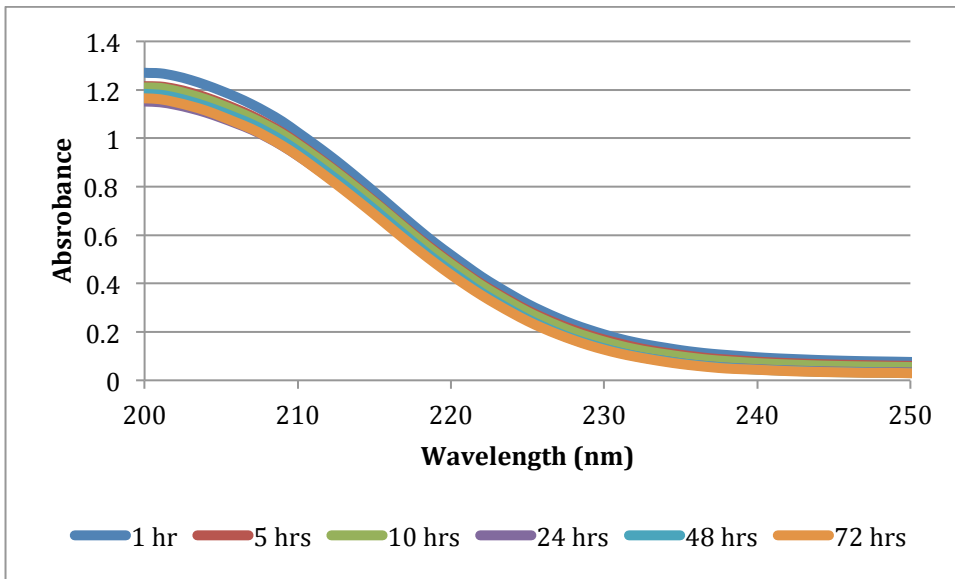


Figure 62. Moselle UV-Derived Kinetics

## Analysis with Fluorescence Spectroscopy

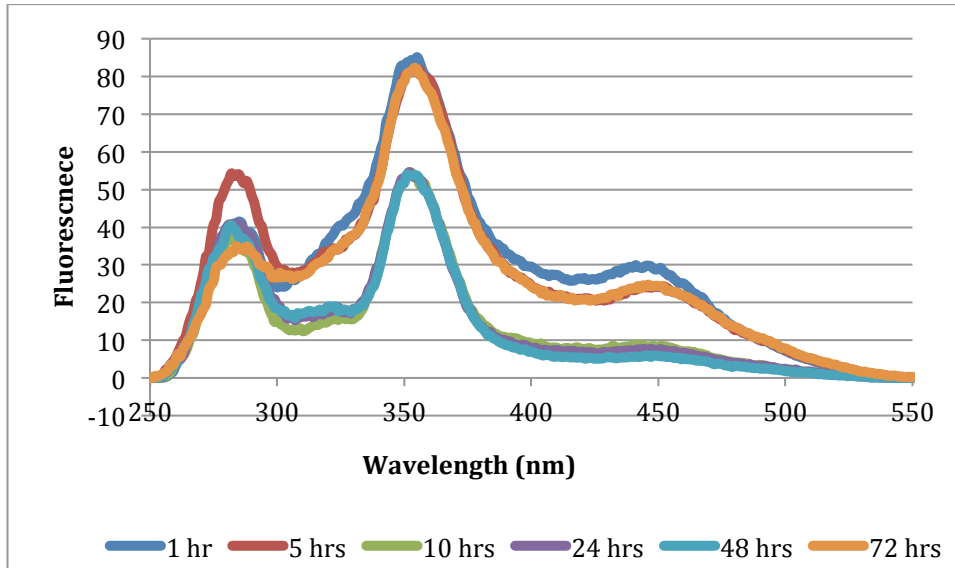


Figure 63. Humic Acid ( $C_0=10$  mg/L) Fluorescence-Derived Kinetics

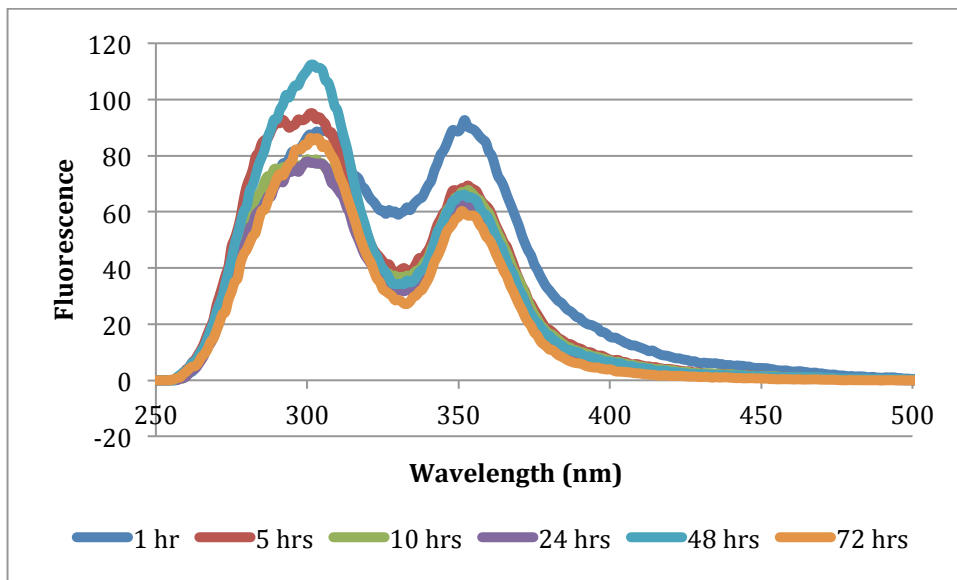


Figure 64. Madon Fluorescence-Derived Kinetics

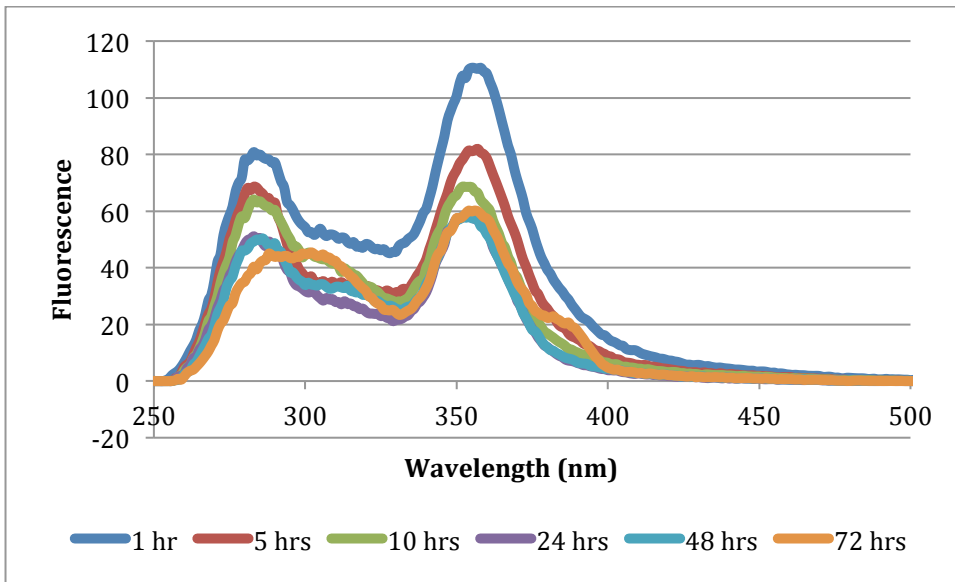


Figure 65. Moselle Fluorescence-Derived Kinetics

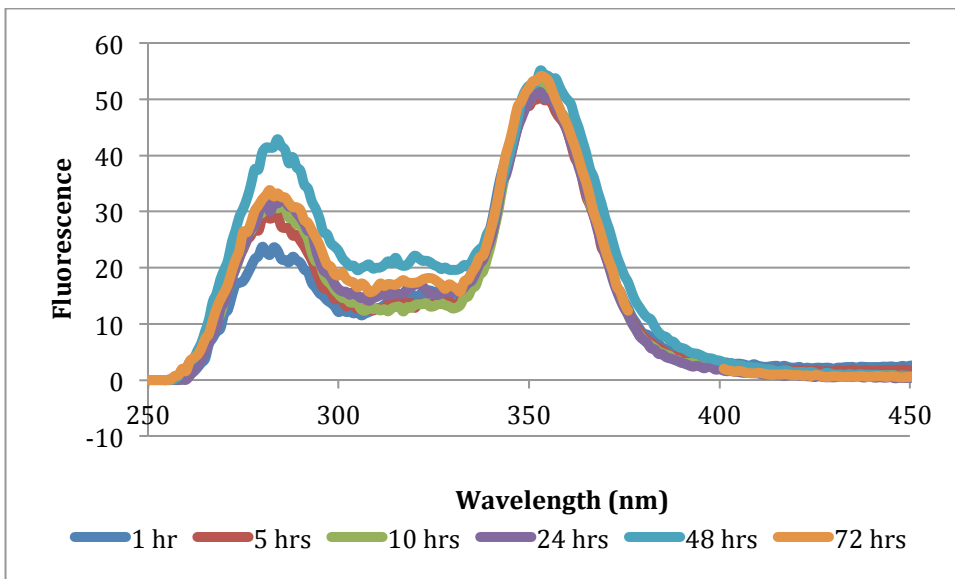


Figure 66. Tylosin ( $C_0=70$  mg/L) Fluorescence-Derived Kinetics

## PH at Start and End of Kinetic Experiments

Table 5. Symbols that Represent Kinetic Solutions

KEY	
Solution	Symbol
Humic acid 10 mg/L	A
Humic acid 80 mg/L	B
Tylosin Tartrate 70 mg/L	T
Tylosin Tartrate 70 mg/L + HA 10 mg/L	C
Madon	D
Moselle	S

The number next to each symbol represents the number of contact hours for the solution.

Table 6. PH Values at the Beginning and End of Kinetic Experiments

	pH at start	pH at end
A1	7.09	5.28
A5	7.09	7.54
A10	7.09	5.32
A24	7.09	6.24
A48	7.09	6.14
A72	7.07	5.9
B1	7.12	6.43
B5	7.12	6.74
B10	7.12	6.46
B24	7.12	6.64
B48	7.12	6.98
B72	7.07	6.72

T1	7.33	6.18
T5	7.09	6.12
T10	7.09	6.13
T24	7.09	6.45
T48	7.09	6.8
T72	7.07	6.68
D1	8.07	7.77
D5	8.07	7.77
D10	8.07	7.88
D24	8.06	7.85
D48	8.25	8.06
D72	8.07	
S1	7.75	7.21
S5	7.75	7.21
S10	7.75	7.31
S24	7.68	7.23
S48	8.05	7.34
S72	7.75	
C1	7.07	5.53
C5	7.07	5.26
C10	7.07	
C24	7.07	5.38
C48	7.07	
C72	7.07	

## Appendix C. Additional GAC Acticarbone BGX Photographs

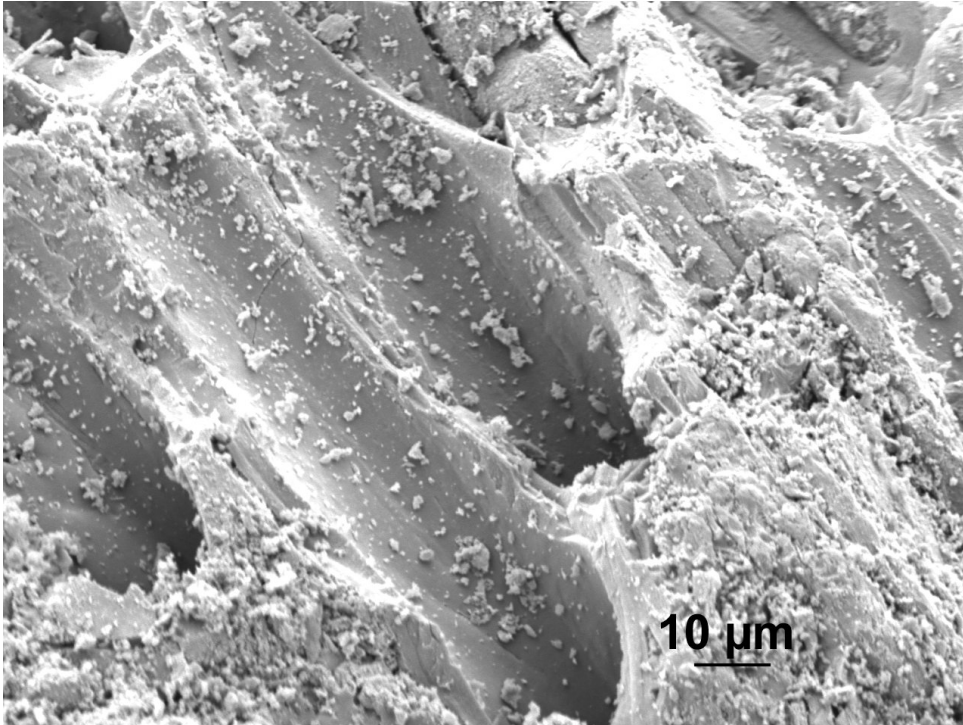


Figure 67. Acticarbone BGX Image (ACCEL\_VOLT 5 KV, MAG 1000)

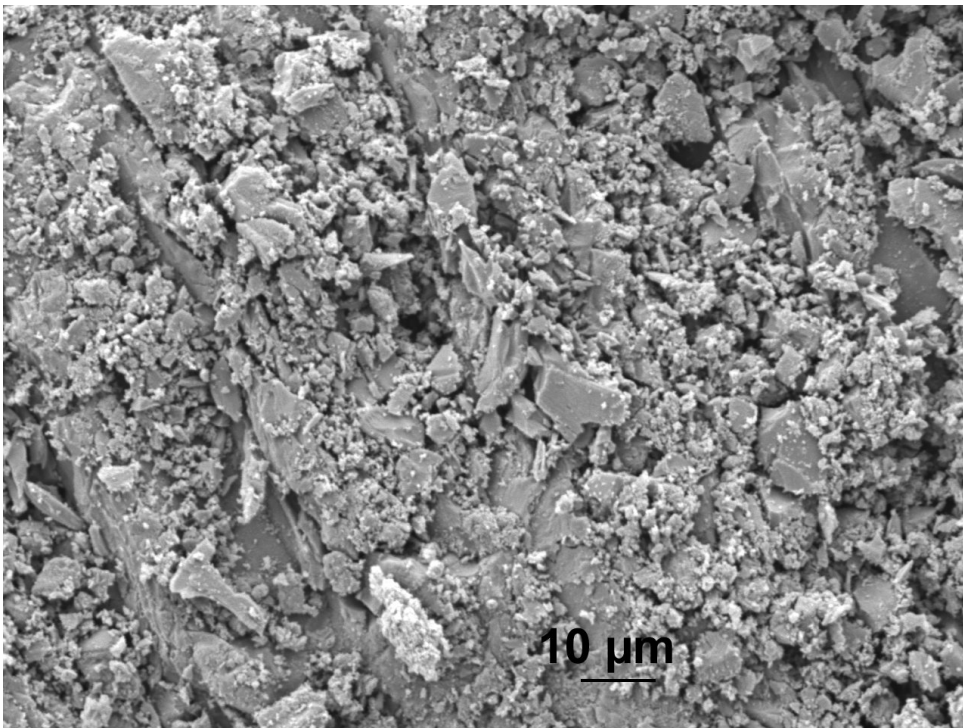


Figure 68. Acticarbone BGX Image (ACCEL\_VOLT 5 KV, MAG 1000)

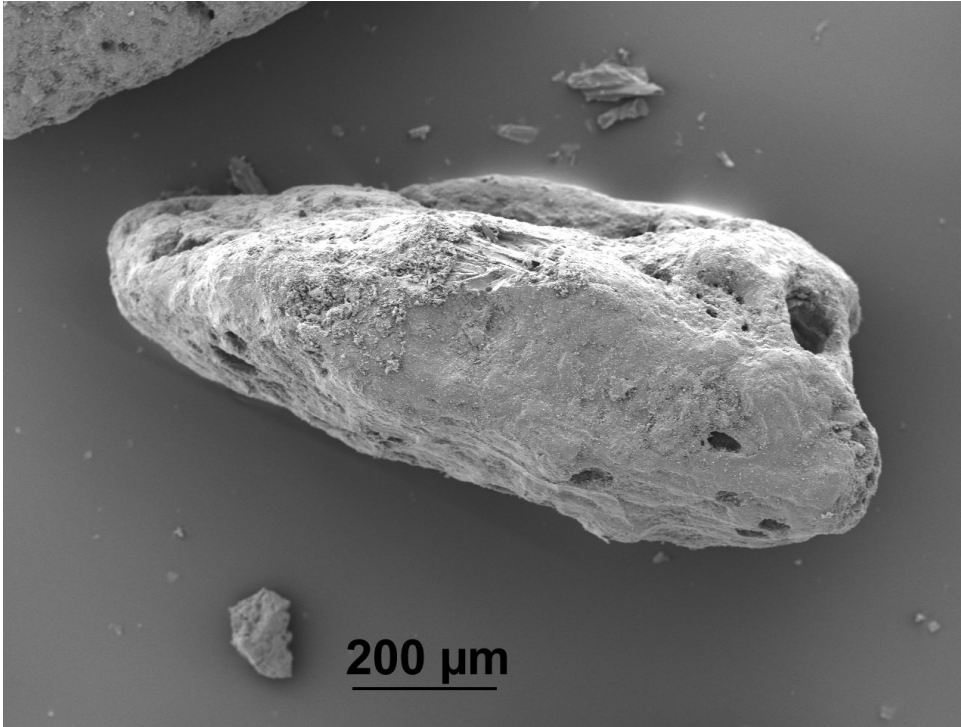


Figure 69. Acticarbonone BGX Image (ACCEL\_VOLT 5 KV, MAG 95)

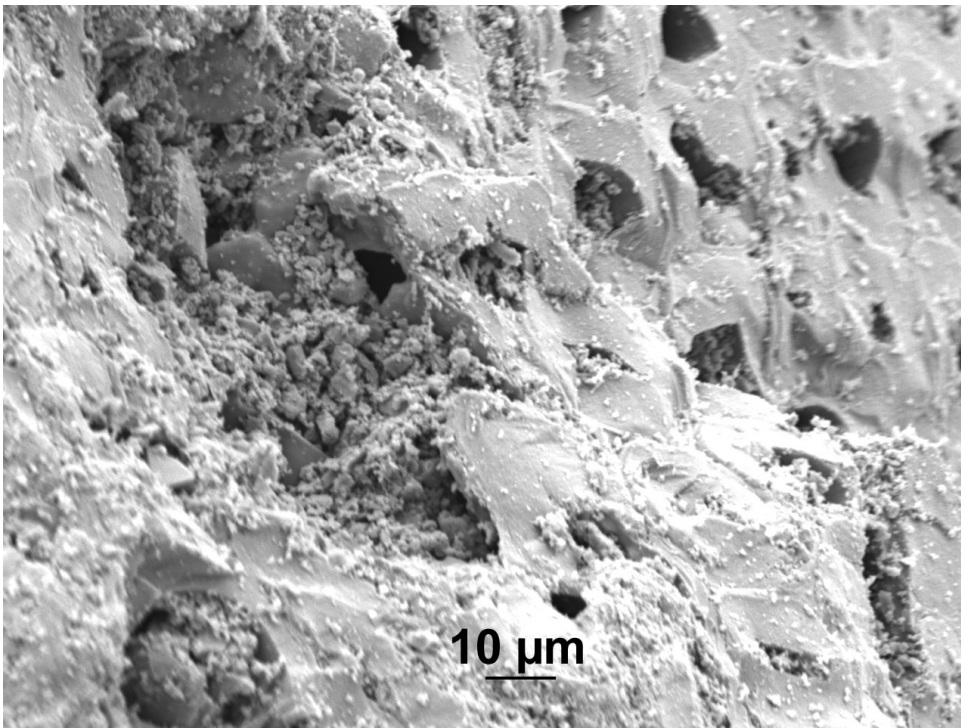


Figure 70. Acticarbonone BGX Image (ACCEL\_VOLT 5 KV, MAG 1000)

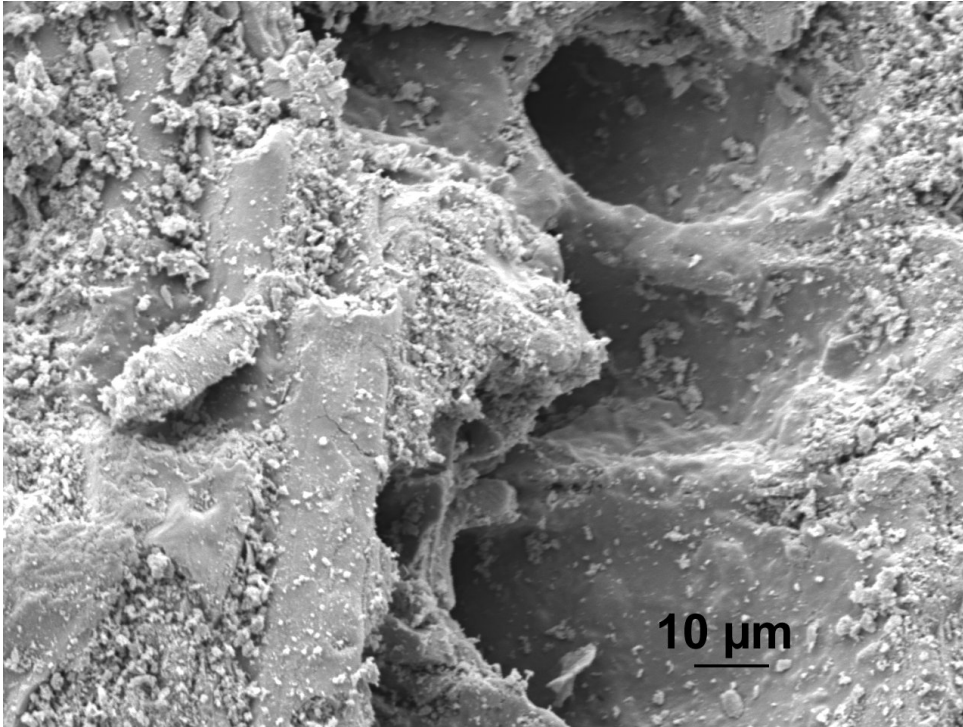


Figure 71. Acticarbon BGX Image (VOLT 5 KV, MAG 1000)

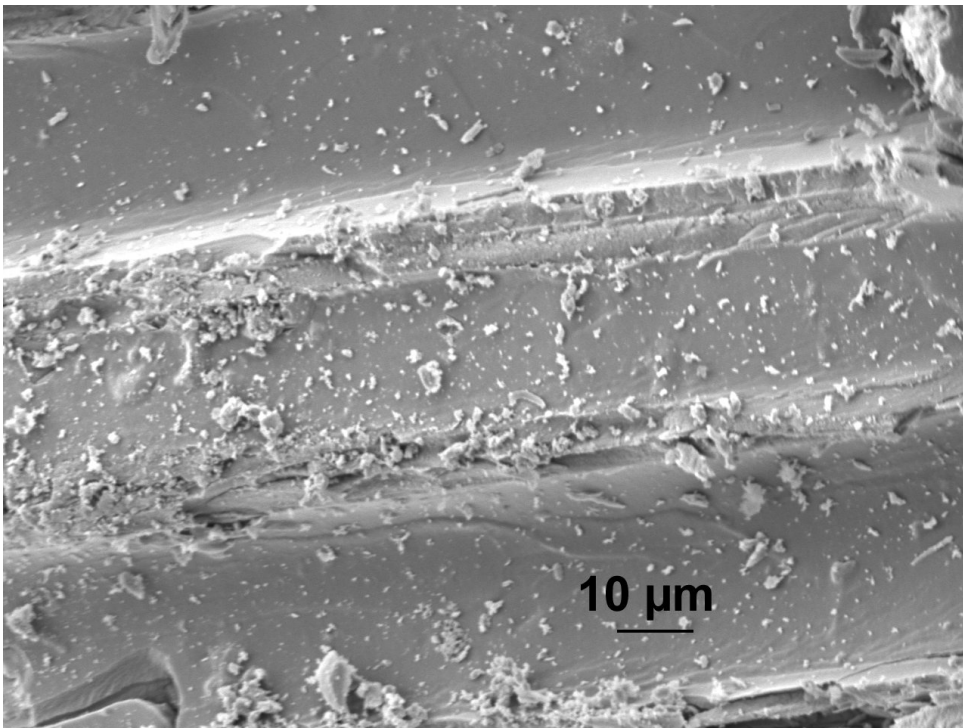


Figure 72. Acticarbon BGX Image (VOLT 5 KV, MAG 1000)

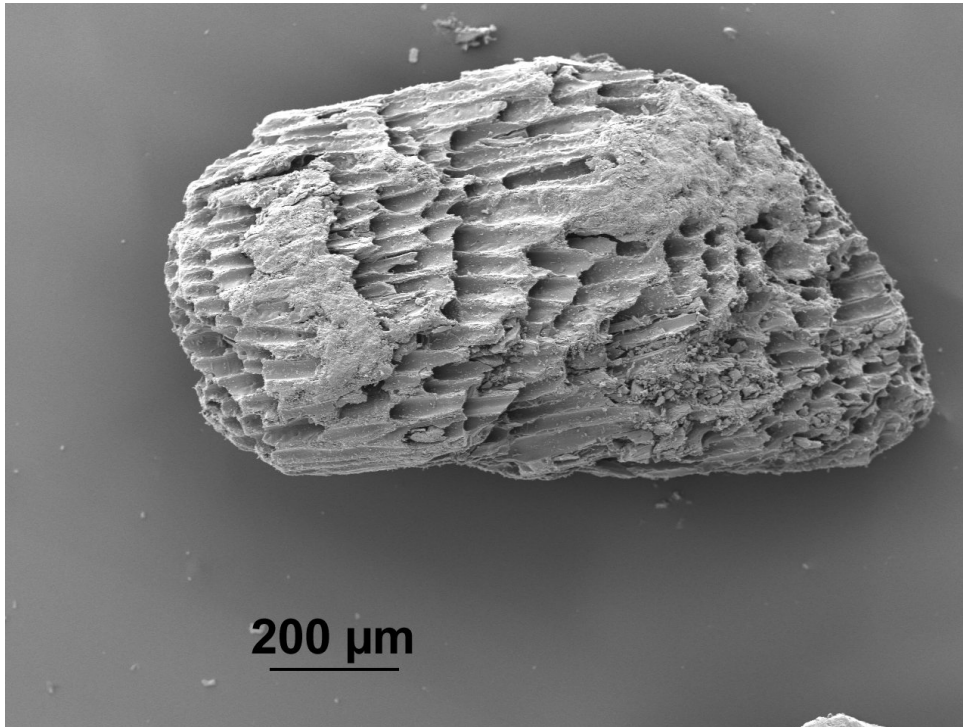


Figure 73. Acticarbonone BGX Image (VOLT 5, MAG 85)

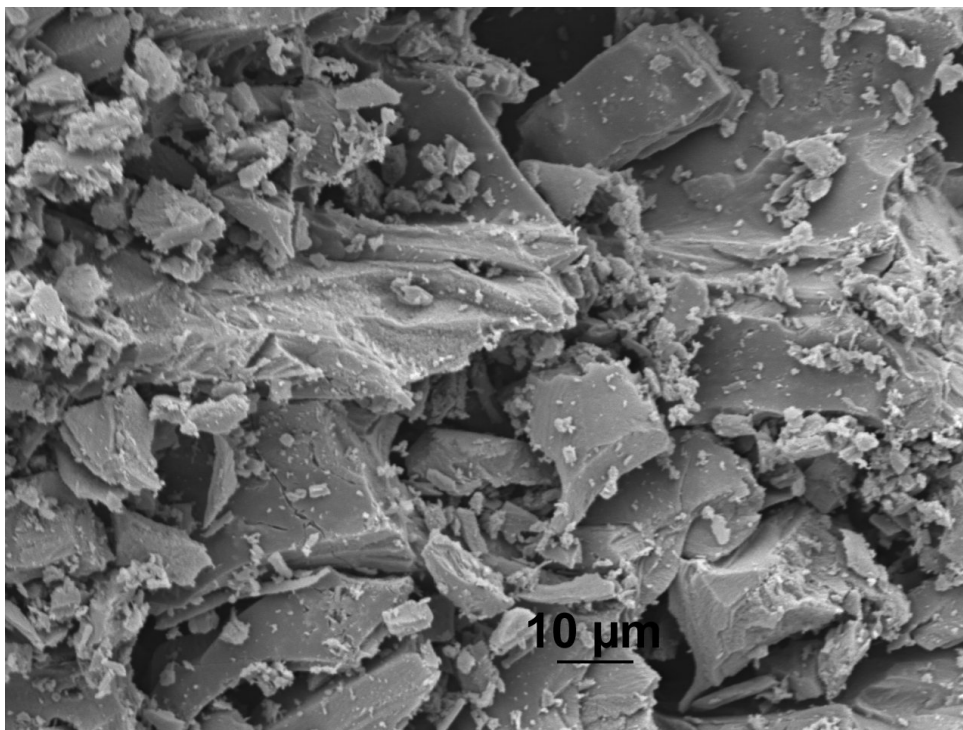


Figure 74. Acticarbonone BGX Image (VOLT 5 KV, MAG 1000)